

LESS IS MORE: OXYGEN AND STEM CELL REGENERATION

Thesis by

Marie Elizabeth Csete MD

In Partial Fulfillment of the Requirements

For the Degree of

Doctor of Philosophy

California Institute of Technology

Pasadena, California

2000

(Submitted March 11, 2000)

© 2000

Marie Elizabeth Csete

All rights reserved

Without Joe Gabel, I would not be writing a dissertation. Joe was Chair of the Anesthesiology Department at UCLA. He had the courage to extend his vision for the department beyond the next fiscal reports, and his encouragement to train as a scientist made my time at Caltech possible. Joe's feistiness often overstepped the boundaries of good judgment but his support for me never flagged, despite the advice of his senior research people that I was meant to be a clinician and never a bench researcher. The grace with which he handled his last days was a surprise to me. In our last meeting, when his death was just a few days away, he didn't rail at the injustice—He wanted to talk about where my science was going! It really saddens me that he is not around to celebrate and get some credit for whatever I've managed to accomplish at Caltech.

Luckily, Joe has a successor, and at a time when academic anesthesiology departments around the country are crumbling, I have found a place where my colleagues believe in the importance of my ideas and are willing to invest in the future of those ideas. So I thank my new colleagues in Ann Arbor, as well as my anesthesiology friends on the UCLA liver transplant service, Drs. Gundappa Neelakanta, Michele

Braunfeld, Randy Steadman, Michael Sopher, and Susan Chan.

I know your workload increased with my departure.

One of the good things about graduate school at Caltech is the committee system in the Biology Division. Instead of reading theses (or not reading them) at the last minute, the committee serves as a balanced feedback mechanism. My committee was thought-provoking and no-nonsense. Though Scott Fraser never managed a committee meeting in real time, I appreciated his input as well as that of the other committee members: Drs. Jim Strauss, Paul Sternberg, and David Baltimore.

Jim and Ellen Strauss provided an oasis for me throughout grad school. I knew I could say anything in their office, and I'd get a reasoned response, and usually come out laughing. I also travelled vicariously and enjoyed their delicious stories about exotic destinations. Thank you, Jim, for your common sense and honest approach to the world.

And then there is Ray...Dr. Ray Owen taught me that successful scientists can actually operate by emphasizing the good in others. He has a genius for match-making and through Ray, I met collaborators, friends, and saw the future of our best and brightest medical students. Ray's meticulous hand-written notes in my box, his clippings of interesting articles (both scientific and amusing) and cartoons, and his refusal to let me pay for lunch all made me feel incredibly special, though I know he lavishes his care on many others.

I have had the good fortune to learn from a number of talented scientists during short collaborations. I thank them all for teaching me the details of their systems and becoming friends in the process: Drs. Gabriela Hernandez-Hoyos, Pam Eversole-Cire, Randy Walikonis, and Carol Readhead were all superb teachers during our work together. Part of the work with Pam Eversole-Cire, a post-doc in Prof. Mel Simon's lab, is presented in Chapter 3. Collaboration with Sean Morrison (then a post-doc in Prof. David Anderson's lab, now at the University of Michigan) also contributed to Chapter 3. I also appreciated the considerable, informal wisdom of post-docs in the Wold lab:

Drs. Sonya Zabudoff, Jeong Yoon, and Brian Williams. I thank Dr. Ron McKay at the National Institutes of Health for hosting me in his laboratory and for introducing me to Dr. Lorenz Studer, now an Assistant Member at Sloan-Kettering. Ron's skepticism and then enthusiasm were rites of passage for me. Lorenz is a committed, creative researcher and I was honored to interact with him. Our work together constitutes Chapter 3 of this thesis, and he also contributed to the work in Chapter 5. Lorenz and I were assisted by Nadine Kabbani (now a grad student in Hershey) and Sang-Hun Lee at the NIH, a post-doctoral fellow in the McKay lab from Hanyang University in Seoul.

The work in Chapter 5 was done in collaboration with Randy Walikonis, a post-doc in Prof. Mary Kennedy's lab. Randy isolated the hippocampal neurons necessary for this work and produced the beautiful confocal images.

My advisor, Prof. Barbara Wold, knows more facts than I will ever imagine, and that knowledge is both intimidating and inspiring. I am grateful to Barbara for allowing me to go in a direction she would not have chosen for me—It's the right path for me to have chosen and the right path for me

to build on. I learned a lot from Barb, and though both of us would probably not choose to repeat much of the last four years, her scientific talents and insights will leave a lasting impression. I particularly appreciated Barb's willingness to hear the "medical" interpretation of biological literature, allowing me to integrate my new education with my old one.

The work in Chapter 4 grew out of discussions with Prof. John Doyle (CDS) and Mark Borisuk, Ph.D., a CDS post-doc. The models were derived by John and Mark after discussions based on my results in a variety of stem cell systems, some not discussed in this work.

Thank you to Jean Walikonis for your attention to all our experiments and for your significant input into this thesis work, as well as the sparkle you brought into our shared space. I was incredibly fortunate to have you as a working partner at the end of graduate school. Jean contributed to the work of Chapters 2, 3, and 5 of the thesis.

To love is not to gaze steadfast at one another: it is to
look together in the same direction.

St. Exupery, *Terres des Hommes*

And especially...a million thanks to the one and only John
Doyle

Abstract

Recent years have witnessed an explosion in the identification and understanding of stem cells, affording new cellular reagents for the study of regeneration in vitro. Traditionally, regeneration is studied in tissue culture in which the gaseous environment surrounding the cells contains about 20% oxygen. Cells in our bodies are never exposed to such high levels of oxygen, well out of normal physiologic range. In this work, stem cell regeneration in several systems was studied in traditional 20% oxygen culture and in oxygen levels more reflective of normal physiology. These lower oxygen-cultured progenitors behaved differently than those cultured in traditional environments. In several stem cell systems low oxygen significantly increased proliferation of progenitor populations, and in central nervous system stem cells, also decreased apoptotic death. More physiologic levels of oxygen in culture also led to regeneration of different daughter progeny populations with a distribution of phenotypes distinct from that generated in 20% oxygen. For example in CNS stem cells, a significantly greater yield of dopaminergic and serotonergic neurons was generated in low oxygen compared to 20% oxygen. Skeletal muscle satellite

stem cells in high oxygen were significantly more likely to assume an adipocyte phenotype than those cultured in low oxygen. Furthermore, genes expressed during regeneration in physiologic vs. 20% oxygen were different from each other in timing and in abundance. These data suggest that oxygen manipulations will be useful to increase the survival and expansion of progenitor populations for research and possible transplantation, as well as for the survival and expansion of selected regenerated progeny. Furthermore, oxygen levels are a useful manipulation to help isolate and identify pathways used during regeneration and differentiation.

Table of contents

1. **Chapter 1:** Physiologic oxygen and stem cells
Text: Pages 1-12
References: Pages 13-20
2. **Chapter 2:** A new satellite trajectory
Text: Pages 1-41
Figures: Pages 42-66
References: Pages 67-87
Appendix (Materials and Methods): Pages 88-93
3. **Chapter 3:** CNS stem cell regeneration in vitro benefits
from a low oxygen environment
Text: Pages 1-27
Figures: Pages 28-63
References: Pages 64-78
Appendix (Materials and Methods): Pages 79-87
4. **Chapter 4:** A simple mathematical model
Text: Pages 1-7
5. **Chapter 5:** Speculation
Text: Pages 1-18
Figures: Pages 19-54
References: Pages 55-68
Appendix (Materials and Methods): Pages 69-72

"We receive most of our oxygen from the air around us, but breathing isn't always enough. With the new bio-oxidative therapies you can actually generate more oxygen in your body to achieve optimum health and longevity."

From Oxygen Healing Therapies-2nd edition by Nathaniel Altman. As featured on www.ozoneservices.com

"Until recently, the only forms of oxygen that have been available to the public have been either highly caustic or potentially toxic. But now, thanks to a revolutionary technological breakthrough, science has found a way to harness oxygen and make it available to us in a form that is completely safe and easy to use.

LIFETRONIX OXYBUILD 1200 represents a twenty-first century solution to the challenge of providing our cells with one of the fundamental elements we all need for optimum health and performance. After years of research and development, LifeTronix is proud to be releasing the FIRST and ONLY STABILIZED OXYGEN (pH balanced) SUPPLEMENT.

The effects of oxygen at the cellular level are well known and well documented. But you don't have to take our word for it. LIFETRONIX OXYBUILD 1200 is not only the FIRST oxygen supplement of its kind, it is also 100% DEMONSTRATABLE!"

From www.uslink.net/~johnb/lifetrnx

Chapter 1. Physiologic Oxygen and Stem Cells

Standard conditions for culture of mammalian cells are 37°C in a gas mixture of 5% CO₂ + 95% air. Thus temperature is adjusted to reflect core mammalian levels, and CO₂ to reflect approximate venous concentrations, while in striking contrast O₂ levels in culture are not physiologic. At sea level, room air contains 21% O₂, and a 5% CO₂ + 95% air mix contains 20% O₂. Alveolar air is 14% O₂, arterial O₂ is 12%, venous O₂ levels are 5.3%, and mean tissue intracellular O₂ concentration is 3% (Guyton and Hall, 1996).

Stem cells are generally hard to find in adult tissue. They are rare cells but part of the difficulty in finding them is that we don't know their addresses. A presumption running throughout the stem cell literature is that these cells home to an environment in which their quiescence is maintained, but where signals for regeneration can be received and processed, a specialized stem cell microenvironment. An enormous research effort is now devoted to understanding the hematopoietic stem cell

microenvironment. But what is meant by microenvironment? Most attention has been given to stroma surrounding hematopoietic stem cells. In fact, in animal models stroma has been co-transplanted to increase the success of hematopoietic bone marrow transplants (Almeida-Porada et al., 1999). Stromal-stem cell jagged-notch pathway interactions are recognized to be important in hematopoietic stem cell regulation of cell cycle kinetics and suppression of myeloid differentiation (Carlesso et al., 1999) and stroma also selectively binds secreted proteins for presentation to stem cells. Thus cell-cell interactions are the "microenvironment" discussed in stem cells biology. Even in review articles, inducible and constitutive locally secreted factors, as well as matrix proteins and surface receptors presented by stromal cells (Torok-Storb et al., 1998) are equated with the microenvironment.

The *in vivo* gaseous microenvironment of the best characterized stem cells (hematopoietic stem cells) is given a vague nod, but has in fact been very scantily studied. Nonetheless, these are the only stem cells for which the consequences of changing oxygen levels have been examined at all. Marrow presents a particular problem

because of its bony encasement, so blood flow is often measured, but direct measurement of oxygen in various regions of marrow is simply quite inaccessible because of its bony encasement. Consequently, blood flow to marrow has often been measured but direct assessment of oxygen levels in marrow is rarely reported in humans. In adult humans, oxygen levels in the femoral head just below the bony surface were measured at 63 torr (or 8.3% oxygen) and subchondral oxygen levels were significantly lower in patients of similar age with osteoarthritis (Kiaer et al., 1988). This number is in general agreement with other studies suggesting that overall marrow oxygenation is similar to that in jugular venous blood (Grant and Root, 1947). In dog long bone medulla, oxygen was directly measured at 23.5-27.7 torr (3.1-3.6%) (Tondevold et al., 1979). Newer indirect measurements of oxygen, based on oxygen-dependent drug binding to marrow components, suggest that some marrow elements may normally be exposed to even lower oxygen tensions than those cited above (Allalunis et al., 1983, and Allalunis-Turner, 1990), and that these regions of low oxygen tension may contain clonogenic potential. However, the gold standard of microregional measurement of oxygen using established Clark electrode techniques coupled with functional assessment of

hematopoietic stem cell potential has not been done, nor is it likely to be feasible.

All work citing measures of marrow oxygenation concentrates on global marrow blood flow, and not regional distribution of blood in the marrow microenvironment. Overall, marrow accounts for approximately 1-2.5% of total body weight (Donahoe et al., 1958) but receives about 2-4% of the cardiac output (Lahtinen et al., 1982). Acute increases in overall marrow blood flow are induced by acute anemia (Chen et al., 1986), but chronic compensated anemia, systemic hypoxemia, or exogenous erythropoietin do not induce increases in marrow flow (Schoutens et al., 1990). Although there is a general presumption that increased blood flow to marrow occurs in parallel to increased marrow cellularity (Iverson, 1997), there are no hard data to support this conclusion.

Since variations in the local gaseous environment in bone marrow have not been directly measured, the location of hematopoietic stem cells in marrow vis-a-vis oxygen supply is largely a matter of conjecture from indirect data. For example, progenitor cells that reside in compact bone, where capillary density is less than in marrow core, are

thought to prefer a relatively "hypoxic" environment (Allalunis-Turner and Chapman, 1986), but oxygen levels in these two environments have not been directly measured and compared. Oxygen delivery may be equivalent despite the difference in capillary density.

It should also be noted that the normal physiologic, protective environment of hematopoietic stem cells that continue to carry out regeneration may be low in oxygen compared to other sites in the body, but should not be deemed "hypoxic" since this term denotes cellular stress. The term "hypoxia" has led to major confusion in the literature since it is used to denote both relatively low levels of physiologic oxygen availability as well as to denote true oxygen limitation. The term should be, for the sake of clarity, limited to situations in which a lack of oxygen initiates cellular stress responses (Murphy et al., 1999).

Oxygen availability is a direct function of distance from the capillary supply of oxygen-carrying erythrocytes. (Very little oxygen is delivered in solute; the vast majority is delivered by red cells.) Thus, capillary density in relation to cellular density in each organ is a

prime determinant of the localized oxygen milieu, but oxygen availability is also regulated by other factors. Arterioles in some vascular beds may contribute significantly to oxygen delivery (Torres Filho et al., 1996) complicating the direct relationship between capillary density and oxygen availability. Oxygen availability and delivery are extremely complex processes dependent on red cell spacing, viscosity, hemoglobin concentration, other gases that bind heme proteins, and myriad other factors. Furthermore, both capillary density and cellular density are dynamic processes in marrow. Increased capillary density is initiated by localized hypoxia in marrow as elsewhere. Capillaries can also regress in normal and pathological responses. Local tissue pH also changes as a function of distance from a capillary source: At 10 micrometers away from a capillary with internal pH 7.4, pH falls to about 7.25 and at 30 micrometers, pH falls to about 7.1 (Martin and Jain, 1994). It is likely that pH and oxygen levels are tightly related in tissue, and pH may play an independent role in hematopoietic differentiation. In cell lines, erythroid differentiation is inhibited or slowed by low pH (McAdams et al., 1998).

In marrow, cellular density changes dramatically with response to physiologic stress, such as anemia (McClugage et al., 1971), with both hematopoietic cellular proliferation and fat proliferation. Cellular density in part determines oxygen utilization and therefore impacts local oxygen availability. Again, access to information about physiologic variation in cellular density and capillary density is limited by the bony surface. (Compare, for example, retina in which gross capillary density is directly visible on ophthalmoscopic examination.) So it is not surprising that little hard evidence about the gaseous microenvironment for hematopoietic stem cells exists.

Technical limitations are largely responsible for the lack of information about the gaseous environment inside bone. Noninvasive techniques give some information, but in general these techniques have not gained wide acceptance or are not applicable to marrow. For example, NITP, a nitroimidazole with a theophylline ligand, was developed to label hypoxic fractions of tumors (Hodgkiss et al., 1991). The drug is taken up by "hypoxic" cells and the theophylline ligand can then be labelled immunocytochemically. However, the drug is not absolutely specific for hypoxic (stressed) cells (Levin M et al.,

1999). Furthermore, in normal rats, as much as 15% of the marrow can take up this drug (Mortensen et al., 1998). When bone marrow is infiltrated by leukemic cells, the marrow environment becomes both acidic (by direct pH measurement) and increasingly "hypoxic" as assessed by NITP uptake. Successful treatment of the leukemia results in recovery of hematopoietic function, indirect evidence that stem cells in the marrow may be relatively insensitive to low oxygen levels (Mortensen et al., 1998).

Another new technique, oxygen-dependent phosphorescence quenching, has been better calibrated to actual high-accuracy electrode measurements of tissue oxygen levels (Lo et al., 1996). After injection of the phosphor probe, the tissue of interest is illuminated with flashes of light (630 nm), then emitted phosphorescence is imaged (Vinogradov et al., 1996). Unfortunately, this technique requires relatively transparent tissue for imaging of oxygen profiles (Torres Filho et al., 1994).

Electron paramagnetic resonance is also used to measure oxygen directly *in vivo*. This technology is based on changes in spectral patterns of paramagnetic probes to oxygen concentration, independent of local changes in pH

and redox status (Swartz et al., 1991). Regional measurements of marrow oxygenation have not been published with this technology.

Although the exact nature of the stem cell microenvironment in bone marrow (or elsewhere) has yet to be defined, tissue oxygen levels are likely to be closer to 2% than 20% oxygen, and this order of magnitude difference is rarely reflected in tissue culture models of stem cell regeneration. One group with long-term clinical marrow transplant experience estimates the marrow oxygen environment to vary between 1.3 to 6.6% (Smith and Broxmeyer, 1986) and has shown that culture of cord blood in low oxygen benefits in vitro hematopoiesis.

Hematopoietic stem cells are the only stems for which some attempt has been made to examine the influence of lower oxygen on maintenance and proliferation (see chapter 2). Although difficult to interpret because of the variety of culture conditions and additives, the different lineages assayed and the exact end-points of assay, there is some suggestion that low oxygen culturing may help to maintain marrow repopulating ability, and therefore may be a useful manipulation before bone marrow transplantation (Reykdal et

al., 1999; Ivanovic et al., 2000). Cytokine regulators of hematopoiesis may be more effective in the presence of physiologic oxygen in culture (vs. traditionally 20% oxygen) (Koller et al., 1992), but cytokine inhibitors of hematopoietic progenitor growth may also be more effective in physiologic oxygen levels (Broxmeyer et al., 1985). The major limitation of these and other studies demonstrating potential beneficial effects of low oxygen culturing on hematopoietic stem cells or progenitors is that they were not followed up with long-term transplantation studies (Bradley et al., 1978; Rich et al., 1982; Lu and Broxmeyer, 1985; Maeda et al., 1986; Pennathur-Das and Levitt, 1987; Broxmeyer et al., 1990; Cipolleschi et al., 1997; LaIuppa et al., 1998).

Outside of stem cell biology, low oxygen culturing has been used in the analysis of vasculogenesis/angiogenesis, a process known to be significantly regulated by oxygen levels surrounding the tissue. Yet, even when low oxygen is used for these purposes, the controls are cultures grown in aphysiologic, 20% oxygen (Tufro-McReddie et al., 1997). The results presented in this thesis make a strong case for considering the oxygen environment of in vitro disease models more carefully. Depending on the end-points of

analysis, cultures grown in 20% oxygen vs. mid-range physiologic oxygen vs. hypoxic conditions are all likely to have distinct patterns of message and protein expression patterns as well as overtly distinct behavior. Although not every parameter is changed by the oxygen environment, significant proliferative, cell death, fate choice, and gene expression pattern differences can be dramatically affected by oxygen levels. Physiologic gases, then, deserve a basic reconsideration as part of tissue culture models of regeneration.

REFERENCES

- Allalunis, M.J., Chapman, J.D., Turner, A.R. (1983). Identification of a hypoxic population of bone marrow cells. *Int. J. Radiat. Oncol. Biol. Phys.* **9**, 227-232.
- Allalunis-Turner, M.J. (1990) Reduced bone marrow pO₂ following treatment with radioprotective drugs. *Radiat. Res.* **122**, 262-267.
- Allalunis-Turner, M.J., Chapman, J.D. (1986). The in vitro sensitivities to radiation and misonidazole of mouse bone marrow cells derived from different microenvironments. *Int. J. Radiat. Biol. Relat. Stud. Phys. Chem. Med.* **49**, 415-422.
- Almeida-Porada, G., Flake, A.W., Glimp, H.A., Zanjani, E.D. (1999). Cotransplantation of stroma results in enhancement of engraftment and early expression of donor hematopoietic stem cells in utero. *Exp. Hematol.* **27**, 1569-1575.
- Bradley, T.R., Hodgson, G.S., Rosendall, M. (1978). The effect of oxygen tension on haemopoietic and fibroblast cell proliferation in vitro. *J. Cell. Physiol.* **97**, 517-522.

Broxmeyer, H.E., Cooper, S., Rubin, B.Y., Taylor, M.W. (1985). The synergistic influence of human interferon-gamma and interferon-alpha on suppression of hematopoietic progenitor cells is additive with the enhanced sensitivity of these cells to inhibition by interferons at low oxygen tension in vitro. *J. Immunol.* **135**, 2502-2506.

Broxmeyer, H.E., Cooper, S., Lu, L., Miller, M.E., Langefeld, C.D., Ralph, P. (1990). Enhanced stimulation of human bone marrow macrophage colony formation in vitro by recombinant human macrophage colony-stimulating factor in agarose medium and at low oxygen tension. *Blood* **76**, 323-329.

Carlesso, N., Aster, J.C., Sklar, J., Scadden, D.T. (1999). Notch1-induced delay of human hematopoietic progenitor cell differentiation is associated with altered cell cycle kinetics. *Blood* **93**, 838-848.

Chen, L.T., Chen, M.F., Porter, V.L. (1986). Increased bone marrow blood flow in rabbits with acute hemolytic anemia. *Am. J. Hematol.* **22**, 35-41.

Cipolleschi, M.G., D'Ippolito, G., Bernabei, P.A., Caporale, R., Nannini R., Mariani, M., Fabbiani, M., Rossi-Ferrini, P., Olivotto, M., Sbarba, P.D. (1997). Severe hypoxia enhances the formation of erythroid

bursts from human cord blood cells and the maintenance of BFU-E in vitro. *Exp. Hematol.* **25**, 1187-1194.

Donahoe, D.M., Gabrio, B.W., Finch, C.A. (1958).

Quantitative measurement of hemopoietic cells of the marrow. *J. Clin. Invest.* **37**, 1564-1570.

Grant, W.C., Root, W.S. (1947). The relation of O₂ in bone

marrow blood to post-hemorrhagic erythropoiesis. *Am. J. Physiol.* **150**, 618-620, 1947.

Hodgkess, R.J., Jones, G., Long, A., Parrick, J., Smith,

K.A., Stratford, M.R., Wilson, G.D. (1991). Flow cytometric evaluation of hypoxic cells in solid experimental tumours using fluorescence immunodetection. *Br. J. Cancer* **63**, 119-125.

Ivanovic, Z., Bartolozzi, B., Bernabei, P.A., Cipolleschi,

M.G., Rovida, E., Milenkovic, P. Praloran, V., Sbarba, P.D. (2000). Incubation of murine bone marrow cells in hypoxia ensures the maintenance of marrow-repopulating ability together with the expansion of committed progenitors. *Br. J. Haematol.* **108**, 424-429.

Iverson, P.O. (1997). Blood flow to the haemopoietic bone

marrow. *Acta Physiol.Scand.* **159**, 269-276.

Kiaer, T., Gronlund, J., Sorensen, K.H. (1988).

Subchondral pO₂, pCO₂, pressure, pH, and lactate in

human osteoarthritis of the hip. *Clin. Orthop.* **229**, 149-155.

Koller, M.R., Bender, J.G., Papoutsakis, E.T., Miller, W.M. (1992). Effects of synergistic cytokine combinations, low oxygen, and irradiated stroma on the expansion of human cord blood progenitors. *Blood* **80**, 403-411.

Lahtinen, R., Lahtinen, T., Romppanen, T. (1982). Bone and bone-marrow blood flow in chronic granulocytic leukemia and primary myelofibrosis. *J. Nucl. Med.* **23**, 218-224.

LaIuppa, J.A., Papoutsakis, T., Miller W.M. (1998). Oxygen tension alters the effects of cytokines on the megakaryocyte, erythrocyte, and granulocyte lineages. *Exp. Hematol.* **26**, 835-843.

Levin, M., Bjornheden, T., Evaldsson, M., Walenta, S., Wiklund, O. (1999). A bioluminescence method for the mapping of local ATP concentrations within the arterial wall, with potential to assess the in vivo situation. *Arterioscler. Thromb. Vasc. Biol.* **19**, 950-958.

Lo, L.W., Koch, C.J., Wilson, D.F. (1996). Calibration of oxygen-dependent quenching of the phosphorescence of Pd-meso-tetra (4-carboxyphenyl) porphine: a phosphor with general application for measuring oxygen

concentration in biological systems. *Anal. Biochem.* **236**, 153-160.

Lu, L., Broxmeyer, H.E. (1985). Comparative influences of phytohemagglutinin-stimulated leukocyte conditioned medium, hemin, prostaglandin E, and low oxygen tension on colony formation by erythroid progenitor cells in normal human bone marrow. *Exp. Hematol.* **13**, 989-993.

Maeda, H., Hotta, T., Yamada, H. (1986). Enhanced colony formation of human hemopoietic stem cells in reduced oxygen tension. *Exp. Hematol.* **14**:930-934.

Martin G.R., Jain, R.K. (1994). Noninvasive measurement of interstitial pH profiles in normal and neoplastic tissue using fluorescence ratio imaging microscopy. *Cancer Res.* **54**, 5670-5674.

McAdams, T.A., Miller, W.M., Papoutsakis, E.T. (1998). pH is a potent modulator of erythroid differentiation. *Br. J. Haematol.* **103**, 317-325.

McClugage, S.G. Jr., McCuskey, R.S., Meineke, H.A. (1971). Microscopy of living bone marrow in situ. II. Influence of the microenvironment on hemopoiesis. *Blood* **38**, 96-107.

Mortensen, B.T., Jensen, P.O., Helledie, N., Iversen, P.O., Ralfkiaer, E., Larsen, J.K., Madsen, M.T. (1998). Changing bone marrow micro-environment during

- development of acute myeloid leukaemia in rats. *Br. J. Haematol.* **102**, 458-464.
- Murphy, S.J., Song, D., Welsh, F.A., Wilson, D.F., Pastuszko, A. (1999). Regional expression of heat shock protein 72 mRNA following mild and severe hypoxia in neonatal piglet brain. *Adv. Exp. Med. Biol.* **471**, 155-163.
- Pennathur-Das, R., Levitt, L. (1987). Augmentation of in vitro human marrow erythropoiesis under physiological oxygen tensions is mediated by monocytes and T lymphocytes. *Blood* **69**, 899-907.
- Reykdal, S., Abboud, C., and Liesveld, J. (1999). Effect of nitric oxide production and oxygen tension on progenitor preservation in ex vivo culture. *Exp. Hematol.* **27**, 441-450.
- Rich, I.N., Kubanek, B. (1982). The effect of reduced oxygen tension on colony formation of erythropoietic cells in vitro. *Br. J. Haematol.* **52**, 579-588.
- Schoutens, A., Verhas, M., Dourov, N., Verschaeren, A., Mone, M., Heilporn, A. (1990). Anaemia and marrow blood flow in the rat. *Br. J. Haematol.* **74**, 514-518.
- Smith, S., Broxmeyer, H.E. (1986). The influence of oxygen tension on the long-term growth in vitro of

haematopoietic progenitor cells from human cord blood.

Br. J. Haematol. **63**, 29-34.

Swartz, H.M., Boyer, S., Gast, P., Glockner, J.F., Hu, H., Liu, K.J., Moussavi, M., Norby, S.W., Vahidi, N., Walczak, T., Wu, M., Clarkson, R.B. (1991).

Measurements of pertinent concentrations of oxygen *in Vivo*. *Magnet. Res. Med.* **20**, 333-339.

Tondevold, E., Erikson, J., Jansen, E. (1979).

Observations on long bone medullary pressures in relation to arterial pO₂, pCO₂ and pH in the anaesthetized dog. *Acta Orthop. Scand.* **50**, 645-651.

Torok-Storb, B., Iwata, M., Graf, L., Gianotti, J., Horton, H., Byrne, M.C. (1998). Dissecting the marrow microenvironment. *Ann. N. Y. Acad. Sci.* **872**, 164-170.

Torres Filho, I.P., Leunig, M., Yuan, F., Intaglietta, M., Jain, R.K. (1994). Noninvasive measurement of microvascular and interstitial oxygen profiles in a human tumor in SCID mice. *Proc. Natl. Acad. Sci.* **91**, 2081-2085.

Torres Filho, I.P., Kerger, H., Intaglietta, M. (1996). PO₂ measurements in arteriolar networks. *Microvasc. Res.* **51**, 202-212.

Tufro-McReddie, A., Norwood, V.F., Aylor, K.W., Botkin, S.J., Carey, R.M., Gomez, R.A. Oxygen regulates

vascular endothelial growth factor-mediated
vasculogenesis and tubulogenesis. *Dev. Biol.* **183**,139-
149.

Vinogradov, S.A., Lo, L.W., Jenkins, W.T., Evans, S.M.,
Koch, C., Wilson, D.F. (1996). Noninvasive imaging of
the distribution in oxygen in tissue in vivo using
near-infrared phosphors. *Biophys. J.* **70**, 1609-1617.

Chapter 2. A new satellite trajectory

Introduction

Satellites as stem cells. Skeletal muscle satellites are ubiquitous but rare mononucleate cells in adult human skeletal muscle. For many years, satellites were presumed to be the only source of regenerated postnatal skeletal muscle. Satellites were also assumed to be relatively homogeneous cells, destined only to become skeletal muscle when stimulated to exit their normal quiescent state. Satellite cells are considered stem-like, despite the assumption of monopotentiality, because of their large proliferative capacity, because they do not express skeletal muscle-specific transcription factors when quiescent (Cornelison and Wold, 1997), and because they are thought to self-renew (Beauchamp et al., 1999).

Self-renewal can imply population-level mechanisms to retain stem cell potency (a subset of stem cells is set aside to remain in a quiescent state or to generate other stem cells). These mechanisms of self-renewal do not necessarily imply asymmetric division of individual stem cells. At the population level, self-renewal implies that

some cells are functionally reserved which have the capacity to execute all the differentiation pathways of a particular stem cell. At the single cell (clonal) level, self-renewal implies asymmetric division into one daughter identical to the original stem cell and another more differentiated progeny.

Lessons from hematopoietic stem cells (HSC), much more extensively studied than satellite stem cells, highlight the difficulty in demonstrating self-renewal at either level. HSC may be heterogeneous with regard to self-renewal while maintaining the same differentiation potential. For HSC, functional self-renewal was demonstrated by long-term marrow reconstitution after transplantation of a single pluripotent stem cell (Osawa et al., 1996). Asymmetric division may or may not occur in this *in vivo* model. In theory HSC may first divide into other HSC which are reserved for future regeneration; the subsequent regeneration episodes follow the same pattern of symmetric division succeeded by differentiation from some pluripotent cells. Elegant time-lapse studies demonstrate asymmetric division of early hematopoietic progenitors (Huang et al., 1999), but still fall short of demonstrating asymmetric division of the HSC.

Tissue culture models for studying HSC self-renewal have been problematic: Over time, the cells generally lose their repopulating capacity (van der Loo, 1995), most likely because the environment that maintains stem cells *in vivo* cannot be completely replicated *in vitro*. Considerable effort has gone into mimicking the *in vivo* environment of HSC, for example by co-culture with stroma (Szilvassy et al., 1996) and/or addition of complex mixes of growth factors (Yagi et al., 1999). Stroma is critical in providing notch-jagged interactions that are involved in maintaining early progenitor populations (Varnum-Finney, 1998). Cytokines play complex permissive roles in hematopoiesis, and further, are modulated by the stromal environment. It may be possible to create a tissue culture model that replicates a marrow supportive of HSC survival, but the localized fluctuations in physiologic conditions likely to play a role in stem cell fate will be difficult to replicate. Microenvironmental physiologic fluctuations are cited as one basis for the stochastic model of HSC differentiation (Ogawa M, 1999).

By comparison to HSC, the demonstration of satellite stem cell self-renewal is even more indirect. In transplant

models of a single HSC, some self renewal is necessary to account for long-term repopulation of blood progenitors that are continually turned over. Skeletal muscle models of transplantation do not have the luxury of similar endpoints for analysis. Skeletal muscle is not normally continually turned over. Furthermore, in models of skeletal precursor transplants, the classical satellite identity of the transplanted cells is usually not established, largely for technical reasons. For example, skeletal muscle progenitors for transplantation are often derived by enzymatic digestion of muscle such that satellites are likely to be mixed in with other muscle cells and potentially other non-muscle (endothelial and blood) cells (Beauchamp et al., 1999 and Rando and Blau, 1997). Self-renewal in these models is assumed by the demonstration of a small population of transplanted cells that selectively survive, proliferate slowly in the immediate post-transplant period, but then contribute significantly to regenerated muscle (Beauchamp et al., 1999).

Other evidence for self-renewal of satellites derives from observations during development: Myonuclei increase in number dramatically but the number of satellite stem cells

stays relatively constant in developing rats (Gibson and Schultz, 1983). These numbers are based on microscopy of particular muscle subsets, which may or may not be statistically representative of all muscle populations. Models to induce continuous regeneration also suggest that satellites, at least functionally, self renew. Intramuscular injection of concentrated (0.75%), large volumes of bupivacaine (a commonly used local anesthetic) causes myonecrosis, and repeated injections into the same rat leg muscle at weekly intervals have been reported to cause a continuous regeneration cycle with regenerative capacity maintained over many such cycles (Sadeh et al., 1985). In light of recent findings that satellites or other skeletal muscle precursors (below) can be recruited from other-than-local muscle sources, self-renewal potential as the only explanation for these observations requires re-evaluation.

Satellites are not alone: Other sources of postnatal skeletal muscle regeneration. Recently, the demonstration that cells other than classical satellites can contribute to skeletal muscle regeneration raises new questions about relationship of satellites to these other potential stem cells. The demonstration of bone marrow derived muscle

progenitors may have been anticipated by muscle biologists who suggested that the number of resident satellite cells was below the number of committed myogenic progenitors (Grounds et al., 1992). Multipotent mesenchymal stem cells resident in murine bone marrow, that can differentiate into connective tissue, cartilage and bone, were demonstrated in marrow transplant studies after culture manipulation (Pereira et al., 1995). Stromal or bone marrow derived cells with chondrocyte, osteocyte, adipocyte and myoblast potential have been known, in fact, for decades (Prockop, 1997), but their functional *in vivo* myogenic potential was only recently demonstrated. Transplantation of marked bone marrow cells into mice with chemically damaged skeletal muscle (to induce differentiation) demonstrated that marrow-derived cells can also contribute to muscle regeneration (Ferrari et al., 1999). Whether these two populations of marrow-derived cells are the same (and the mesenchymal stem cells become restricted in culture), or whether the two populations are distinct, cannot be established from available data. (In fact there is considerable confusion about whether "mesenchymal stem cells" in marrow are indeed a uniform pluripotent population or whether multiple types of progenitors live in

marrow. Their identity independent of stroma which support hematopoietic stem cell growth is not yet clear.)

Functional myoblasts can also be explanted from murine dorsal aorta. These cells of paraxial mesoderm origin retain a rounded morphology (like satellites) in culture, and fuse to become myotubes when cultured in a muscle differentiation medium. They express MyoD, myf-5, desmin, MNF, c-Met and M-cadherin like satellites, but also express the endothelial/smooth muscle markers VEGF-receptor 2, α M-integrin, VE-integrin, β 3 integrin, P-selectin, PECAM and α -actin (De Angelis et al., 1999). Again the relationship of these cells to the bone marrow-derived myoblast/satellites is not clear. The cells have migratory potential, and so, may migrate to a protected marrow environment. These cells could also be endothelial-myoblast stem cells that are distinct both from satellite cells in muscle and from bone marrow-derived mesenchymal cells. However, the same sets of markers have not been examined in the various cell populations (marrow-derived myoblasts and aorta-derived myoblasts), nor has migration from aorta to marrow been followed. Such studies will be necessary to clarify the relationship between these non-satellite sources of

skeletal muscle and the classical muscle-associated satellites.

So though the somite was presumed to be the original source of adult satellite cells, the options have been expanded. Cells which traffic from aorta, marrow, the systemic circulation and skeletal muscle must now be considered potential sources of satellites.

Satellites may be pluripotent after all. Considerable excitement has been generated by reports that satellites may also be able to produce hematopoietic daughters. Jackson et al. reported that cells derived from minced adult murine skeletal muscle displayed remarkable hematopoietic stem cell potential (Jackson et al., 1999). However, the acknowledged weakness of this report was that the cells with hematopoietic stem cell potential were not tested for myogenic differentiation capability (Lemischka, 1999), and so are only assumed at this point to be satellite cells. Formally, the possibility that these are satellites distinct from the classical satellites intimately associated with muscle fibers or are other cells altogether (endothelial cells, perhaps) remains open. Nonetheless further support that muscle-derived cells have

hematopoietic potential was demonstrated when muscle preparations of sorted mononuclear cells were also demonstrated to have hematopoietic potential (Gussoni et al., 1999). Again the satellite identity of these cells was not established but these mononuclear cells undergo myogenic differentiation.

Central nervous system stem cells were also recently demonstrated to have hematopoietic potential (Bjornson et al., 1999) in transplantation experiments using mice transgenic for LacZ. Thus transplantation experiments, rather than clonal *in vitro* analyses, have been particularly successful in expanding our understanding of the repertoire of genetic programs that can be activated in stem cell populations. Culture systems, with progressive loss of potentiality, may be inherently limited in demonstrating these less well-used genetic programs, simply because they require so much time to be expressed. Or culture systems may not adequately replicate the normal environmental influences that preserve or promote pluripotency.

The reports of muscle stem cells that make blood and CNS stem cells that make blood raise the question of whether

all organ-specific stem cells have hematopoietic capacity. If an organ is to be properly reconstituted, after all, it requires a circulatory system to develop side by side with parenchyma. Or the hematopoietic programs may simply be remnants of development without significant functional physiologic input. Furthermore, it is possible that only a subset of CNS stems and muscle/mesenchymal stems have hematopoietic potential.

Reports of a "new" potential for stem cells allow a rethinking of approaches for analyzing how stem cells determine their differentiation fate. The muscle-blood common progenitor analysis will be facilitated by the well-characterized surface markers of hematopoietic stem cells. In this work, I observe cells with distinct adipocyte phenotype emerging from fibers in the normal position of skeletal muscle satellites. This observation may represent a new fate for satellites which has been anticipated by muscle biologists (Seale and Rudnicki, 2000). Mesenchymal stem cells derived from bone marrow can be induced to differentiate into adipocytes as well as myotubes (Wakitani et al., 1995). Various mesenchymal stem cell lines have multipotent capacity including adipocyte and skeletal muscle plus other daughter cell types (Taylor and Jones,

1979). Myoblast lines and myoblasts subjected to forced co-expression of the adipocyte differentiation factors PPAR γ and C/EBP α undergo adipogenesis (Hu et al., 1995). However, satellites resident in adult muscle fiber have to date only been determined to execute a muscle (and now, hematopoietic) fate. In our work, environmental influences (in this case high oxygen) may be facilitating the unmasking of a phenotype (fat) rather than influencing a true stem cell fate choice. Verification of the hypothesis that satellites can take at least two fates, muscle and fat, will require clonal analysis. Single cell tracing experiments done in vivo with retroviral markers have been powerful tools to analyze stem cell potential in a variety of other systems including CNS (Morshead et al., 1998). Clonal analyses in vitro have also been powerful tools to analyze stem cell potential in other systems including spinal cord (Kalyani et al., 1997) and keratinocyte stem cell proliferation (Kolodka et al., 1998).

The choice of daughter type by a stem cell is often attributed to microenvironmental influences (Seale and Rudnicki, 2000). The major environmental influences examined in regeneration fate choices are growth factors and cell-cell interactions (Torok-Storb et al., 1999). The

gaseous microenvironment has been largely ignored in tissue culture models of regeneration. In fact, virtually all cell culture is performed in a gaseous environment (20% oxygen) that exposes cells to high levels of oxygen completely out of physiologic range. Our results indicate that the oxygen environment is important in regulating both stem cell proliferation and the generation of specific daughter cell types. For satellite stem cells and mesenchymal stem cell lines, high oxygen enhances adipogenesis and physiologic oxygen levels in culture blunt this fate choice.

Satellite aging. The absolute number of satellites resident in skeletal muscle fibers is thought to diminish with aging in rodents and humans (Bischoff, 1994). A simplistic interpretation of this observation is that the pool of satellites established after skeletal muscle development is complete (about age 10 in humans) are gradually "used up" with sequential injuries to muscle. (An analogy is the apparent depletion of hepatocyte proliferative potential after massive hepatectomy and regeneration (Palmer et al., 1999). But newly regenerated skeletal muscle and its neighboring satellite donor muscle has not been systematically examined for satellite density over time.

In addition, satellites from different muscle groups may initiate regeneration and self-renewal in quantitatively different ways, and very few muscles (mostly rodent leg muscles) have been examined. Furthermore, localized satellite counts are only part of the story since some contribution to muscle regeneration is likely made by a circulating pool of cells from marrow, which may home selectively to only certain muscle groups.

Satellite proliferative potential also decreases with age in rodents (Schultz and Lipton, 1982). In muscle fibers, satellites are normally quiescent, located between the fiber plasmalemma and basal lamina (Schultz, 1976). In cultures of adult single muscle fibers, satellites are easily observed emerging from this fiber microenvironment, pulling basal lamina behind them, then completely breaking away from the fiber. This process mimics the migration of satellites across basal lamina during muscle development (Hughes and Blau, 1990) and during postnatal regeneration (Bischoff, 1997).

Tissue culture models of regenerative capacity of skeletal muscle suggest that aging is indeed associated with decreased regeneration potential or at least a regeneration

delay (Yablonka-Reuveni et al., 1999, and Lescaudron et al., 1997) though other transplant studies suggest that environment determined by host age is a major determinant of skeletal muscle regeneration potential (Carlson and Faulkner, 1989). As satellites age, they may lose the potential to respond to mitogens released locally by muscle fibers (in addition to an age-associated generalized growth factor decline), thus both arms of normal muscle paracrine responses are blunted with aging. Not surprisingly, skeletal muscle mass generally declines with age, and this aging-related atrophy is likely due to both satellite and myofiber changes.

Proliferation decreases with aging in many cell types including vascular smooth muscle (Ruiz-Torres et al., 1999), hepatocytes (Palmer et al., 1999), osteoblasts (Bergman et al., 1996), and fibroblasts (Cristofalo and Pignolo, 1993). The relationship between aging and loss of proliferative potential is based largely on tissue culture models and in culture, the relationship between proliferative potential and life-span is not that clear-cut. Without their normal environmental cues, cultured cells may differentiate or cycle more than they would *in vivo* (Bell et al., 1978). Furthermore, aged cells are subject to an aged environment

including profound hormonal changes such that cellular explants from aged animals may reflect systemic changes rather than intrinsic changes in cellular proliferative potential. Tissue culture models may be less able to clarify this distinction than transplant models.

A major hormonal influence on muscle aging is insulin-like growth factor-1, which is produced at maximal levels in puberty then circulating levels decline steadily thereafter (Hall et al., 1999). IGF-1 has multiple effects of skeletal muscle growth and development, differentiation, and hypertrophy and illustrates the complexity of analyzing satellite contributions to post-natal regeneration and muscle preservation. In culture systems IGF-1 induces both satellite proliferation and differentiation (Allen and Boxhorn, 1989). In fully differentiated cardiac and skeletal muscle, IGF-1 induces hypertrophy via calcineurin (Musaro et al., 1999), and prevents aging-related atrophy of muscle in mouse models. The mechanism by which IGF-1 prevents age-induced atrophy was attributed largely to satellite activation, based on interpretation of gross histologic changes after viral-mediated delivery of the hormone. However, some hypertrophy of skeletal muscle occurs in response to IGF-1 after satellite proliferation

is abrogated by irradiation (Barton-Davis et al., 1999). Increased fiber protein synthesis independent of satellite proliferation also contributes to IGF-1-induced muscle hypertrophy. Although satellites are not cited as part of this independent fiber response, they may well play a role in local production of survival or proliferative factors. For example, in single cell PCR analyses of satellites we found that many express vascular endothelial growth factor (below). A possible precedent for satellite involvement in fiber restructuring is bone formation: VEGF is expressed by chondrocytes, plays an important role in longitudinal bone growth, with VEGF receptors expressed on osteoblasts. The role of VEGF in bone growth is integrated with rather than confined to its role in local angiogenesis (Gerber et al., 1999).

More directly relevant to this work, longterm exposure to oxygen radicals plays an important role in the pathophysiology of aging in all cell types (Beckman and Ames, 1998). Largely post-mitotic tissues such as muscle and central nervous system may be most susceptible to accumulation of oxidative damage (Mecocci et al., 1999). Oxygen radicals are the necessary byproducts of normal cellular metabolism, particularly mitochondrial metabolism,

but also accumulate with radiation and chemical/xenobiotic exposure (Collins, 1999). The free radical theory of aging is supported by evidence that oxidative damage is cumulative with aging and that the usual defenses against oxidative stress (free radical scavenging and detoxification systems) are gradually diminished with aging.

RESULTS

Differentiation of mesenchymal stem cell lines into fat is oxygen dependent

Both 10T1/2 and 3T3 cells grown in standard laboratory incubator gas conditions (20% O₂, 5% CO₂) demonstrated significant adipocyte differentiation when exposed to standard differentiation paradigms. Differentiated adipocytes were easily identified by morphologic criteria (Figure 1A) or with oil red O staining (Figure 2A). However, adipocyte differentiation was markedly reduced when the same cells were grown in 6% O₂ (Figures 1B and 2B). Furthermore, 3T3 cells stained with antibody against the adipogenic nuclear receptor PPAR γ after a week in differentiation conditions revealed significantly more cells with distinct nuclear signals in 20% (Figure 3A) vs.

6% oxygen cultures (Figure 3B). In 20% O₂, 36.0% of the cells were α -PPAR γ positive and in 6% O₂, 12.1% of the cells were positive (Chi2=64, p<<0.001). Anti-myf5 staining after a week of differentiation revealed occasional cells with a myoblast appearance in 6% O₂ cultures (not shown). Surprisingly, the antibody also labelled many cells with a distinct adipocyte morphology under 20% O₂ conditions (Figure 4).

Human myoblasts can become adipogenic

Human myoblasts were expanded and serially passaged after reaching 60-80% confluence. Several attempts to induce terminal differentiation of these cells by culturing in 0.5%, 1% or 2% horse serum (with and without added insulin and dexamethasone) failed to induced myotube formation. After the cells were confluent for several weeks in culture, they were still able to re-enter the cell cycle and proliferate when passaged. After 4 or more weeks in culture in 20% O₂, occasional adipocytes were seen in the cultures, confirmed by oil red O staining (Figure 5). Parallel 6% O₂ cultures did not reveal adipocytes, but the conversion in 20% O₂ was a rare event.

Adult murine satellites are adipogenic

After a week in culture at either 6% or 20% O₂, single muscle fibers were stained with oil red O to identify adipocytes. In 20% O₂ conditions, adipocytes were intensely stained in an anatomic location that suggested that they were satellite cells (Figure 6). In 6% O₂ conditions, some adipocytes were similarly identified but they were significantly less frequent on gross examination. Because of the formal possibility that these cells could represent adipocytes that had adhered to the fiber, single fibers were plated on Matrigel, such that all cells which migrated from the fiber were captured on the coating. The fibers were scanned by eye twice daily. After a week in 20% O₂ cultures, clear adipocytes were seen emerging from the fiber, still adherent to the fiber basal lamina (Figure 7). Two of 24 such fibers that survived for a week in 20% O₂ had apparent adipocytes emerging from the fiber, and none of 24 fibers cultured in 6% O₂.

When these single fiber preparations were grown for about 2 weeks, 20% O₂ cultures had prominent fat cells scattered over the culture plate (Figure 8A) whereas 6% O₂ cultures contained few (Figure 8B) or extremely rare (Figure 8C) adipocytes.

Mrf expression in individual satellites from adult muscle fibers

Single-cell PCR was used to determine the frequency of expression of individual mrf family genes in cultured satellites at 24, 48, and 96 hours after culture in either 6% or 20% O₂. The percentage of cells expressing these genes over time is shown in Table 1 below. At 24 hours, all four mrf's were more likely to be expressed in satellites grown in 6% than in 20% O₂. At that time 13% of the cells grown in 6% oxygen expressed three mrf's simultaneously vs. 6% of the cells in room air cultures (p<0.05). By 96 hours in culture, the satellites grown in 20% O₂ were more likely to express mrf4 and myf5 than those grown in 6% O₂.

Table 1. Expression of individual mrf genes in single adherent skeletal muscle satellite cells in single fiber cultures. Data for each gene in a cell from cultures at either 6 or 20% oxygen are expressed as the percentage of satellite expressing the gene (raw data in parentheses).

		<u>24 hr</u>	<u>Chi²</u>	<u>p value</u>
MyoD	20%	52 (24/46)	4.25	<0.05
	6%	72 (43/60)		
mrf4	20%	4 (2/46)	0.02	ns
	6%	5 (3/60)		
myf5	20%	24 (11/46)	6.61	<0.03
	6%	48 (29/60)		
mgn	20%	15 (7/46)	1.52	ns
	6%	25 (15/60)		
		<u>48 hr</u>	<u>Chi²</u>	<u>p value</u>
MyoD	20%	81 (21/26)	2.01	ns
	6%	92 (28/30)		
mrf4	20%	23 (6/26)	1.77	ns
	6%	10 (3/30)		
myf5	20%	58 (15/26)	0.01	ns
	6%	55 (17/30)		
mgn	20%	16 (4/26)	3.21	ns
	6%	35 (11/30)		

Table 1, cont. Expression of individual mrf genes in single adherent skeletal muscle satellite cells in single fiber cultures.

		<u>96 hr</u>	<u>Chi²</u>	<u>p value</u>
MyoD	20%	71 (39/55)	2.71	ns
	6%	84 (43/51)		
mrf4	20%	52 (29/55)	8.20	<0.005
	6%	25 (13/51)		
myf5	20%	35 (31/55)	4.72	<0.05
	6%	35 (18/51)		
mgn	20%	61 (34/55)	0.09	ns
	6%	65 (33/51)		

An alternative approach to analysis of the single cell data is to look at the distribution of the 15 possible combinations of mrf expression:

Table 2. mrf expression pattern combinations in individual adherent satellite cells from single fiber cultures over time in 6% or 20% cultures.

	24-20%	24hr-6%	48-20%	48-6%	96-20%	96-6%
	(n=46)	(n=60)	(n=26)	(n=30)	(n=55)	(n=51)
<u>mrf</u> s						
4	0	0	0	0	2	0
5	0	0	0	1	1	2
D	3	4	3	5	4	7
G	3	2	1	0	4	1
4+5	0	0	0	0	0	0
4+D	0	0	0	0	2	0
4+G	0	1	0	0	0	0
5+D	2	6	1	5	2	2
5+G	0	0	0	0	0	0
D+G	1	0	0	3	2	7
4+5+D	0	1	0	0	1	0
4+5+G	0	0	0	0	1	0
5+D+G	0	2	0	2	3	1
4+D+G	0	1	0	0	1	3
4+5+D+G	0	0	0	1	6	5

These data, in a general way, recapitulate the temporal expression patterns of mrf's during embryonic development, with early expression of myf5 and MyoD most prominent and mrf4 and myogenin expression delayed. In addition, when only two mrf genes are expressed, a pairing of one early and one late gene is unlikely. Myf5 and mrf4 are not expressed together as the only two mrf's in any cell, and myf5 and myogenin are also never similarly paired.

The absence of myf5 expression in many satellites early during regeneration is somewhat unexpected because myf5 is prominently expressed in early somitic myogenesis (Ott et al., 1991) and in postnatal models of regenerating muscle (Cooper et al., 1999). Variability in myf5 expression in satellites just emerging from adult cultured fibers was confirmed at the protein level by observation of similar fibers obtained from a myf5-LacZ knock-in mouse (courtesy of Dr. Margaret Buckingham). Emerging satellites that did not stain for LacZ were seen throughout culture (Figure 9). Furthermore, satellite pairs in which one cell stained for LacZ and the other did not were also common (Figure 10).

Occasional asymmetric expression patterns in apparent satellite pairs were also seen for myogenin using immunohistochemistry (Figures 11 and 12).

Satellite cell and myoblast proliferation are enhanced in 6% vs. 20% O₂ cultures

Because differentiation and cell cycling are coordinately regulated, proliferation of satellites and myoblasts in lowered vs. 20% O₂ conditions was examined using BrdU uptake and labeling. Human myoblasts in these experiments were grown in 2% O₂ or 20% O₂. After a BrdU pulse of 3.5 hr, 3.5% of the myoblasts grown in 20% stained with ^3H -BrdU vs. 10.3% of the cells in low oxygen ($\text{Chi}^2=9.73$, $p<0.005$). After a 25 hr BrdU pulse, 26.6% of myoblasts grown in 20% O₂ were BrdU-positive vs. 64.1% of myoblasts grown in 2% O₂.

Proliferation of satellites in single muscle fiber cultures was similarly enhanced in 6% vs. 20% O₂ conditions (Table 3). At each 12-hour interval in culture over the first three days, more proliferating satellites were present on fibers cultured in 6% than 20% O₂. The greatest statistical difference in proliferation between the two oxygen conditions was in the first 24 hours in culture.

Table 3.

BrdU-positive adherent satellites per unit length of cultured fiber after serial 12-hour BrdU pulses. Data were not normally distributed, and are expressed as median with range in parentheses. Comparisons between oxygen conditions were made using Mann-Whitney U testing.

Time of BrdU pulse	<u>BrdU+cells/U length</u>		conf. Interval	p value
	20% O ₂	6% O ₂		
0-12	0	rare		
12-24	0.6 (0-1.1)	1.6 (1.1-4.0)	95.1% (0.6-1.4)	0.0001
24-36	0.4 (0-1.8)	1.2 (0-3.2)	95.6% (0-2.7)	0.056
36-48	2.8 (0-14.0)	4.0 (0-28.0)	95.1% (-0.4->4.0)	0.20
48-60	2.0 (0-10.0)	6.0 (1-16.0)	95.0% (0-6.0)	0.009

Survival of single skeletal muscle fibers in culture is greater in 6% vs. 20% O₂.

Survival of single adult muscle fibers was assessed in both floating cultures and in single fiber assays with the individual fibers adherent to Matrigel. For floating

cultures, 5 fibers were transferred into each well of a 24-well Primaria plate after isolation, and were scored daily for live vs. dead fibers. After 48 hr in floating culture, 70% of the fibers were alive in 6% O₂ vs. 31% alive in 20% O₂ (n=80, Chi²=24.03, p<<0.001). After 10 days in 6% O₂, 30% of the fibers were still alive vs. only 5% in room air cultures (n=80, Chi²=17.32, p<<0.001). Among single adherent fibers after 48 hr in 6% O₂, 74% of the fibers were alive (n=72) vs. 22% in room air (n=96, Chi²=44.68, p<<0.001).

DISCUSSION

The optimal oxygen concentration for skeletal muscle regeneration cannot be determined from our data. Oxygen levels significantly above and significantly below physiologic norms can induce production of reactive oxygen species. It is likely, then, that optimal culture conditions will be close to physiologic norms, but further oxygen dose-response curves in specially constructed laboratory facilities will be necessary to determine the best gas conditions for satellite growth and differentiation. Physiologic norms for skeletal muscle vary over a fairly wide range. In adult mice, one group

estimated skeletal muscle tissue oxygen levels at 3.3% using both microelectrode and EPR measurements (Goda et al., 1997). In anesthetized rats, crural muscle O₂ was 2.5% (Seekamp et al., 1997) and cremasteric muscle 4.7% (Kunert et al., 1996). In anesthetized dogs, mean skeletal muscle oxygen tension has been reported at 3.7% (Hutter et al., 1999), 4.0% (McKinley et al., 1998) and 5.5% (McKinley and Butler, 1999). In resting rabbit anterior tibialis muscle, mean O₂ is 2.4% but varies widely depending on electrode placement in the muscle from 1.8-10.5% (Greenbaum et al., 1997). In adult human extremities normal skeletal muscle (specific muscle not specified) tissue O₂ has been estimated at about 3.1% (Seekamp et al., 1995). In human anterior tibialis at rest pO₂ has been measured at 2.1% (Heinrich et al., 1987) and 2.5% (Evers et al., 1997), and 5.0% (Kunze, 1976). Newer methods of measuring intracellular muscle oxygen such as phosphorescence quenching appear to work well in skeletal muscle (Hogan, 1999), but have not yet been used to report normal physiologic levels.

The direct observation of satellite stem cells apparently emerging from adult skeletal muscle and assuming an adipocyte phenotype is novel. Several reasons why this

observation has not been made before may relate to technical details of the culture systems. In floating single muscle fiber preparations, the adherent cells that stained with oil red O as they emerged from the fiber were grossly indistinguishable from other satellites. Partly because these small, early-emerging cells have a grossly uniform appearance, they have been presumed to be myogenic (only) precursors. Furthermore, single fiber preparations are often maintained for less than a week or are prepared from rat rather than mouse (Yablonka-Reuveni and Rivera, 1994) and adipogenesis was a late phenomenon in our cultures. Direct observation of adherent single fibers was necessary to indisputably catch adult satellites in the act of adipogenesis. These particular assays are not common, but when done, the fibers may be isolated from younger mice than those used in this study (Rosenblatt et al., 1996).

The pattern of oil red O staining in the cultured single fibers suggests that the stained fat was not a function of fatty degeneration of the fiber, as reported in muscular dystrophies (Bachmann, 1996). Staining was confined to cells which appeared to be emerging from the fiber (or were perhaps adherent to the fiber), and was never seen in myonuclei or the body of the fiber itself. Furthermore,

degenerating fibers stained with the same cellular/satellite pattern as live fibers.

Adipogenesis from satellites has been anticipated by previous work. Adipocyte transdifferentiation of a myoblast cell line was induced by forced co-expression of the adipogenic factors PPAR γ and C/EBP α (Hu et al., 1995). Ectopic expression of either PPAR γ or C/EBP α alone in these cells inhibited myogenesis but did not induce adipogenesis. Treatment of the C2C12 myogenic cell line with thiazolidinedione (a high affinity ligand for PPAR γ) and fatty acids induced adipogenesis. Furthermore, primary myoblasts/satellites isolated from newborn mice (satellite identity was not formally established) exposed to the same treatment also became adipogenic, but this phenomenon could not be replicated in vivo (Hallakou et al., 1998).

Future plans include analysis of these cells for expression of developmental regulators of adipogenesis as well as for other regulators of muscle differentiation. During human fetal development, adipocytes are not seen on pathologic sections until the second trimester. At that time the primitive fat lobules are organized in groups with early

vascular cells. Areas of proliferation of the vascular cells appear to mark areas in which adipocyte proliferation will soon follow (Poissonnet et al., 1983). Foci of fat development appear in various parts of the body (head first) starting as early as week 14 of development. Animal surgical work demonstrates that the morphogenetic link between vasculogenesis and adipogenesis is maintained in adult animals (Roth et al., 1981). Based on pathologic observations of mammary gland development, the immature ends of early mammary ducts may be hypoxic, which initiates a vasculogenic response followed by accumulation of capillaries and adipocytes around mature mammary ducts (Hausman, 1982). Adipocytes and capillaries may share a common precursor, at least in mammary gland: Cultured mammary stromal cells can differentiate into either adipocytes or capillary structures (Zangani et al., 1999). Furthermore, leptin, one of the few secreted products of adult fat cells, is angiogenic (Bouloumie et al., 1998).

Transcriptional control of adipogenesis is dominated by two gene families, C/EBP's (CCAAT/enhancer binding proteins are bZIP transcription factors) and PPAR's (peroxisome proliferator-activated receptor family of nuclear hormone receptors). Both families contribute not only to adipocyte

development and differentiation, but also to adipocyte metabolism and energy homeostasis after fat cell maturation (Fruchart et al., 1999; Wang et al., 1995). Furthermore, throughout adipocyte differentiation the two families mutually cross-regulate (Mandrup and Lane, 1997; Wu et al., 1999), in addition to the basic time course of transcriptional events described below.

The most important early transcriptional regulators of adipogenesis are C/EBP α , C/EBP β and the bHLH/leucine zipper transcription factor ADD1/SREBP1. PPAR γ is expressed in low abundance during early in vitro adipogenesis. Although ADD1/SREBP1 can independently induce adipogenesis in permissive cells, it also plays a role in adipogenesis by inducing transcriptional activation of PPAR γ /RXR α heterodimers (Kim and Spiegelman, 1996). PPAR's act with retinoid X receptors as heterodimers to activate transcription on target genes containing PPRE response elements (Ijpenberg et al., 1997). Similarly, C/EBP β and C/EBP δ work in part by inducing expression of PPAR γ and C/EBP α .

A critical component of adipocyte differentiation is coordinated control of cell cycle exit. In vitro quiescent preadipocytes are characterized by E2F binding predominantly to the Rb-related protein p130. Just before differentiation, a round of mitosis is initiated, and E2F becomes bound predominantly to p107 (Richon et al., 1997). E2F transcription factors play a complex regulatory role in cell cycle progression and in many differentiation pathways (DeGregori et al., 1995). pRB (retinoblastoma protein) in turn controls the transition from G1 to S by repressing E2F. In adipocytes Rb may play a role opposite of its usual function, by interacting with C/EBP's to promote adipocyte terminal differentiation (Chen et al., 1996). However, transactivation of PPAR γ is not dependent on pRB (Hansen et al., 1999).

In preadipocytes, PREF-1 (preadipocyte factor) is an important negative regulator of adipocyte differentiation (Smas and Sul, 1993). PREF-1 is similar to delta-like and secreted dlk variants functionally substitute for PREF-1 in adipocyte differentiation suppression (Garces et al., 1999).

Late transcriptional mediators of terminal differentiation are C/EBP α and PPAR γ 2. (PPAR γ 1 is widely expressed whereas

PPAR γ 2 expression is adipocyte specific.) Shortly after activation of these genes, the adipocyte specific genes such as leptin, adiponectin, and angiotensinogen are expressed.

This outline of adipogenesis points out some but not all features shared in common with skeletal myogenic pathways. C/EBP family members, like bHLH family members involved in myogenesis, have DNA binding domains as well as domains that mediate homo- and heterodimerization. Thus the functional overlap of C/EBP in adipogenesis is similar to the functional overlap of myogenic bHLH factors in myogenesis, related to their ability to interact dynamically with each other and with other partners. Furthermore, Id family members, HLH transcription factors, are negative regulators of both myogenesis and adipogenesis. Id proteins (particularly Id2 and Id3) interact with ADD1/SREBP1 to negatively regulate both adipogenesis and later expression of adipocyte terminal differentiation markers partly under the control of ADD1/SREBP1 (Moldes et al., 1999).

The "master regulator" genes of both adipogenesis and myogenesis have independent cell cycle regulatory effects. MyoD is an inhibitor of cell cycling (Crescenzi et al.,

1990) through interaction with multiple cell cycle regulators (Skapek et al., 1995; Zhang et al., 1999; Cenciarelli et al., 1999). Similarly PPAR γ inhibits cycling by dramatically decreasing DNA binding of E2A/DP complexes (Altiok et al., 1997).

Both pathways use the transcriptional coactivator p300. In myogenesis p300 interacts with MyoD to enhance muscle differentiation (Sartorelli et al., 1997). PPAR γ was recently reported to interact with p300 as well, such that docking of PPAR γ to its DNA binding site is part of a process that traps p300 to enhance transcription from that site (Puigserver et al., 1999). In the context of this work, it should be noted that p300 is induced under hypoxic conditions (Arany et al., 1996) and plays an important role in regulating HIF-1 α function under hypoxic conditions (Carrero et al., 2000).

Finally overlapping growth factors including IGF-1 and PDGF induce proliferative responses in both muscle and adipocyte precursors (Butterwith et al., 1991). Furthermore, IGF-1 induces similar signal transduction pathways in myoblasts and adipocytes (Petley et al., 1999).

The data presented here indicate that high oxygen conditions support a "spontaneous" adipocyte phenotype in adult satellites as well as mesenchymal stem cell lines and human myoblasts. Low oxygen culturing (2.5% O₂) was reported to increase myogenesis in 5-azacytidine-treated 10T1/2 cells (Storch, 1990) as assessed by counting of unstained myocytes. No mention of adipocytes is made in this report.

The high levels of oxygen implied by usual laboratory conditions (20%) are never encountered by cells *in vivo* such that usual culture conditions may actually represent oxygen-toxic levels. Thus, "spontaneous" differentiation of adipocytes from satellites may be initiated by pathologic responses to aphysiologically high oxygen levels in cell culture. One hypothesis to explain these findings is that usual laboratory conditions are associated with high levels of oxidative activity from reactive oxygen intermediates (Tanaka et al., 1998). Oxidative stress may in turn selectively activate and inhibit a variety of transcriptional pathways (Adler et al., 1999).

Aphysiologic, high oxygen standard cultures may, in fact, mimic the cumulative free radical damage associated with cellular aging (Beckman and Ames, 1998) rather than adequately reflecting the microenvironment in which normal development takes place. Furthermore, the reactive oxygen species can independently promote proliferation in 3T3 (Shibanuma et al., 1990) and other cells. Mn-superoxide dismutase (antioxidant) overexpression in 3T3 cells inhibits cell cycling (Li et al., 1998). Antioxidant defenses in skeletal muscle are developmentally regulated, and differentiated myotubes may be more susceptible to oxidative stress than undifferentiated myoblasts (Franco et al., 1999). Furthermore, humans accumulate markers of oxidative DNA damage, lipid peroxidation and oxidative damage to proteins in skeletal muscle as they age (Mecocci et al., 1999). Pro-oxidants may also independently promote differentiation in some cells (Chenais et al., 2000). Glycation of proteins followed by oxidation in the presence of transition metals produces superoxide radicals in a variety of cells (Loske et al., 1998). In mesangial cells such advanced glycation end products induces expression of PPAR γ , and antioxidants block this response (Iwashima et al., 1999). Thus, specific pathways related to adipogenesis may be affected in satellites by perturbations

in environmental oxygen sufficient to induce oxidant stress.

The pattern of decreased proliferation of satellites in the 20% oxygen conditions also parallels the decreased proliferative potential or delay in proliferation characteristic of aging satellites (Yablonka-Reuveni et al., 1999). Nonetheless, differences in gene expression patterns in satellite cells exposed to low or 20% oxygen conditions may yield clues to the determinants of myogenesis vs. adipogenesis differentiation choice.

The oxygen-influenced adipogenic potential of satellites may also be related to the decreased survival of fibers in 20% oxygen conditions, and pathways that are induced as the fibers die. In addition, the increased rate of proliferation of satellites in 6% vs. 20% O₂ conditions may play a role in the differentiation fate choice. Satellite cell activation after muscle injury is thought to be initiated by growth factors released from traumatized muscle and from surrounding matrix. Another possibility for the effect of oxygen in promoting satellite proliferation, then, is that some mitogens may function

more efficiently in physiologic rather than hyperoxic conditions (Nurse and Vollmer, 1997).

Single satellite cell PCR analysis of the major myogenic transcription factors suggested that expression of these factors may be affected by the oxygen environment. Early in culture, the fraction of satellites that expressed myogenic bHLH factors in 6% O₂ was greater than that in 20% O₂. Taken together with the morphologic observations, these results suggest that early expression of multiple mrf's in satellites may be associated with less diversion to adipogenesis. This interpretation of the results is in accord with the vast amount of data from knockout studies of myogenic bHLH genes: Their complex, mutually compensatory roles suggest that a critical threshold level of combinations of these genes is necessary to activate muscle differentiation (Arnold and Winter, 1998).

Later in culture, single satellite PCR analysis revealed that myf5 (and mrf4) were more likely to be expressed by satellites exposed to 20% vs. 6% O₂. Furthermore, myf5 protein was detected in adipocytes generated from mesenchymal stem cells in 20% oxygen. Myf5 expression has not been previously reported in adipocytes, but its

expression is not limited to skeletal muscle. Myf5 is transcribed normally in differentiated embryonic neurons, but myf5 protein cannot be detected simultaneously in brain regions where transcript is found (Daubas et al., 2000). However, when these same neurons are cultured, myf5 protein can be induced. One explanation for these findings which was not discussed by the authors of this report is that the high oxygen conditions associated with traditional cultures may play a role in the post-transcriptional regulation of myf5. Oxygen-regulated stability of proteins is not unprecedented. Hypoxia-inducible factor 1alpha contains an oxygen dependent domain of about 200 amino acids that mediates its proteasomal breakdown when oxygen is abundant (Huang et al., 1998), but the protein is stable in low oxygen conditions. Furthermore, oxidative stress can induce proteasomal breakdown of some proteins (Ullrich et al., 1999).

In summary we present direct observation of an expanded phenotypic repertoire for the adult muscle satellite. Satellites can express an adipogenic phenotype and expression of this phenotype is significantly affected by the oxygen environment. Traditional culture in 20% oxygen is associated with increased adipocyte appearance on

skeletal muscle in a characteristically satellite location. Similar patterns of oxygen-influenced adipocyte appearance were observed in mesenchymal stem cells and human myoblasts. These data suggest that the gaseous environment surrounding satellite can be used as a tool to dissect patterns of phenotype decisions.

Figure legends**Figure 1**

- A. 10T1/2 fibroblasts differentiated in 3 μ M 5-azacytidine in 20% O_2 for 9 days. Numerous adipocytes are seen in all fields.
- B. Parallel cultures grown in 2% O_2 showing no adipocyte phenotype after 9 days in differentiation conditions.

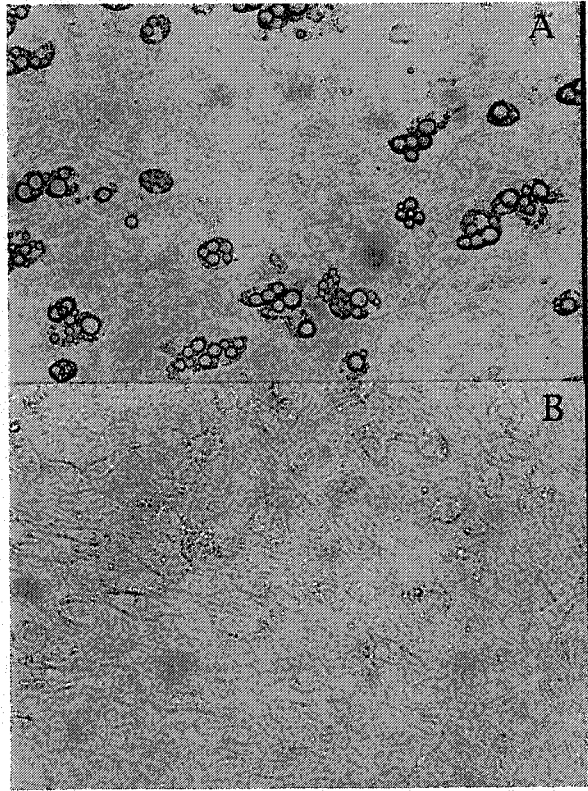


Figure 1.

Figure 2.

- A. 3T3 cells differentiated for 1 week in insulin, dexamethasone, and isomethylbutylxanthine in 20% O₂, then stained for the presence of adipocytes with oil red O. Prominent adipocyte development was seen throughout the culture plates.
- B. Parallel 3T3 cultures differentiated as above but grown in 2% O₂, and stained with oil red O. Most fields contained no adipocytes.

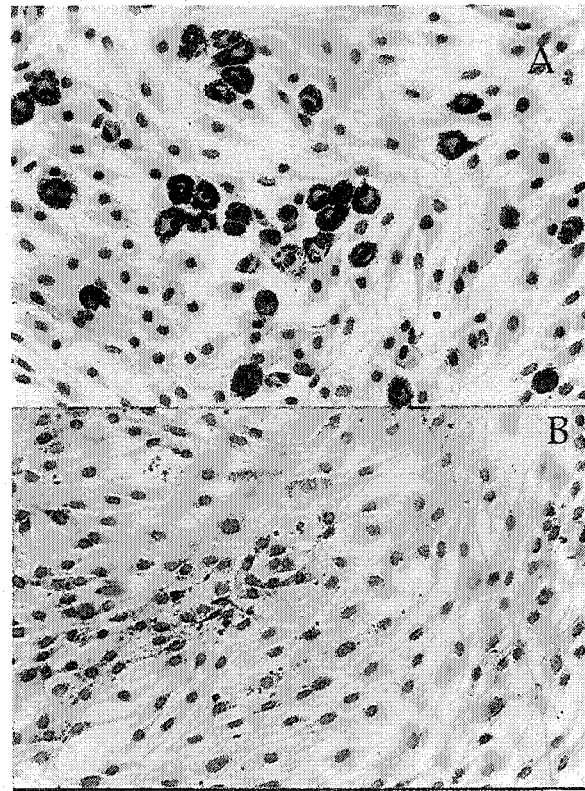


Figure 2.

Figure 3.

- A. 3T3 cells stained with α -PPAR γ after one week of differentiation in 20% O₂, with paired DAPI stain. A nuclear PPAR γ signal was seen in 35% of the cells.
- B. 3T3 cells stained with α -PPAR γ after 1 week of differentiation in 6% O₂. A nuclear signal was detected in 12% of cells.

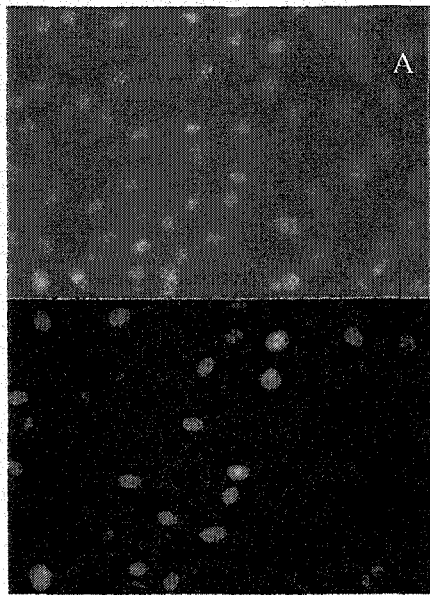


Figure 3A.

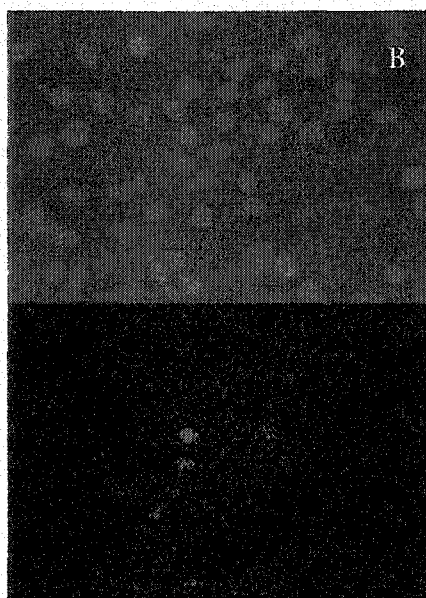


Figure 3B.

Figure 4.

3T3 cells differentiated for 1 week in 20% O₂, stained with α -myf5 antibody. Fluorescent cells characteristically contained large unstained areas in cytoplasm and appeared to be adipocytes.

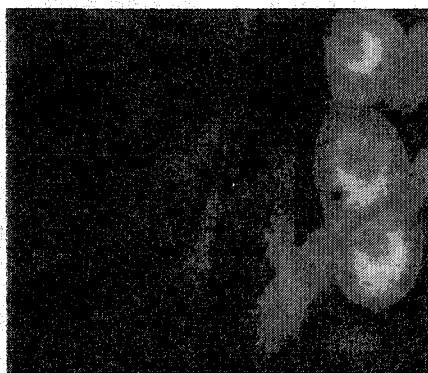


Figure 4.

Figure 5.

Adult human myoblasts cultured in 20% oxygen for one month, then stained with oil red O. Occasional adipocytes were identified.



Figure 5.

Figure 6.

Single adult mouse muscle fiber maintained in floating culture for 1 week in 20% O₂, stained with oil red O. Cells which appear to be emerging satellites stained prominently.

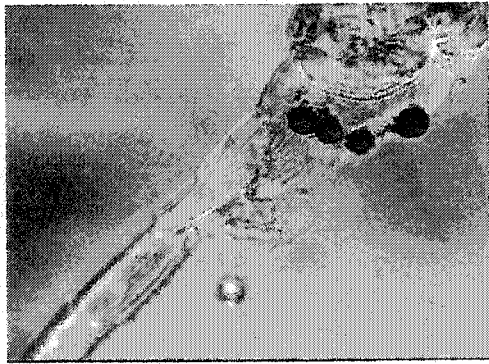


Figure 6.

Figure 7.

Single adult skeletal muscle fiber grown for 8 days on Matrigel in 20% O₂. Several cells emerging from the fiber, with basal lamina still adherent, have adipocyte morphology.

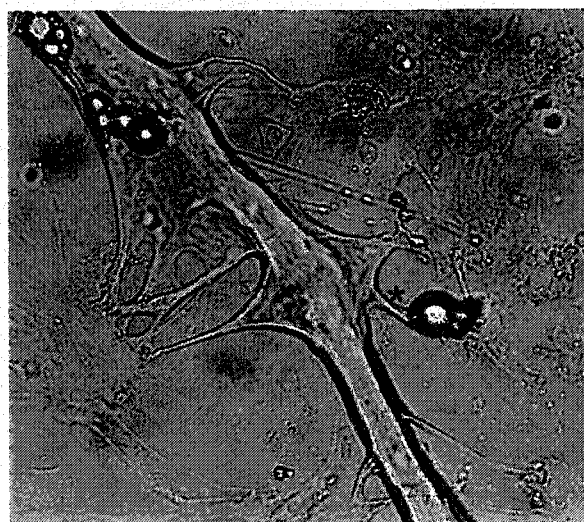


Figure 7.

Figure 8.

- A. Single murine skeletal muscle fiber grown on Matrigel for 2 weeks in 20% O₂. About 50% of the cells on the plate are adipocytes based on gross morphology.
- B. Single murine skeletal muscle fiber grown on Matrigel for 2 weeks in 6% O₂. Fewer adipocytes are present compared to 20% O₂ cultures.
- C. Single fiber grown on Matrigel for 2 weeks in 6% O₂. Very few adipocytes are present.

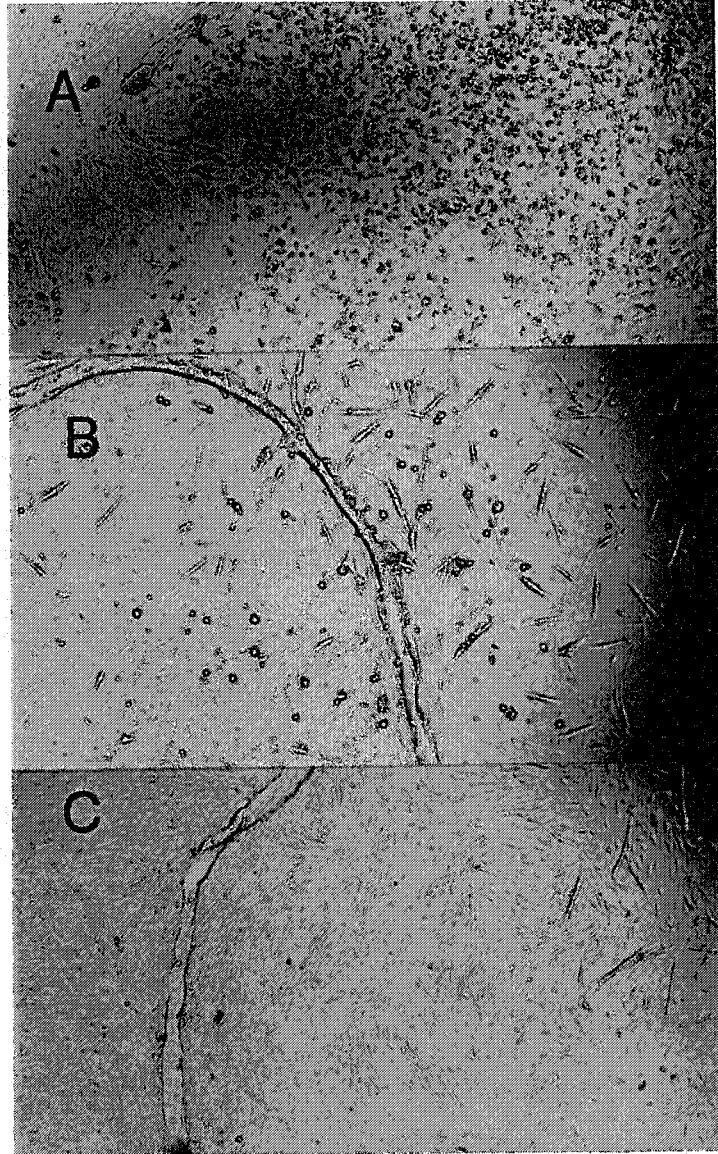


Figure 8.

Figure 9.

A. Cultured single adult skeletal muscle fiber from a myf5-LacZ knock-in mouse after 48 hours in culture in 6% oxygen. X-gal staining reveals multiple stained myonuclei. An emerging satellite pair (basal lamina still attached) (*) does not stain for LacZ.

B/C. Satellite pair (*) (two nuclei by DAPI staining, C) emerging from a myf5-LacZ knock-in fiber after two weeks in culture in 6% oxygen. X-gal staining reveals LacZ in several myonuclei but the emerging satellites are negative.

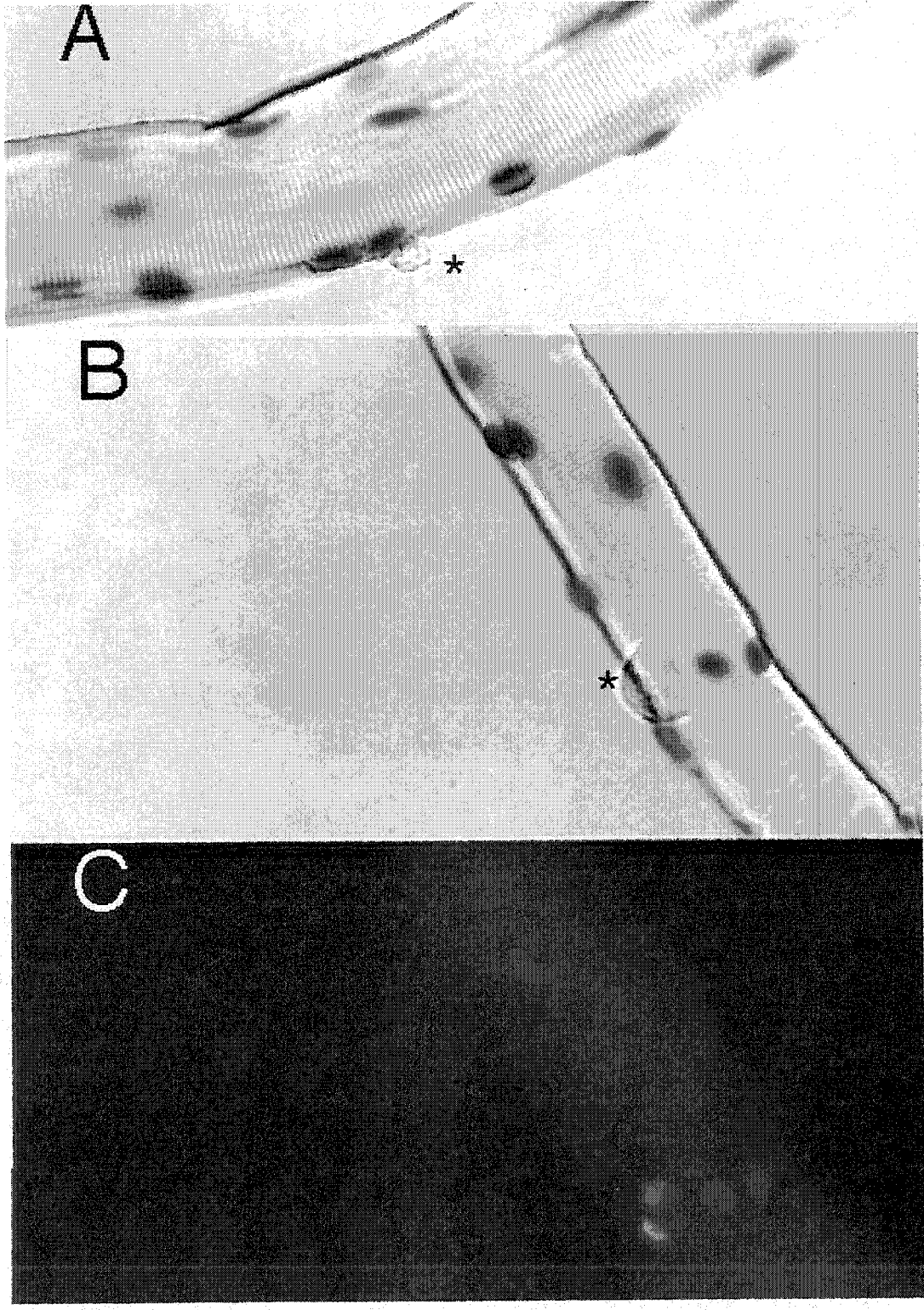


Figure 9.

Figure 10.

- A. Single adult skeletal muscle fiber from a myf5-LacZ knock-in mouse stained for LacZ after 48 hours in culture in 6% oxygen. An emerging satellite pair contains one intensely stained cell and one cell without LacZ expression.
- B. Single adult skeletal muscle fiber from a myf5-LacZ knock-in mouse stained for LacZ after 2 weeks in culture in 20% oxygen. An emerging satellite pair contains one intensely stained cell and one cell without LacZ expression.

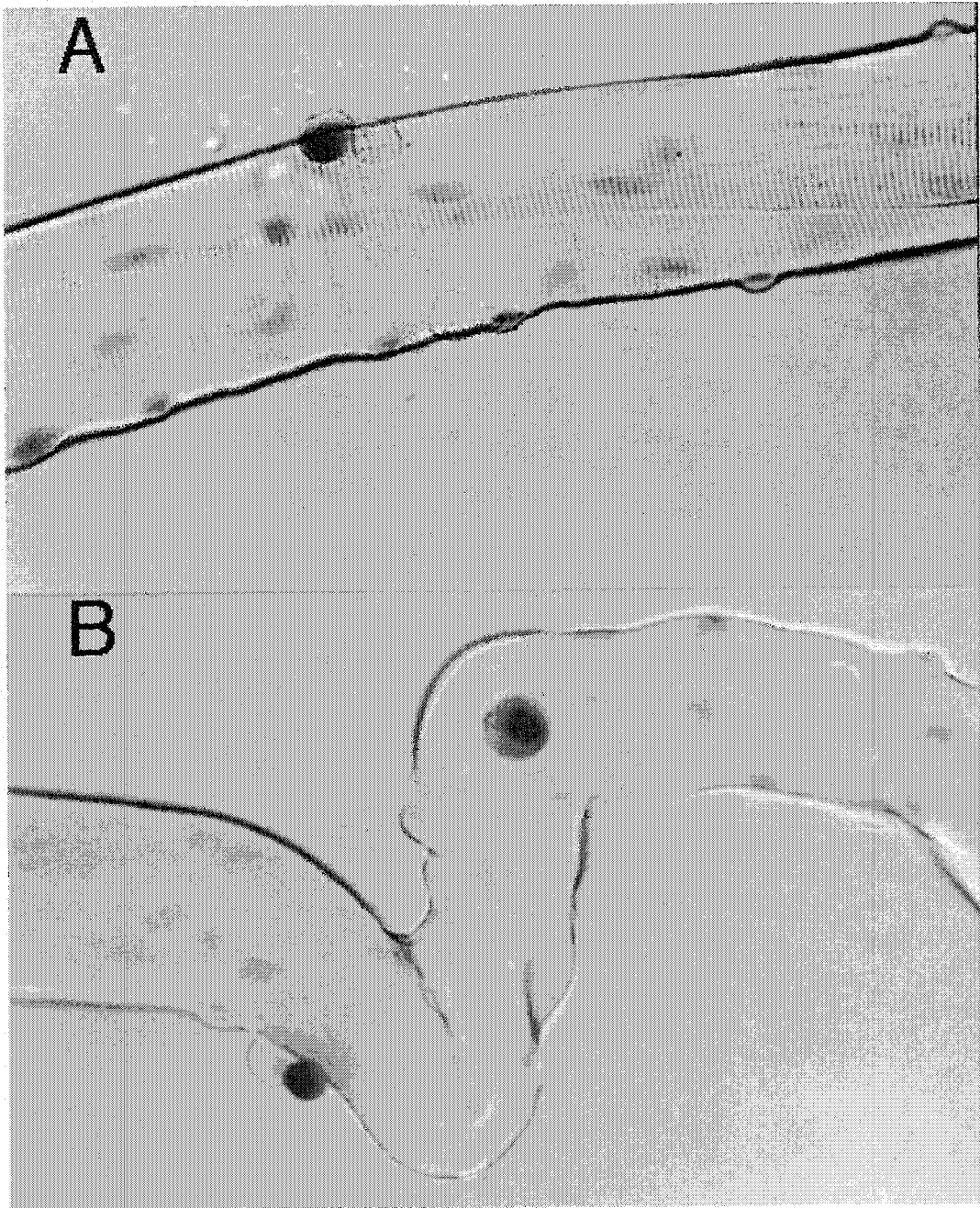


Figure 10.

Figure 11.

- A. Satellite pair on cultured single adult muscle fiber maintained in 6% oxygen for 48 hours. One cell of the pair is intensely immunoreactive for myogenin and the other cell has a signal below background.
- B. DAPI staining of the same section showing the two nuclei of the satellite pair.

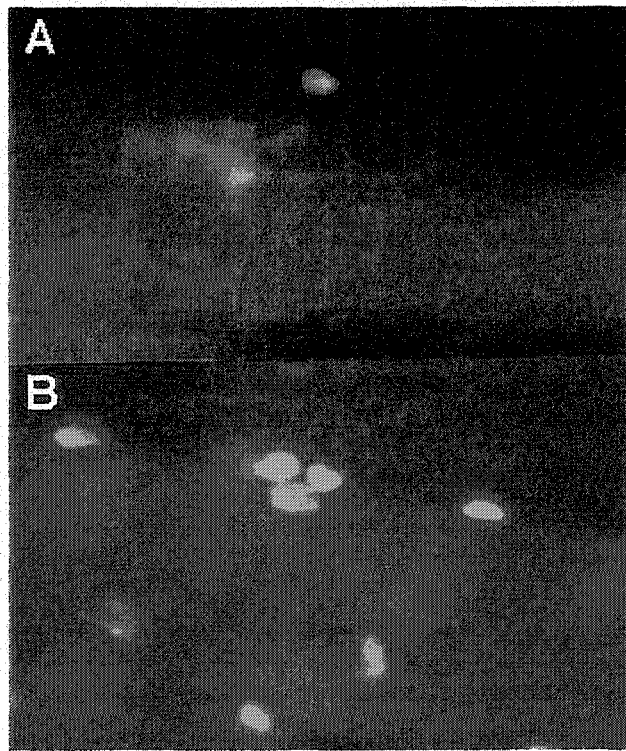


Figure 11.

Figure 12.

- A. Emerging satellites on an isolated single skeletal muscle fiber after 48 hours of culture in 6% oxygen. One of the three cells is intensely immunoreactive for myogenin, and the others are nonreactive.
- B. DAPI stain of the same field showing three nuclei in the satellite group.

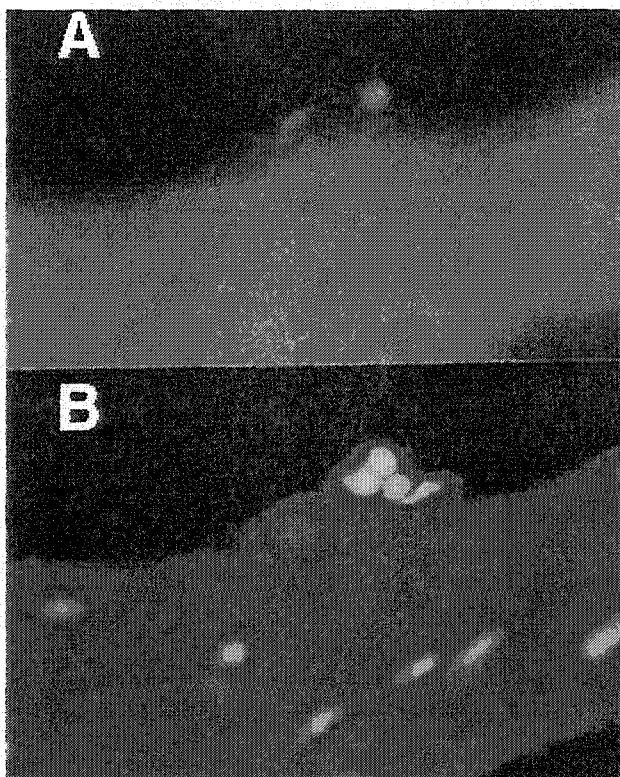


Figure 12.

REFERENCES

- Adler, V., Yin, Z., Tew, K.D., Ronai, Z. (1999). Role of redox potential and reactive oxygen species in stress signaling. *Oncogene* **18**, 6104-6111.
- Allen, R.E., Boxhorn, L.K. (1989). Regulation of skeletal muscle satellite cell proliferation and differentiation by transforming growth factor-beta, insulin-like growth factor I, and fibroblast growth factor. *J. Cell Physiol.* **138**, 311-315.
- Altiok, S., Xu, M., Spiegelman, B.M. (1997). PPAR induces cell cycle withdrawal: inhibition of E2F/DP DNA-binding activity via down-regulation of PP2A. *Genes Dev.* **11**, 1987-1998.
- Arany, Z., Huang, L.E., Eckner, R., Bhattacharya, S., Jiang, C., Goldberg, M.A., Bunn, H.F., Livingston, D.M. (1996). An essential role for p300/CBP in the cellular response to hypoxia. *Proc. Natl. Acad. Sci.* **93**, 12969-12973.
- Arnold, H-H., Winter, B. (1998). Muscle differentiation: more complexity to the network of myogenic regulators. *Curr. Biol.* **8**, 539-544.
- Bachmann, G., Damian, M.S., Koch, M., Schilling, G., Fach, G., Stoppler, S. (1996). *Neuroradiology* **38**, 629-635.

- Barton-Davis, E.R., Shoturma, D.I., Musaro, A., Rosenthal, N., Sweeney, H.L. (1998). Viral mediated expression of insulin-like growth factor I blocks the aging-related loss of skeletal muscle function. *Proc. Natl. Acad. Sci.* **95**, 15603-15607.
- Barton-Davis, E.R., Shoturma, D.I., Sweeney, H.L. (1999). Contribution of satellite cells to IGF-I induced hypertrophy of skeletal muscle. *Acta Physiol. Scand.* **167**, 301-305.
- Beauchamp, J.R., Morgan, J.E., Pagel, C.N., Partridge, T.A. (1999). Dynamics of myoblast transplantation reveal a discrete minority of precursors with stem-like properties as the myogenic source. *J. Cell. Biol.* **144**, 1113-1122.
- Beckman, K.B., Ames, B.N. (1998). The free radical theory of aging matures. *Physiol. Rev.* **78**, 547-581.
- Bell, E., Marek, L.F., Levinstone, D.S., Merrill, C., Sher, S., Young, I.T., Eden, M. (1978). Loss of division potential in vitro: aging or differentiation? *Science* **202**, 1158-1163.
- Bergman, R.J., Gazit, D., Kahn, A.J., Gruber, H., McDougall, S., Hahn, T.J. (1996). Age-related changes in osteogenic stem cells. *J. Bone Miner. Res.* **11**, 568-577.

- Bischoff, R. (1994). The satellite cell and muscle regeneration. In "Myogenesis" (A.G. Engel and C. Franzini-Armstrong, eds.), Vol. 2, pp.97-117, McGraw-Hill, New York.
- Bischoff, R. (1997). Chemotaxis of skeletal muscle satellite cells. *Dev. Dyn.* **208**, 505-151.
- Bjornson, C.R., Rietze, R.L., Reynolds, B.A., Magli, M.C., Vescovi, A.L. (1999). Turning brain into blood: a hematopoietic fate adopted by adult neural stem cells in vivo. *Science* **283**, 534-537.
- Bouloumie, A., Drexler, H.C.A., Lafontan, M., Busse, R., (1998). Lepin, the product of the *Ob* gene, promotes angiogenesis. *Circ. Res.* **83**, 1059-1066.
- Butterwith, S.C., Goddard, C. (1991). Regulation of DNA synthesis in chicken adipocyte precursor cells by insulin-like growth factors, platelet-derived growth factor and transforming growth factor-beta. *J Endocrinol.* **131**, 203-209.
- Carlson, B.M., Faulkner, J.A. (1989). Muscle transplantation between young and old rats: age of host determines recovery. *Am. J. Physiol.* **256**, C1262-C1266.
- Carrero, P., Okamoto, K., Coumailleau, P., O'Brien, S., Tanaka, H., Poellinger, L. (2000). Redox-regulated

recruitment of the transcriptional coactivators CREB-binding protein and SRC-1 to hypoxia-inducible factor 1alpha. *Mol. Cell. Biol.* **20**, 402-415.

Cenciarelli, C., De Santa, F., Puri, P.L., Mattei, E., Ricci, L., Bucci, F., Felsani, A., Caruso, M. (1999). Critical role played by cyclin D3 in the MyoD-mediated arrest of cell cycle during myoblast differentiation. *Mol. Cell. Biol.* **19**, 5203-5217.

Chen, P.L., Riley, D.J., Chen, Y., Lee, W.H. (1996). Retinoblastoma protein positively regulates terminal adipocyte differentiation through direct interaction with C/EBPs (1996). *Genes Dev.* **10**, 2794-2804.

Chenais, B., Andriollo, M., Guiraud, P., Belhoussine, R., Jeannesson, P. (2000). Oxidative stress involvement in chemically induced differentiation of K562 cells. *Free Radic. Biol. Med.* **28**, 18-27.

Collins, A.R. (1999). Oxidative DNA damage, antioxidants, and cancer. *BioEssays* **21**, 238-246.

Cooper, R.N., Tajbakhsh, S., Mouly, V., Cossu, G., Buckingham, M., Butler-Browne, G.S. (1999). In vivo satellite cell activation via Myf5 and MyoD in regenerating mouse skeletal muscle. *Cell Sci* **112**, 2895-2901.

- Cornelison, D.D.W., Wold, B. (1997). Single-cell analysis of regulatory gene expression in quiescent and activated mouse skeletal muscle satellite cells. *Dev. Biol.* **191**, 270-283.
- Crescenzi, M., Fleming, T.P., Lassar, A.B., Weintraub, H., Aaronson, S.A. (1990). MyoD induces growth arrest independent of differentiation in normal and transformed cells. *Proc. Natl. Acad. Sci.* **87**, 8442-8446.
- Cristofalo, V.J. and Pignolo, R.J. (1993). Replicative senescence of human fibroblast-like cells in culture. *Physiol. Rev.* **73**, 617-638.
- Daubas, P., Tajbakhsh, S., Hadchouel, J., Primig, M., Buckingham, M. (2000). Myf5 is a novel early axonal marker in the mouse brain and is subjected to post-transcriptional regulation in neurons. *Development* **127**, 319-331.
- De Angelis, L., Berghella, L., Coletta, M., Lattanzi, L., Zanchi, M., Cusella-De Angelis, M.G., Ponzetto, C., Cossu, G. (1999). Skeletal myogenic progenitors originating from embryonic dorsal aorta coexpress endothelial and myogenic markers and contribute to postnatal muscle growth and regeneration. *J. Cell Biol.* **147**, 869-877.

- DeGregori, J., Kowalik, T., Nevins, J.R. (1995). Cellular targets for activation by the E2F1 transcription factor include DNA synthesis- and G1/S-regulatory genes. *Mol. Cell. Biol.* **15**, 4215-4224.
- Evers, B., Odemis, V., Gerngroß, H. (1997). Intramuscular oxygen partial pressure in patients with chronic exertional compartment syndrome. *Adv. Exp. Med. Biol.* **428**, 311-316.
- Ferrari, G., Cusella-De Angelis, G., Coletta, M., Paolucci, E., Stornaiuolo, A., Cossu, G., Mavilio, F. (1998). Muscle regeneration by bone marrow-derived myogenic progenitors. *Science* **279**, 1528-1530.
- Franco, A.A., Odom, R.S., Rando, T.A. (1999). Regulation of antioxidant enzyme gene expression in response to oxidative stress and during differentiation of mouse skeletal muscle. *Free Radic. Biol. Med.* **27**, 1122-1132.
- Fruchart, J.C., Duriez, P., Staels, B. (1999). Peroxisome proliferator-activated receptor-alpha activators regulate genes governing lipoprotein metabolism, vascular inflammation and atherosclerosis. *Curr. Opin. Lipidol.* **10**, 245-257.
- Garces, C., Ruiz-Hidalgo, M.J., Bonvini, E., Goldstein, J., Laborda, J. (1999). Adipocyte differentiation is

modulated by secreted delta-like (dlk) variants and requires the expression of membrane-associated dlk. *Differentiation* **64**, 103-114.

Gerber, H.-P., Vu, T.H., Ryan, A.M., Kowalski, J., Werb, Z., Ferrara, N. (1999). VEGF couples hypertrophic cartilage remodeling, ossification and angiogenesis during endochondral bone formation. *Nature Medicine* **5**, 623-628.

Gibson, M.C., Schultz, E. (1983). Age-related differences in absolute numbers of skeletal muscle satellite cells. *Muscle Nerve* **6**, 574-580.

Goda, F., O'Hara, J.A., Liu, K.J., Rhodes, E.S., Dunn, J.F., Swartz, H.J. (1997). Comparisons of measurements of pO₂ in tissue in vivo by EPR oximetry and micro-electrodes. *Adv. Exp. Med. Biol.* **411**, 543-549.

Greenbaum, A.R., Etherington, P.J., Manek, S., O'Hare, D., Parker, K.H., Green, C.J., Pepper, J.R., Winlove, C.P. (1997). Measurements of oxygenation and perfusion in skeletal muscle using multiple microelectrodes. *Muscle Res. Cell Motil.* **18**, 149-159.

Grounds, M.D., Garrett, K.L., Lai, M.C., Wright, W.E., Beilharz, M.W. (1992). Identification of skeletal

muscle precursor cells in vivo by use of MyoD1 and myogenin probes. *Cell Tissue Res.* **267**, 99-104.

Gussoni, E., Soneoka, Y., Strickland, C.D., Buzney, E.A., Khan, M.K., Flint, A.F., Kunkel, L.M., Mulligan, R.C. (1999). Dystrophin expression in the *mdx* mouse restored by stem cell transplantation. *Nature* **401**, 390-394.

Hall, K., Hilding, A., Thoren, M. (1999). Determinants of circulating insulin-like growth factor-I. *J. Endocrinol. Invest.* **22**, 48-57.

Hallakou, S., Foufelle, F., Doare, L., Kergoat, M., Ferre, P. (1998). Pioglitazone-induced increase of insulin sensitivity in the muscles of obese Zucker *fa/fa* rats cannot be explained by local adipocyte differentiation. *Diabetologia* **41**, 963-968.

Hansen, J.B., Petersen, R.K., Larsen, B.M., Bartkova, J., Alsner, J., Kristiansen, K. (1999). Activation of peroxisome proliferator-activated receptor gamma bypasses the function of the retinoblastoma protein in adipocyte differentiation. *J. Biol. Chem.* **274**, 2386-2393.

Hausman, G.J. (1982). Adipocyte development in subcutaneous tissue of the young rat. *Acta Anat.* **112**, 185-192.

- Heinrich, R., Gunderoth-Palmowski, M., Grauer, W., Machac, N., Dette, S., Egberts, E. (1987). Gewebe-pO₂ M. Tibialis ant. Gesunder Probanden bei normovolämischer Hamodilution mit 10%iger HES 200. *VASA* **16**, 18-323, 1987.
- Hogan, M.C. (1999). Phosphorescence quenching method for measurement of intracellular PO₂ in isolated skeletal muscle fibers. *J. Appl. Physiol.* **86**, 720-724.
- Hu, E., Tontonoz, P., and Spiegelman, B.M. (1995). Transdifferentiation of myoblasts by the adipogenic transcription factors PPAR γ and C/EBP β . *Proc. Natl. Acad. Sci.* **92**, 9856-9860.
- Huang, L.E., Gu, J., Schau, M., Bunn, H.F. (1998). Regulation of hypoxia-inducible factor 1 α is mediated by an O₂-dependent degradation domain via the ubiquitin-proteasome pathway. *Proc. Natl. Acad. Sci.* **95**, 7987-7992.
- Huang, S., Law, P., Francis, K., Palsson, B.O., Ho, A.D. (1999). Symmetry of initial cell divisions among primitive hematopoietic progenitors is independent of ontogenic age and regulatory molecules. *Blood* **94**, 2595-2604.

- Hughes, S.M., and Blau H.M. (1990). Migration of myoblasts across basal lamina during skeletal muscle development. *Nature* **345**, 350-353.
- Hutter, J., Habler, O., Kleen, M., Tiede, M., Podtschaske, A., Kemming, G., Corso, C., Batra, S., Keipert, P., Faithfull, S., Messmer, K. (1999). Effect of acute normovolemic hemodilution on distribution of blood flow and tissue oxygenation in dog skeletal muscle. *J. Appl. Physiol.* **86**, 860-866.
- Ijpenberg, A., Jeannin, E., Wahli, W., Desvergne, B., (1997). Polarity and specific sequence requirements of peroxisome proliferator-activated receptor (PPAR)/Retinoid X receptor heterodimer binding to DNA. *J Biol. Chem.* **272**, 20108-20117.
- Iwashima, Y., Eto, M., Horiuchi, S., Sano, H. (1999). Advanced glycation end product-induced peroxisome proliferator-activated receptor gamma gene expression in the cultured mesangial cells. *Biochem. Biophys. Res. Commun.* **264**, 441-448.
- Jackson, K.A., Mi, T., and Goodell, M.A. (1999). Hematopoietic potential of stem cells isolated from murine skeletal muscle. *Proc. Natl. Acad. Sci.* **96**, 14482-14486.

- Kalyani, A., Hobson, K., Rao, M.S. (1997). Neuroepithelial stem cells from the embryonic spinal cord: isolation, characterization, and clonal analysis. *Dev. Biol.* **186**, 202-223.
- Kim, J.B., Spotts, G.D., Halvorsen, Y.D., Shih, H.J., Ellenberger, T., Towle, H.C., Spiegelman, B.M. (1995). Dual DNA binding specificity of ADD1/SREBP1 controlled by a single amino acid in the basic helix-loop-helix domain. *Mol. Cell. Biol.* **15**, 2582-2588.
- Kolodka, T.M., Garlick, J.A., Taichman, L.B. (1998). Evidence for keratinocyte stem cells in vitro: long term engraftment and persistence of transgene expression from retrovirus-transduced keratinocytes. *Proc. Natl. Acad. Sci.* **95**, 4356-4361.
- Kunert, M.P., Liard, J.F., Abraham, D.J., Lombard, J.H. (1996). Low-affinity hemoglobin increases tissue PO₂ and decreases arteriolar diameter and flow in the rat cremaster muscle. *Microvasc. Res.* **52**, 58-68.
- Kunze, K. (1976). Spontaneous oscillations of PO₂ in muscle tissue. *Adv. Exp. Med. Biol.* **75**, 631-637.
- Lemischka, I. (1999). The power of stem cells reconsidered? *Proc. Natl. Acad. Sci.* **96**, 14193-14195.
- Lescaudron, L., Creuzet, S.E., Li, Z., Paulin, D., Fontaine-Perus, J. (1997). Desmin-lacZ transgene

- expression and regeneration within skeletal muscle transplants. *J. Muscle Res. Cell Motil.* **18**, 631-641.
- Li, N., Oberley, T.D., Oberley, L.W., Zhong, W. (1998). Inhibition of cell growth in NIH/3T3 fibroblasts by overexpression of manganese superoxide dismutase: Mechanistic studies. *J. Cell. Physiol.* **175**, 359-369.
- Mandrup, S.M., Lane, M.D. (1997). Regulating adipogenesis. *J. Biol. Chem.* **272**, 5367-5370.
- McKinley, B.A., and Butler, B.D. (1999). Comparison of skeletal muscle PO₂, PCO₂, and pH with gastric tonometric P(CO₂) and pH in hemorrhagic shock. *Crit. Care Med.* **27**, 1869-1877.
- McKinley, B.A., Parmley, C.L., Butler, B.D. (1998). Skeletal muscle PO₂, PCO₂, and pH in hemorrhage, shock, and resuscitation in dogs. *J. Trauma* **44**, 119-127.
- Mecocci, P., Fano, G., Fulle, S., MacGarvey, U., Shinobu, L., Polidori, M.C., Cherubini, A., Vecchiet, J., Senin, U., Beal, M.F. (1999). Age-dependent increases in oxidative damage to DNA, lipids, and proteins in human skeletal muscle. *Free Rad. Biol. Med.* **26**, 303-308.
- Mezzogiorno, A., Coletta, M., Zani, B.M., Cossu, G., Molinaro, M. (1993). Paracrine stimulation of

senescent satellite cell proliferation by factors released by muscle or myotubes from young mice. *Mech. Ageing Dev.* **70**, 35-44.

Moldes, M., Boizard, M., Liepvre, X.L., Fève, B., Dugail, I., Pairault, J. (1999). Functional antagonism between inhibitor of DNA binding (Id) and adipocyte determination and differentiation factor 1/sterol regulatory element-binding protein-1c (ADD1/SREBP1c) trans-factors for the regulation of fatty acid synthase promoter in adipocytes. *Biochem. J.* **344**, 873-880.

Morshead, C.M., Craig, C.G., van der Kooy, D. (1998). In vivo clonal analyses reveal the properties of endogenous neural stem cell proliferation in the adult mammalian forebrain. *Development* **125**, 2251-2261.

Musaro, A., McCullagh, K.J.A., Naya, F.J., Olson, E.N., Rosenthal, N. (1999). IGF-1 induces skeletal myocyte hypertrophy through calcineurin in association with GATA-2 and NF-Atc1. *Nature* **400**, 581-585.

Nurse, C.A., Vollmer, C. (1997). Role of basic FGF and oxygen in control of proliferation, survival, and neuronal differentiation in carotid body chromaffin cells. *Dev. Biol.* **184**, 197-206.

- Ogawa, M. (1999). Stochastic model revisited. *Int. J. Hematol.* **69**, 2-5.
- Osawa, M., Hanada, K., Hamada, H., Nakauchi, H. (1996). Long-term lymphohematopoietic reconstitution by a single CD34-low/negative hematopoietic stem cell. *Science* **273**, 242-245.
- Ott, M.O., Bober, E., Lyons, G., Arnold, H., Buckingham, M. (1991). Early expression of the myogenic regulatory gene, myf-5, in precursor cells of skeletal muscle in the mouse embryo. *Development* **111**, 1097-1107.
- Palmer, H.J., Tuzon, C.T., Paulson, K.E. (1999). Age-dependent decline in mitogenic stimulation of hepatocytes. Reduced association between Shc and the epidermal growth factor receptor is coupled to decreased activation of Raf and extracellular signal-regulated kinases. *J. Biol. Chem.* **274**, 11424-11430.
- Pereira, R.F., Halford, K.W., O'Hara, M.D., Leeper, D.B., Sokolov, B.P., Pollard, M.D., Bagasra, O., Prockop, D.J. (1995). Cultured adherent cells from marrow can serve as long-lasting precursor cells for bone, cartilage, and lung in irradiated mice. *Proc. Natl. Acad. Sci.* **92**, 4857-4861.
- Petley, T., Graff, K., Jiang, W., Yang, H., Florini, J. (1999). Variation among cell types in the signaling

- pathways by which IGF-1 stimulates specific cellular responses. *Horm. Metab. Res.* **31**, 70-76.
- Poissonnet, C.M., Burdi, A.R., Bookstein, F.L. (1983). Growth and development of human adipose tissue during early gestation. *Early Hum. Dev.* **8**, 1-11.
- Prockop, D.J. (1997). Marrow stromal cells as stem cells for nonhematopoietic tissues. *Science* **276**, 71-74.
- Puigserver, P., Adelmant, G., Wu, Z., Fan, M., Xu, J., O'Malley, B., Spiegelman, B.M. (1999). Activation of PPARgamma coactivator-1 through transcription factor docking. *Science* **286**, 1368-1371.
- Rando, T.A., Blau, H.M. (1997). Methods for myoblast transplantation. *Methods Cell Biol.* **52**, 261-272.
- Richon, V.M., Lyle, R.E., McGehee, R.E. Jr. (1997). Regulation and expression of retinoblastoma proteins p107 and p130 during 3T3-L1 adipocyte differentiation. *J. Biol. Chem.* **272**, 10117-10124.
- Rosenblatt, J.D., Parry, D.J., and Partridge, T.A. (1996). Phenotype of adult mouse muscle myoblasts reflects their fiber type of origin. *Differentiation* **60**, 39-45.
- Roth, J., Greenwood, M.R., Johnson, P.R. (1981). The regenerating fascial sheath in lipectomized Osborne-Mendel rats: morphological and biochemical indices of

- adipocyte differentiation and proliferation. *Int. J. Obes.* **5**, 131-143.
- Ruiz-Torres, A., Gimeno, A., Melon, J., Mendez, L., Munoz, F.J., Macia, M. (1999). Age-related loss of proliferative activity of human vascular smooth muscle cells in culture. *Mech. Ageing Dev.* **110**, 49-55.
- Sadeh, M., Czyewski, K., Stern, L.Z. (1985). Chronic myopathy induced by repeated bupivacaine injections. *J. Neurol. Sci.* **67**, 229-238.
- Sartorelli, V., Huang, J., Hamamori, Y., Kedes, L. (1997). Molecular mechanisms of myogenic coactivation by p300: direct interaction with the activation domain of MyoD and with the MADS box of MEF2C. *Mol. Cell. Biol.* **17**, 1010-1026.
- Schultz, E. (1976). Fine structure of satellite cells in growing skeletal muscle. *Am. J. Anat.* **147**, 49-70.
- Schultz, E., Lipton, B.H. (1982). Skeletal muscle satellite cells: changes in proliferation potential as a function of age. *Mech. Ageing Dev.* **20**, 377-383.
- Seale, P., Rudnicki, M.A. (2000). A new look at the origin, function, and "stem-cell" status of muscle satellite cells. *Dev. Biol.* **218**, 115-124.

- Seekamp, A., van Griensven, M., Ziegler, M., Gunderoth, M. (1995). Transcutaneous PO₂ measurement in compound fractures. *Eur. J. Emerg. Med.* **2**,69-74.
- Seekamp, A., Van Griensven, M., Blankenburg, H., Regel, G. (1997). Intramuscular partial oxygen tension monitoring in compartment syndrome--an experimental study. *Eur. J. Emerg. Med.* **4**,185-192.
- Shibanuma, M. Kuroki, T., Nose, K. (1990). Stimulation by hydrogen peroxide of DNA synthesis, competence family gene expression and phosphorylation of a specific protein in quiescent Balb/3T3 cells. *Oncogene* **5**, 1025-1032.
- Skapek, S.X., Rhee, J., Kim, P.S., Novitch, B.G., Lassar, A.B. (1996). Cyclin-mediated inhibition of muscle gene expression via a mechanism that is independent of pRB hyperphosphorylation. *Mol. Cell. Biol.* **16**, 7043-7053.
- Smas, C.M., Sul, H.S. (1993). Pref-1, a protein containing EGF-like repeats, inhibits adipocyte differentiation. *Cell* **73**, 725-734.
- Storch, T.G. (1990). Oxygen concentration regulates 5-azacytidine-induced myogenesis in C₃H/10T1/2 cultures. *Biochim. Biophys. Acta* **1055**, 126-129.

Szilvassy, S.J., Weller, K.P., Lin, W., Sharma, A.K., Ho, A.S., Tsukamoto, A., Hoffman, R., Leiby, K.R., Gearing, D.P. (1996) Leukemia inhibitory factor upregulates cytokine expression by a murine stromal cell line enabling the maintenance of highly enriched competitive repopulating stem cells. *Blood* **87**, 4618-4628.

Tanaka, K., Pracyk, J.B., Takeda, K., Yu, Z-X., Ferrans, V.J., Deshpande, S.S., Ozaki, M., Hwang, P.M., Lowenstein, C., Irani, K., Finkel, T. (1998). Expression of Id1 results in apoptosis of cardiac myocytes through a redox-dependent mechanism. *J. Biol. Chem.* **273**, 25922-25928.

Taylor, S.M., Jones, P.A. (1979). Multiple new phenotypes induced in 10T1/2 and 3T3 cells treated with 5-azacytidine. *Cell* **17**, 771-779.

Teboul, L., Gaillard, D., Staccini, L., Inadera, H., Amri, E.Z., Grimaldi, P.A. (1995). Thiazolidinediones and fatty acids convert myogenic cells into adipose-like cells. *J. Biol. Chem.* **270**, 28183-28187.

Torok-Storb, B., Iwata, M., Graf, L., Gianotti, J., Horton, H., Byrne, M.C. (1999). Dissecting the marrow microenvironment. *Ann. N. Y. Acad. Sci.* **872**, 164-170.

- Ullrich, O., Ruinheckel, T., Sitte, N., Hass, R., Grune, T., Davies, K.J. (1999). Poly-ADP ribose polymerase activates nuclear proteasome to degrade oxidatively damaged histones. *Proc. Natl. Acad. Sci.* **96**, 6223-6228.
- van der Loo, J.C., Ploemacher, R.E. (1995). Marrow- and spleen-seeding efficiencies of all murine hematopoietic stem cell subsets are decreased by preincubation with hematopoietic growth factors. *Blood* **85**, 2598-2606.
- Varnum-Finney, B., Purton, L.E., Yu, M., Brashem-Stein, C., Flowers, D., Staats, S., Moore, K.A., Le Roux, I., Mann, R., Gray, G., Artavanis-Tsakonas, S., Bernstein, I.D. (1998). The Notch ligand, Jagged-1, influences the development of primitive hematopoietic precursor cells. *Blood* **91**, 4084-4091.
- Wakitani, S., Saito, T., and Caplan, A.I. (1995). Myogenic cells derived from rat bone marrow mesenchymal stem cells exposed to 5-azacytidine. *Muscle Nerve* **18**, 1417-1426.
- Wang, N.D., Finegold, M.J., Bradley, A., Ou, C.N., Abdelsayed, S.V., Wilde, M.D., Taylor, L.R., Wilson, D.R., Darlington, G.J. (1995). Impaired energy

- homeostasis in C/EBP alpha knockout mice. *Science* **269**, 1108-1112.
- Wu, Z., Rosen, E.D., Brun, R., Hauser, S., Adelmant, G., Troy, A.E., McKeon, C., Darlington, G.J., Spiegelman, B.M. (1999). Cross-regulation of C/EBP alpha and PPAR gamma controls the transcriptional pathway of adipogenesis and insulin sensitivity. *Mol. Cell* **3**, 151-158.
- Xue, J-C., Schwarz, E.J., Chawla, A., Lazar, M.A. (1996). Distinct stages in adipogenesis revealed by retinoid inhibition of differentiation after induction of PPAR γ . *Mol. Cell. Biol.* **16**, 1567-1575.
- Yablonka-Reuveni, Z., Rivera, A.J. (1994). Temporal expression of regulatory and structural muscle proteins during myogenesis of satellite cells on isolated adult rat fibers. *Dev. Biol.* **164**, 588-603.
- Yablonka-Reuveni, Z., Seger, R., Rivera, A.J. (1999). Fibroblast growth factor promotes recruitment of skeletal muscle satellite cells in young and old rats. *J. Hisotchem. Cytochem.* **47**, 23-42.
- Yagi, M., Ritchie, K.A., Sitnicka, E., Storey, C., Roth, G.J., Bartelmez, S. (1999). Sustained ex vivo expansion of hematopoietic stem cells mediated by thrombopoietin. *Proc. Natl. Acad. Sci.* **96**, 8126-8131.

Zangani, D., Darcy, K.M., Masso-Welch, P.A., Bellamy, E.S.,
Desole, M.S., Ip, M.M. (1999). Multiple
differentiation pathways of rat mammary stromal cells
in vitro: acquisition of a fibroblast, adipocyte or
endothelial phenotype is dependent on hormonal and
extracellular matrix stimulation. *Differentiation* **64**,
91-101.

Zhang, J.M., Zhao, X., Wei, Q., Paterson, B.M. (1999).
Direct inhibition of G(1) cdk kinase activity by MyoD
promotes myoblast cell cycle withdrawal and terminal
differentiation. *EMBO J.* **18**, 6983-6993.

Appendix I.**MATERIALS AND METHODS****Culture of mesenchymal stem cell lines and human myoblasts**

C3H/10T_{1/2} cells were grown in DMEM + 10% fbs with added penicillin/streptomycin and glutamine. At confluence differentiation was induced by the addition of 3 uM 5-azacytidine (Taylor and Jones, 1979) for 24 hr. 3T3 cells derived from wild type C57Bl6 mice were grown in DMEM + 10% calf serum with added pen/strep and glutamine. At confluence, the cells were induced to differentiate with 10 ug/ml insulin, 1 uM dexamethasone, and 0.5 mM isomethylbutylxanthine (Xue et al., 1996). When differentiation conditions were induced, the cultures were divided into either 6% oxygen/5% CO₂/89% N₂ conditions in a modular incubator (Billups-Rothenberg, Del Mar, CA) or traditional 20% O₂/5% CO₂/75% N₂ incubators. Human myoblasts (Clonetics, San Diego CA) were grown in F10 with 15% fbs and 0.5% chick embryo extract.

Isolation and culture of adult murine single muscle fibers

B6D2F1 female mice, 100-200 days old, were euthanized with CO₂ inhalation. After 70% ethanol prep of the skin, a large inguinal incision was continued circumferentially around

the hip, then the skin peeled off over the ankle. The legs were amputated at the hip and ankle and placed into DMEM + high glucose + 25 mM Hepes without phenol under a dissection microscope. Fat, large blood vessels and other non-muscle tissue (tendons) were removed as much as possible, and the muscle groups dissected into smaller groups to facilitate enzymatic digestion. Muscle was transferred into pre-warmed 400 U collagenase type I in the same medium (10 ml) and digestion continued in a 35.5°C water bath for 1 hr. The contents were put into a fresh petri dish and individual live fibers were picked into a small-bore Pasteur pipet, and placed into pre-warmed DMEM + 25 mM Hepes + 4% chick embryo extract + 10% horse serum + antibiotics/antimycotic (with phenol red). Live fibers were distinguished by their transparent appearance whereas contracted, opaque fibers were dead. Live fibers were placed in a tissue culture incubator for 30 min to restore pH. The process of segregating live fibers was repeated twice with progressively smaller bore Pasteur pipets to purify the preparation. In the last purification fibers were placed into culture medium without Hepes buffer. The preparations were split into either 6% O₂/5% CO₂ or 20% O₂/5% CO₂ conditions as above.

Culture of individual skeletal muscle fibers on matrix

24-well Primaria (Falcon) plates were coated with 10% Matrigel in DMEM, then placed in a 37°C incubator until used. Fibers were isolated as described above, then individual fibers were placed singly in each well (15 ul volume). After about 5 min, 500 ul culture medium was added gently to each well. The cultures were then divided into 6% or 20% oxygen conditions.

Oil red O staining for identification of adipocytes

Floating fibers or mesenchymal stem cells were washed with PBS, then fixed in 10% formalin for 15 min at room temperature, rinsed with 60% isopropanol, then stained with oil red O for 10 min. Cells were then rinsed with 60% isopropanol, 30% isopropanol (floating fibers only), then water. Fibers were transferred to microscope slides with fine forceps for microscopy. Mesenchymal stem cell lines were counterstained with hematoxylin under direct vision (30 sec to 2 min). After two water rinses, Scott solution (2 g/L Na bicarbonate, 20 g/L MgSO₄) was added for 3 min, then a final rinse in water.

Immunohistochemistry for myf5 and PPAR γ

Cells were washed three times with PBS, then fixed in 4% paraformaldehyde for 15 min at room temp, then washed X 3 with PBS. Block was performed with 10% donkey serum for 30 min at RT, removed, then primary antibody was applied (1:50) in 1.5% donkey serum/PBS overnight at 4°C (both primaries from Santa Cruz Biotechnology). Three washes with 1.5% ds/PBS were followed by 1:100 of appropriate secondary conjugated to Cy3 (for 1 hour at room temperature). After three PBS washes cells were mounted with Vectashield containing DAPI (Vector Labs, Burlingame, CA) and counted.

Single cell PCR of satellites adherent to cultured muscle fibers

At 24, 48 and 96 hours after culture, fibers were placed in PBS and transferred to a microscope with attached patch clamp apparatus. Individual satellites were identified by morphology and location on the fiber and drawn into a patch clamp electrode previously back-filled with sterile PBS. The contents of the electrode were transferred to an iced mix containing RT buffer (Boehringer-Mannheim), 40 mM DTT, 0.5 mM dNTP's, 10 U Boehringer RNase inhibitor, and 200 ng random primers in water. The cells were stored on ice until 10 U of M-MLV RT was added and the reverse

transcription reaction run at 37°C for 1 hour. Half this cDNA reaction was used in nested PCR reactions: For the first reaction, outside primers for mrf4, myf5, MyoD, and myogenin were used together (PCR details and primers previously reported in Cornelison and Wold, 1997). The product of the first reaction was diluted 1:500 and then individual PCR reactions run for each of these mrf genes using primer sets internal to the outside sets. PCR products were run on a 2% agarose gel and identified by size. Positive controls were run for each reaction using cDNA from C2C12 cells and negative controls were run on PBS drawn from the assayed fibers at the end of the satellite cell retrieval.

BrdU uptake and immunohistochemistry on isolated single muscle fiber cultures

A series of 12 hour pulses of BrdU (10uM/ml) were performed by adding BrdU to cultures at specified times. After the pulse, fibers were fixed in 4% PFA for 15 min, washed X 3 with PBS then transferred to microscope slides. They were treated with 4 M HCl for 10 min, washed X 3 with PBS, then treated with 1% NP40 in PBS for 4 min and washed X3 with PBS. Primary anti-BrdU antibody (rat monoclonal,

Harlan Sera Labs) was applied overnight at 1:10 dilution in PBS at 4°C. After three PBS washes, secondary donkey anti-rat conjugated to TRITC was added at 1:100 for 1 hour at room temperature. After washing, fibers were mounted and co-labeled with DAPI. Fluorescent labelled satellites were counted as a function of unit length of fiber (one 400X field diameter).

X-gal staining of cultured muscle fibers

Fix was prepared fresh by adding 2.7 ml 37% formaldehyde and 0.4 ml glutaraldehyde to PBS, pH 7.3. Stain was prepared as follows: 0.625 ml 40 mg/ml X-Gal in DMSO + 50 ul 1M MgCl₂, 41 mg potassium ferricyanide, 53 mg potassium ferrocyanide, added to 25 ml PBS.

Fibers were washed in BPS then fixed for 5 minutes at room temp, rinsed three times with PBS, then stained. Development of the stain was followed under a microscope and the stain was removed at the desired intensity (generally 15-45 minutes). Fibers were fixed again, then rinsed in PBS and transferred to a microscope slide for mounting.

Chapter 3. CNS stem cell regeneration in vitro benefits from a low oxygen environment

Introduction

Cultured central nervous system (CNS) stem cells are used extensively to study pathways leading to generation of neuronal and glial lineages (McKay, 1997). Cultured CNS stem cells can self-renew, and after mitogen withdrawal, differentiate into neurons, astrocytes and oligodendrocytes in predictable proportions (Johe et al., 1996). Single extrinsic factors can shift the fate of CNS stem cells toward specific cell lineages (Johe et al., 1996 and Panchision et al., 1998). CNS stems are the subject of intensive study because degenerative and ischemic diseases of the brain are so common and often devastating. Dopaminergic neurons derived from CNS precursors are of special interest given the therapeutic potential of dopaminergic cell replacement for Parkinson's disease (Olanow et al., 1996). Several open trials have suggested that transplantation of fetal CNS stem cells in patients with Parkinson's disease leads to improvement in neurologic function, and better-controlled trials are currently underway in several centers (Freeman et al., 2000)

In mammalian brain, interstitial tissue O₂ levels range from about 1-5% (Table 1). Mean rat cerebral pO₂ was measured at 3.9% (Goda et al., 1997) or 4.2% (Liu et al., 1997), both studies using EPR, and cortical pO₂ in newborn piglets was recently estimated at 5.7% (Tammela et al., 1997). These studies did not employ extensive regional sampling. Data gathered from more extensive sampling suggests that mean brain tissue oxygen levels in rat are about 1.6% (Silver and Erecinska, 1988) and the same in fetal sheep (Koos and Power, 1987). Regional differences in mean tissue oxygen levels in rat brain are presented below (Silver and Erecinska, 1988).

Table 1.

Rat regional brain tissue partial pressures of O₂

<u>Brain area</u>	<u>% O₂</u>
Cortex (gray)	2.5-5.3
Cortex (white)	0.8-2.1
Hypothalamus	1.4-2.1
Hippocampus	2.6-3.9
Pons, fornix	0.1-0.4

The brain is protected by robust acute and chronic control mechanisms to minimize changes in intracranial pressure, blood flow and cerebral oxygenation. The cerebral vasculature is extremely reactive—Vessel radius can change acutely by 50% in response to CO₂ changes (Ursino and Lodi, 1998). This reactivity is used clinically to manipulate brain blood flow in patients with space occupying lesions of the head. The blood-brain barrier assures that cerebral blood flow is constant at mean systemic arterial pressures varying between 50-150 mm Hg (Paulson et al., 1990). Chronic decreases in oxygen availability initiate dramatic restructuring of brain capillary architecture to increase capillary volume by vasodilation, elongation and sprouting (Lauro and LaManna, 1997).

Extreme hypoxia and anoxia are commonly studied in neuronal tissue culture to model the effects of stroke or trauma on the brain (Nieber, 1999). However, controls for these hypoxic cells are almost always parallel cultures grown in a gaseous atmosphere of 20% oxygen (Xu et al., 1999; Hewett et al., 1996), which is very often reported as "normoxic." Outcome comparisons of CNS-derived cultures in frankly anoxic vs. physiologic oxygen conditions have not been done.

Only very rarely are neurons cultured under physiologic oxygen conditions (Colton et al., 1995). One study of cultured cortical neurons grown in 1,5,9,13,21, and 60% oxygen suggested that survival and synthesis of neurofilament were maximal in 9% oxygen (Kaplan et al., 1986). Such reports have not changed common laboratory practice, probably because non-room air culturing is so inconvenient.

Standard gas conditions for CNS stem cell culture is also 20% oxygen and 5% CO₂ (Gage et al., 1995) and during isolation cells may be exposed to even higher levels of oxygen (Hazel and Muller, 1998). In fact, the practice is so accepted that it is often not described when culture methods are cited, assuming that all culture is in room air levels of oxygen (Gage FH, 2000).

We analyzed CNS precursors from embryonic rat mesencephalon and lateral ganglionic eminence in standard 20% O₂-exposed cultures and in more physiologic levels of oxygen (3+2%). Over a wide range of plating densities, the yield of cells regenerated from the precursors was significantly greater in physiologic vs. 20% O₂. Proliferation of precursors was enhanced in the lower oxygen conditions and apoptosis

reduced. Although both conditions yielded the full repertoire of astrocytes, oligodendrocytes and neurons, neuronal yield was greater (as a percentage of total cells) in lower oxygen. Oxygen significantly influenced the distribution of neuronal subtypes generated from cultured CNS precursors: Physiologic oxygen cultures were enriched in dopaminergic and serotonergic neurons. These results suggest that regeneration of specific neuronal subtypes involves coordination of known developmental gene pathways with oxygen-responsive pathways, and that oxygen manipulations can be used to enhance regeneration of specific cells in culture.

Results

Lowered O₂ around cultured CNS precursors augments expansion of striatal and mesencephalic precursors.

E14 rat striatum, widely used for derivation of CNS precursors, was one source for neuroepithelial precursors used to examine growth at either 20% or physiologic oxygen levels. Precursor expansion was performed using a defined medium supplemented with bFGF. Basic FGF is mitogenic for stem cells obtained from the developing brain. EGF or bFGF are mitogens used to expand CNS precursors in culture. Withdrawal of bFGF was used to initiate differentiation,

usually after about 5 days of expansion. Striatal precursors cultured in lowered O₂ yielded an average two- to three-fold more cells than 20% O₂ cultures over a range of plating densities in the presence of bFGF (Figure 1). Identical results were obtained with E12 mesencephalic precursors.

Lowered oxygen culturing affects both precursor proliferation and apoptosis.

To test whether increased cell yield in lowered O₂ is due to increased proliferation, reduced cell death, or both, precursors were pulsed with bromodeoxyuridine (BrdU) for 1 hr before fixation at multiple time points. Mesencephalic and striatal precursors showed increased BrdU labeling indices when grown in lowered O₂ compared to 20% O₂, both in the presence of bFGF and following its withdrawal. BrdU incorporation rates for striatal precursors were: *Day 2 of expansion*: 18 ± 6% in lowered O₂ vs. 11 ± 6% in 20% O₂ (n=24, p < 0.05). *Day 6 of expansion*: 30 ± 8% in lowered O₂ vs. 22 ± 5% in 20% O₂ (n=24, p < 0.05). *Day 4 of differentiation (10 days in vitro)*: 12 ± 5% in lowered O₂ vs. 3 ± 3% in 20% O₂ (n=24, p < 0.05). Mesencephalic

cultures showed similar patterns of BrdU incorporation and are depicted in Figure 2.

CNS precursors were also less likely to undergo apoptosis in lowered vs. 20% O₂. Both mesencephalic and striatal precursors revealed significantly reduced percentages of TUNEL-positive cells both during expansion and after bFGF withdrawal. Mesencephalic TUNEL data are depicted in Figure 3. Similar studies were performed in human CNS precursor cultures (Clonetics, San Diego) grown in either 20% or 2% oxygen. At the end of 13 days in culture, significantly more cells were present in lowered oxygen conditions. TUNEL assays at that time revealed that about 50% of the cells in traditional cultures were undergoing apoptosis whereas few cells in 2% oxygen were labelled in the assay (Figure 4). Proliferation assays were not performed in these cultures. We conclude that reduced apoptosis and increased cell proliferation both contribute to elevated cell yield after expansion in rat CNS stem cells. Cell death is reduced but not entirely eliminated during the differentiation phase by lowered O₂.

We used a series of molecular markers, together with morphologic assessment to characterize how lowered O₂

culturing affects the kinetics and choice of differentiation pathways. Immunoreactivity for the intermediate filament nestin was used to discriminate CNS stem/progenitor cells from more differentiated progeny (Lendahl et al., 1990). Six days after bFGF withdrawal the percentage of nestin-positive cells derived from expanded precursors was grossly reduced in lowered O₂ cultures compared with 20% O₂ cultures, suggesting that differentiation was accelerated in lowered O₂ (Figure 5). The idea of accelerated progression to more differentiated phenotypes was supported by the earlier appearance of neuronal and glial markers in lowered O₂. The antibody 04 which identifies early oligodendrocytes stained cells at 24 hours after withdrawal of bFGF only in low oxygen cultures (Figure 6). Similarly the neuroblast marker PSA-NCAM was seen earlier after bFGF withdrawal in low oxygen cultures (see Figure 7). On the other hand, oligodendrocytes in high oxygen may be selectively lost, since they are known to be particularly susceptible to oxidative injury (Husain and Juurlink, 1995; Laszkiewicz, 1999; Casaccia-Bonofil, 2000).

Five days after bFGF withdrawal, neurons were identified by β -tubulin III (TUJ1) staining, astrocytes by glial fibrillary acidic protein (GFAP), and oligodendrocytes by GalC galactocerebroside staining (Figure 5). Striatal cultures grown in low O₂ contained 46% Tuj1-positive cells vs. 34% in 20% O₂ (n=12, p < 0.05); Six percent were GFAP+ vs. 2% in 20% O₂ (n=12, p < 0.05); and 4% were Gal-C+ vs. 5% in 20% O₂ (p=n.s.). In mesencephalic cultures grown in lowered O₂, 73% were Tuj1+ vs. 63% in 20% O₂ (n=12, p = 0.06); no GFAP+ cells were detected in either condition; 1% were O4+ versus 0% in 20% O₂ (n=12, p < 0.01) (not shown).

To investigate O₂ effects at clonal densities, mesencephalic precursors were expanded in bFGF for 6 days in 20% O₂, replated at a density of 1-5 cells/well, then maintained in either lowered or 20% O₂. After 20 days, 20 ng/mL bFGF was withdrawn. Clonal cultures with typical multi-lineage differentiation responses were observed in both lowered and 20% O₂. However, the efficiency of clone formation was 3 times higher in lowered O₂ and the average clone size increased from <50 cells in 20% O₂ to 50-500 cells in lowered O₂ (Figure 8).

Neuronal subtype differentiation

Previous work from the McKay lab showed that nestin-positive mesencephalic precursors differentiate into functional dopaminergic neurons (Studer et al., 1998). Here we determined that this particular neuronal fate was influenced by lowered O₂. Mesencephalic precursors in lowered O₂ displayed a striking increase in both the absolute number and fraction of neurons expressing TH. In lowered O₂, large neuronal clusters were seen in which virtually all neurons were TH-immunoreactive (Figure 9). On average, 56% of neurons (Tuj1-positive) generated in lowered O₂ were TH+ vs. 18% in traditional cultures (n=12, p < 0.001). Increased TH-immunoreactivity in lowered O₂ correlated with increased TH protein content in Western blots (Figure 10).

Functional dopaminergic capacity of the TH+ neurons was further assessed by reverse phase HPLC, which showed significantly increased levels of dopamine in lowered vs. 20% O₂ (Figure 11). Conditioned medium (24 hours) showed a five-fold increase in dopamine (n=5, p < 0.01). Basal release in HBSS revealed a two- to three-fold increase (n=5, p < 0.05) and evoked release was three-fold increased

(n=5, $p < 0.05$). These results confirm that lowered O_2 favors differentiation of functional dopaminergic neurons.

Mesencephalic precursors give rise to neurons with several distinct neurotransmitter phenotypes in addition to dopaminergic fate. Interestingly, the percentage of serotonergic neurons was also increased in lowered O_2 , $3.2 \pm 1.2\%$ vs. $1.2 \pm 0.3\%$ in 20% O_2 (n=12, $p < 0.05$, Figure 9). On the other hand GABA+ and Glutamate+ neurons were less likely to be generated in lowered O_2 : GABA+ $6.6 \pm 1.8\%$ in lowered O_2 vs. $10.4 \pm 1.5\%$ in 20% O_2 (n=12, $p < 0.05$); Glutamate+ $12.8 \pm 3.8\%$ in lowered O_2 vs. $23.6 \pm 4.0\%$ in 20% O_2 (n=12, $p < 0.01$). No double labeling of TH with GABA was detected indicating that TH immunoreactivity corresponded to differentiated dopaminergic neurons and was not a transient developmental phenomenon described in developing GABAergic neurons (Max et al., 1996). Furthermore, TH-positive neurons were not fated to a noradrenergic phenotype, since no dopamine- β -hydroxylase staining could be demonstrated (not shown).

Since lowered O_2 promoted differentiation of dopaminergic and serotonergic neurons, both ventral phenotypes (Yamada

et al., 1991; Hynes et al., 1995; Ye et al., 1998), we tested whether these changes were associated with an increase in floor plate cells. Immunohistochemistry revealed expanded zones of FP4+ cells in lowered O₂ (Figure 7). A more striking feature was the increase in neurons expressing the transcription factor engrailed-1 (En1) in lowered O₂ (Figure 7). En1 is critical for normal midbrain development (Joyner, 1996; Danelian and McMahon, 1996; Wurst et al., 1994) and has been implicated in control of dopaminergic neuronal fate (Simone et al., 1998).

It is important to establish whether lowered O₂ enhanced dopaminergic differentiation by acting during the proliferation or differentiation phases of culture. Mesencephalic precursors were expanded for 5 days in either lowered or 20% O₂, then subdivided for differentiation in either lowered or 20% O₂. Precursors expanded in lowered O₂ but differentiated in 20% O₂ yielded 38±6% TH+ neurons, similar to those maintained in lowered O₂ throughout (41±7%, n=12, p = n.s.) but significantly higher than those maintained in 20% O₂ throughout (17±4%, n=12, p < 0.01). Exposure to lowered O₂ limited to the differentiation phase did not significantly increase the yield of dopaminergic

neurons ($21 \pm 2\%$, $n=12$, $p=n.s.$) compared to 20% O₂ throughout (Figure 12). We conclude that the major effect of lowered O₂ is during expansion.

Semi-quantitative RT-PCR was used to assay cultures at various time points for differential expression of candidate genes involved in dopaminergic neuron development (Figure 13). A small increase in TH message was detected from lowered O₂ cultures after differentiation, compared to 20% O₂. The Ptx3 homeobox gene has also been implicated in dopamine neuron development (Smidt et al., 1997) and was also expressed at increased levels in lowered O₂ suggesting that these conditions promoted the dopaminergic phenotype, not simply upregulation of TH gene expression. Strong evidence links sonic hedgehog (Echelard et al., 1993) and Nurr1 (Saucedo-Cardenas et al., 1998) to the differentiation of midbrain dopaminergic neurons, but we detected no O₂-dependent changes in their expression. However, En1 was upregulated in lowered O₂, paralleling immunohistochemical results. Fibroblast growth factor 8b (FGF8b) message was dramatically upregulated in lowered O₂ after 4 days of expansion. Messages for other regulators

of dopaminergic differentiation did not differ significantly between O₂ conditions.

We also examined genes previously implicated in mediating O₂ responsiveness or known to be regulated by O₂. As expected, EPO (Figure 14) and vascular endothelial growth factor (VEGF) RNAs were upregulated in lowered vs. 20% O₂, though with different kinetics (VEGF message was increased during expansion). Transcript levels for the tumor suppressor gene, von Hippel Lindau (VHL) and the transcription factor hypoxia inducible factor-1 α (HIF1 α) (Maxwell et al., 1999) did not differ between O₂ conditions.

Based on these results, recombinant proteins and neutralizing antibodies for FGF8b, VEGF or EPO were added to precursors grown in either lowered or 20% O₂ in the presence of bFGF. VEGF or its neutralizing antibody did not affect the ratio of dopaminergic neurons generated in either condition. FGF8 promoted proliferation in mesencephalic precursors: 20% cultures expanded 7.5 ± 1.2 -fold in 5 days, compared to 5.6 ± 1.2 -fold without FGF8 (n=6, p < 0.05). After bFGF withdrawal, continuous FGF8

exposure kept precursor cells proliferating in both O₂ conditions and substantially delayed neuronal differentiation including the generation of TH⁺ cells. Surprisingly, addition of recombinant human EPO (0.5 - 2 U/ml) led to a marked increase in TH⁺ cells in 20% O₂ cultures. Furthermore, addition of EPO neutralizing antibody to both lowered and 20% O₂ cultures dramatically reduced the yield of dopaminergic neurons (Figure 15).

Peripheral nerve stem cells. A parallel story in peripheral nerve stem cells emerged in work performed by Sean Morrison in David Anderson's lab at Caltech. Neural crest stem cells were derived from e15 rat embryonic sciatic nerve (Morrison et al., 1999), then cultured in either 6% or 20% oxygen. These pluripotent cells can generate a variety of neurons and glia in culture and also self-renew in culture. Growth of the neural crest stem cells in low oxygen conditions yielded greater stem cell purity and increased stem cell proliferation. Apoptosis was not examined. In addition when the cells differentiated, low oxygen conditions were associated with an increased yield of the sympathetic neuron (a catecholaminergic) phenotype (manuscript submitted).

Preliminary data suggest increased yield of neurons in low oxygen cultures of newborn mouse retina compared to 20% oxygen conditions.

A well-characterized, robust mouse retinal progenitor culture system does not exist. Part of the difficulty in establishing murine retinal culture models is that retinal stem cells lose their multipotentiality quickly in the post-natal period. In fact, establishment of mouse clones from multipotent retinal progenitors required use of a mouse transgenic for the cell survival factor bcl-2 (Jensen and Raff, 1997). Neonatal rat precursors are used to study retinal development (Belliveau and Cepko, 1999), but much retinal development is studied in either zebrafish or frog, both of which have enormous regenerating capacity as adults.

We developed a mouse newborn retina culture system and divided the cultures between 6% and 20% oxygen conditions. The first observation was that retinal cultures survive longer in low oxygen. Invariably when the cells were grown in room air, the cultures were completely dead after 2 weeks. At that time, cultures grown in low oxygen continued to survive. Preliminary data suggested that some of the cell death seen in the 20% oxygen conditions was due

to apoptosis (Figure 15). Furthermore, after cultures were allowed to differentiate (by withdrawal of EGF), by gross examination, more neurons were generated in low oxygen than in 20% oxygen conditions. All wells of the low oxygen conditions contained some neurons as assessed by TuJ1 immunostaining, vs. only about half the wells in 20% oxygen. Furthermore, the size of neuronal clusters in low oxygen appeared larger than those in 20% oxygen on gross examination (Figure 16). We were able to identify rare dopaminergic neurons only in low oxygen (TH-positive) and none in 20% oxygen (not shown).

Discussion

Lowered O₂ culturing consistently enhanced proliferation of CNS stem cells by two- to four-fold during the proliferation phase when most cells are nestin-positive precursors. This increase in cell number was also maintained after mitogen withdrawal when proliferation was vastly reduced. Although more cells were present in differentiated cultures in lowered O₂, the proportions of neurons and glia were similar in the two O₂ conditions, though there was a tendency for more neurogenesis in lowered O₂. These results together with clonal analysis

confirm that nestin-positive precursors expanded in lowered O_2 have stem cell properties.

In neural tissue, there is one supporting, though specialized, precedent for mitogenic activity of lowered O_2 in neural crest-derived carotid body chromaffin cells (Nurse and Vollmer, 1997). These dopaminergic glomus cells are functionally specialized O_2 -sensitive chemoreceptors, and so would be expected to specifically respond to arterial O_2 levels.

Neurobiologists often use hippocampal slices as models for studying long-term potentiation and other processes. These slices, by universal consensus, are extremely sensitive to hypoxic conditions. The slices are often maintained by bubbling through 95% oxygen. On the other hand, hippocampal neurons are usually cultured on coverslips which are turned upside down after the cells become adherent, and the ability to maintain these cultures has been attributed to low oxygen levels in the resultant sandwich. Reduced oxygen culturing (9%) has, in addition, been shown to increase survival and development of these neurons in culture (Brewer and Cotman, 1989).

Less apoptosis occurs in CNS stem cells cultured in lowered O₂. There is a potential toxic role for reactive oxygen intermediates (ROI) produced in room air cultures. However, it cannot simply be assumed that 20% O₂ cultures generate more oxidative stress than lowered O₂ cultures, since free radicals are generated in frankly ischemic conditions (Perez Velasquez et al., 1997). In fact, perinatal hypoxic injury to brain, still unfortunately common, is now thought to be mediated partly by oxidative stress (Taylor et al., 1999).

CNS stem cells can give rise to multiple neuron types (Johe et al., 1996; Gritti et al., 1996; Kalyani et al., 1998), and the midbrain has been extensively studied as model for neuron subtype specification (Hynes et al., 1995; Ye et al., 1998; Wang et al., 1995; Ericson et al., 1995; Hynes and Rosenthal, 1999). Recently, conditions were established to allow midbrain precursors to differentiate into dopaminergic neurons in vitro (Studer et al., 1998). Here we show that 56% of neurons generated from mesencephalic precursors in lowered O₂ are TH-positive, a marked increase over previous reports. For example, adenoviral-mediated gene transfer to CNS precursors similar to those used in our study led to a 65-84% increase in TH-positive neurons

(Choi-Lundberg et al., 1997). In our studies, with a three-fold expansion in stem cells and a three-fold expansion in the fraction of neurons that are dopaminergic, oxygen was at least ten times as effective as GDNF gene therapy in promoting dopaminergic neuron survival. Exposure to lowered O₂ was most effective in generating dopaminergic neurons during precursor expansion. These results suggest that lowered O₂ conditions enhance the production of ventral fates by a mechanism that acts prior to differentiation.

In the developing brain the initial specification events for dopaminergic neuronal development are mediated through the diffusible factors, SHH and FGF8, thought necessary and sufficient for dopaminergic neuron induction. A gradient of sonic hedgehog (SHH) signaling establishes neuronal identity in the hindbrain (Briscoe et al., 1999) and SHH induces dopaminergic neuron differentiation in explants of the early neural plate (Hynes et al., 1995; Ye et al., 1998; Wang et al., 1995). Later transcriptional mediators of further dopaminergic neuron development include Nurr1, the steroid orphan nuclear receptor, the homeobox gene Ptx1, aldehyde dehydrogenase 2 (Wallen et al., 1999), and En1. Nurr1-deficient mice lack specific populations of

dopaminergic neurons, most importantly those in the substantia nigra and ventral tegmentum, but other populations of dopaminergic neurons develop normally such as those in hypothalamus and diencephalon (Le et al., 1999). Ptx3 expression is restricted to mesencephalic dopaminergic neurons (Smidt et al., 1997). However, Ptx3 expression does not compensate for absence of Nurr1 and Ptx-expressing dopaminergic precursors without Nurr1 undergo apoptosis (Saucedo-Cardenas et al., 1998). Nurr1 plays a role in regulating transcription of tyrosine hydroxylase (Sakurada et al., 1999) and the dopamine transporter (Sacchetti et al., 1999), which mediates reuptake of dopamine from nerve terminals.

Our results suggest that local oxygen levels may play a role at several levels in the dopaminergic developmental pathway. Transcript levels of FGF8 and En1 (Ye et al., 1998; Simone et al., 1998; Shamim et al., 1999), were upregulated in lowered vs. 20% O₂. FGF8 has also been implicated in the commitment of serotonergic neurons (Ye et al., 1998). These findings are consistent with a role for FGF8 in the expansion of dopaminergic and serotonergic neuronal subtypes seen in lowered O₂ cultures. However, addition of FGF8 to 20% O₂ cultures or neutralization of

FGF8 in lowered O₂ did not reproduce the O₂-dependent neuronal subtype differentiation patterns.

En1 mRNA and protein expression were increased in lowered O₂. En1 is thought to act in a pathway with pax2, wnt-1 and FGF8 to regulate the fate of midbrain neurons (Joyner, 1996; Danelian et al., 1996; Wurst et al., 1994, Simone et al., 1998). The FGF8 gene contains a binding site for En1 (Gemel et al., 1999). In addition we found that the FGF8 5'-UTR (accession #AF065607) contains the sequence CCTCCCTCA known to control O₂ responsiveness in VEGF and EPO regulatory elements (Scandurro and Beckman, 1998). We have not yet determined if En1 acts as a direct upstream regulator of FGF8 in our lowered O₂ cultures, or whether they act independently. Nonetheless, the prominent expression of En1 in young neurons suggests it may be a good candidate for regulating neuronal subtype differentiation. In preliminary data we also found increased mRNA abundance for the dopamine transporter at the end of expansion in low oxygen cultures.

EPO levels are known to be regulated by oxygen, and in the brain, asphyxia is associated with increased EPO production of sufficient magnitude to be measured in cerebrospinal

fluid (Juul et al., 1999). EPO and its receptor are expressed in brain from early development through adulthood (Juul et al., 1999a), but no specific role for EPO in CNS development has been described. EPO is thought to be produced by astrocytes with its receptor on neurons, but detailed receptor expression patterns have not been reported. Septal cholinergic neurons are likely to have EPO receptor since EPO significantly improves survival of these cells after fimbria-fornix transection (Konishi et al., 1993). The blood brain barrier is not permeable to EPO, and the paracrine loop of EPO and its receptor in CNS functions in isolation from hematologic effects.

In the adult CNS, however, EPO has received attention as a neuroprotective agent (Sakanaka et al., 1998; Sadamoto et al., 1998), and EPO treatment of PC12 cells has been demonstrated to increase intracellular monoamine levels (Masuda et al., 1993). EPO-mediated increases in dopaminergic neuron yield in 20% O₂ were dose-dependent (not shown), but no additional increase in yield was mediated by EPO in lowered O₂, suggesting that EPO in lowered O₂ was at maximal functional level for this response. Though EPO supplementation of 20% O₂ cultures significantly improves dopaminergic yield, the full effect

of lowered O_2 was not recapitulated, suggesting that additional factors promote dopaminergic differentiation in lowered O_2 . Furthermore, EPO message was not detected until after differentiation, and lowered oxygen restricted to the expansion phase had a major impact on dopaminergic differentiation and survival.

A variety of growth factors mediates survival of transplanted dopaminergic neurons. These include GDNF, bFGF and IGF-1 (Zawada et al., 1998). IGF's and insulin are known to increase EPO expression in cultured astrocytes in physiologic (2% and 5% O_2) and 20% O_2 , with IGF-1 the most potent (Masuda et al., 1997). A neurotrophic sequence in EPO was identified which appears to mediate survival and sprouting in neuroblastoma lines, but does not affect proliferation in mouse spleen cells or erythropoietic cell lines (Campana et al., 1998). EPO may act in the protection of dopaminergic neurons partly as an antioxidant (Bany-Mohammed et al., 1996). In culture, EPO protects neurons from nitric oxide-induced death (Sakanaka et al., 1998). EPO also protects cultured neurons from glutamate toxicity (Morishita et al., 1998). EPO may act as an anti-apoptotic agent (Quelle et al., 1998) as it does in erythroid progenitors (Koury and Bondurant, 1990). These

mechanisms certainly deserve further investigation. Our finding that EPO affects the differentiation patterns of expanded CNS precursors is novel and identifies EPO as a component of increased dopaminergic neuron yield in lowered O₂ conditions, and as a potential mediator of dopaminergic neuron survival during development.

A recent report highlighted increased dopamine content after differentiated dopaminergic mesencephalic neurons were exposed to 0% O₂ conditions (Gross et al., 1999). Others have previously reported release of dopamine after hypoxic stress, probably as a pathologic depolarizing event (Kuo et al., 1998). Another study described a relative increase in TH-expressing neurons in primary neuronal cultures from E14 rats after exposure to 5% O₂ (Colton et al., 1995). It is also known that hypoxic conditions favor expression of the TH gene (Czyzyk-Krzeska et al., 1994; Paulding and Czyzyk-Krzeska, 1999). In our studies, TH upregulation in response to low oxygen was modest at the message level, but significant protein accumulation was demonstrated by western analysis. In one experiment, significantly more message for the dopamine transporter (another phenotypic marker for dopaminergic neurons)

accumulated in low oxygen conditions at the end of the expansion phase (not shown).

Our results suggest that O_2 levels much lower than those traditionally used in culture are useful in mimicking in vivo phenomena. Lowered O_2 culturing has the practical implication of contributing to a more efficient production of dopaminergic neurons for transplant therapy in Parkinson's disease. In fact, current theories of the pathophysiology of Parkinson's disease center on oxidative damage to dopaminergic neurons. Oxidation of dopamine itself locally leads to production of reactive oxygen intermediates, and pathologic sections from striatum of patients with Parkinson's disease suggests that they are deficient in antioxidant enzymes, GSH peroxidase and catalase (Ibi et al., 1999). (GSH peroxidase detoxifies H_2O_2 to H_2O .)

Recently adult neural stem cells were demonstrated to have hematopoietic capacity (Bjornson et al., 1999). Our analysis of differentiation phenotypes included only cells with neuronal or glial markers. The methods of analysis did not account for all cells, and it remains possible that some blood cells were generated in our cultures.

Hematopoietic potential of CNS stem cells as a function of oxygen microenvironment deserves further investigation.

Figure legends**Figure 1.**

Effect of lowered O₂ on precursor yield in vitro at varying plating densities.

Striatal cultures were expanded with bFGF in lowered or 20% O₂, and total cell numbers assessed after 5 days of proliferation when over 95% of cells were nestin-positive precursors. Significantly increased cell numbers were detected at all plating densities in lowered O₂ compared to 20% O₂.

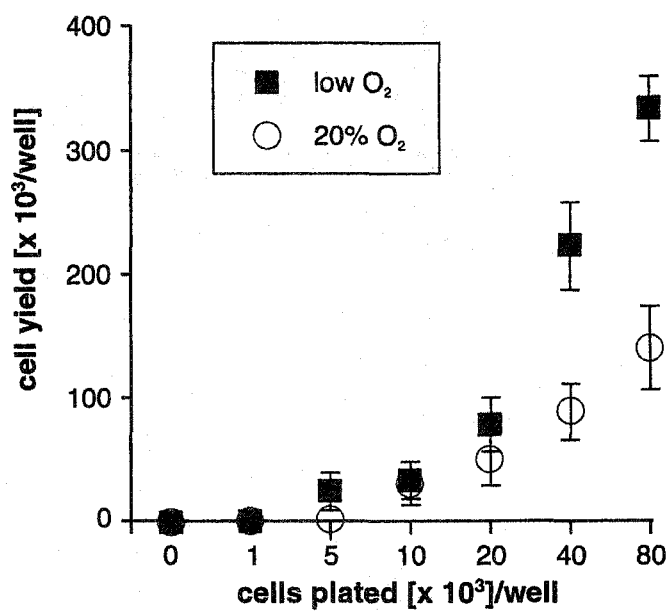


Figure 1.

Figure 2.

Mesencephalic precursors had increased rates of BrdU incorporation during expansion and differentiation when cultured in low vs. 20% oxygen.

- A. anti-BrdU immunohistochemistry after 1 hour BrdU pulses at various times in culture.
- B. Tabulation of cell counts: BrdU-positive and total cells were counted, then results graphed as a percentage of BrdU-positive cells at three times in culture.

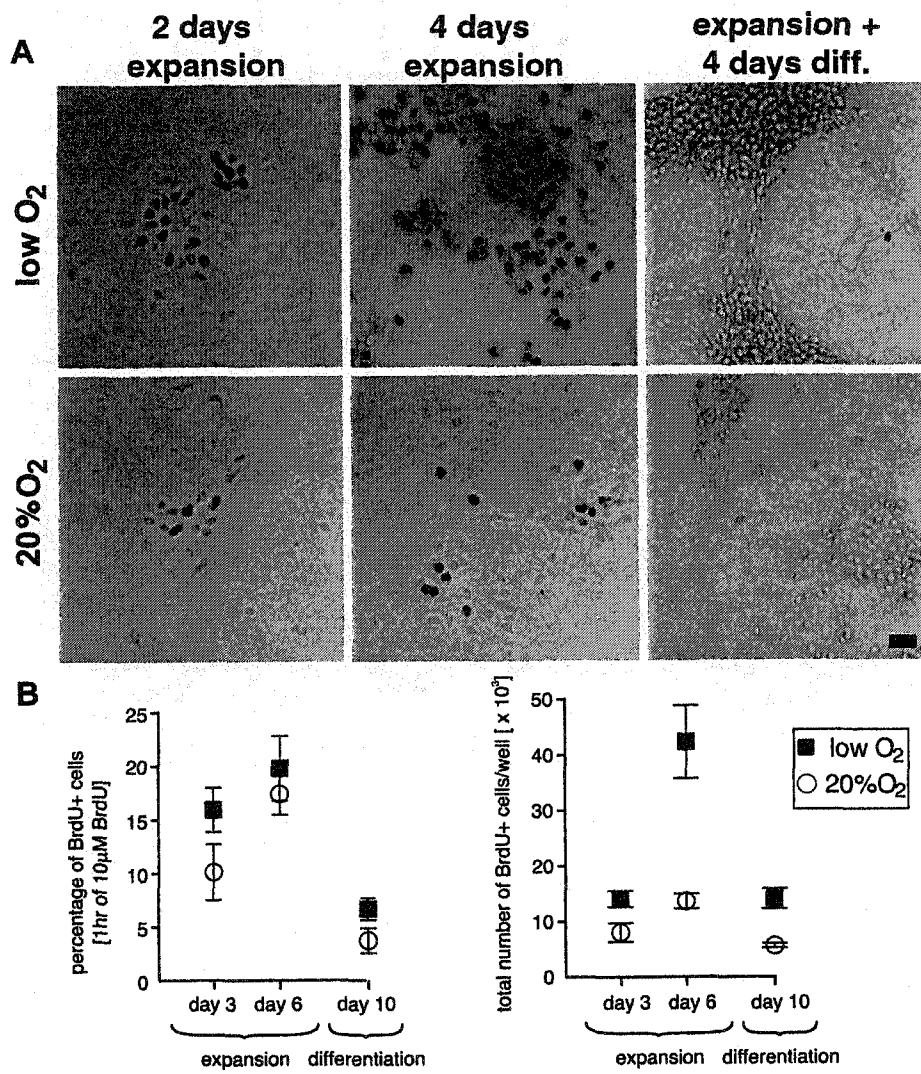


Figure 2.

Figure 3.

CNS precursors cultured in lowered (vs. 20%) O₂ have reduced rates of apoptosis.

- A. TUNEL labeling of mesencephalic precursors showed that precursors cultured in lowered O₂ had significantly less apoptosis than cells cultured in traditional conditions.
- B. Tabulation of cell counts (TUNEL-positive/total cells)

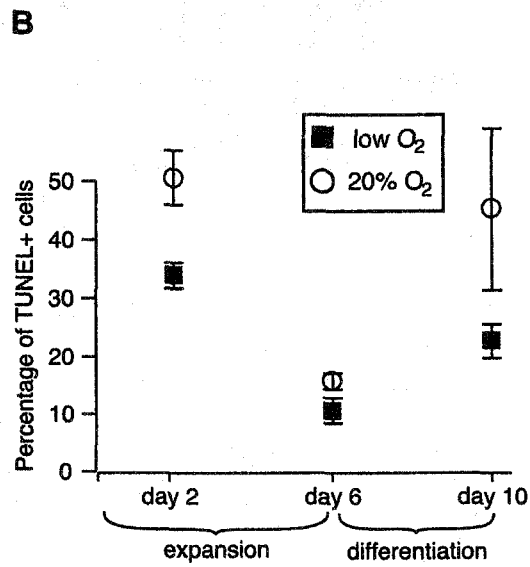
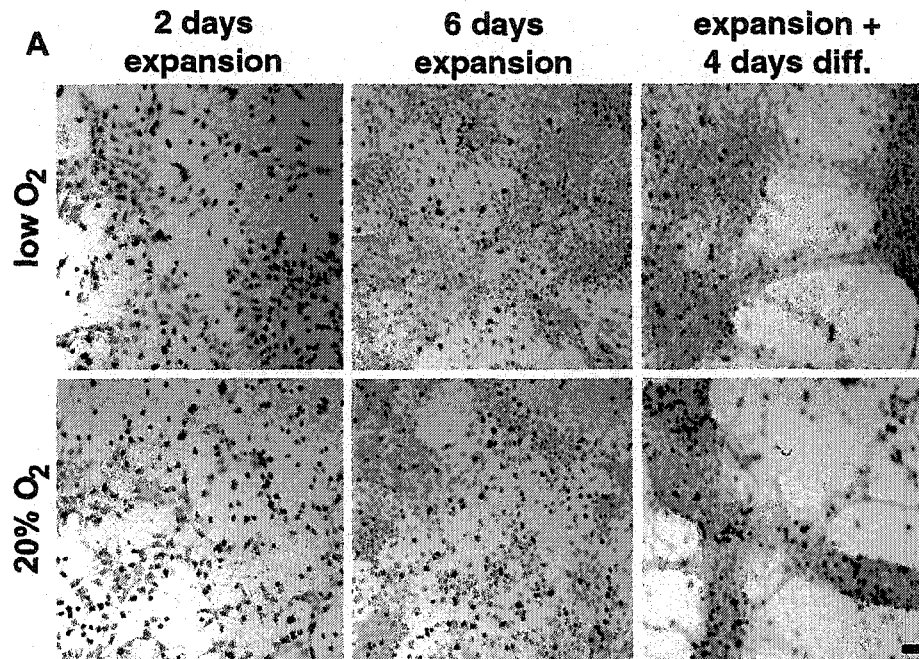


Figure 3.

Figure 4.

A. Human CNS precursors grown in 20% oxygen for 13 days displayed many apoptotic (brown/black) cells.

B. The same precursors grown in 2% oxygen had a significantly lower rate of apoptosis.

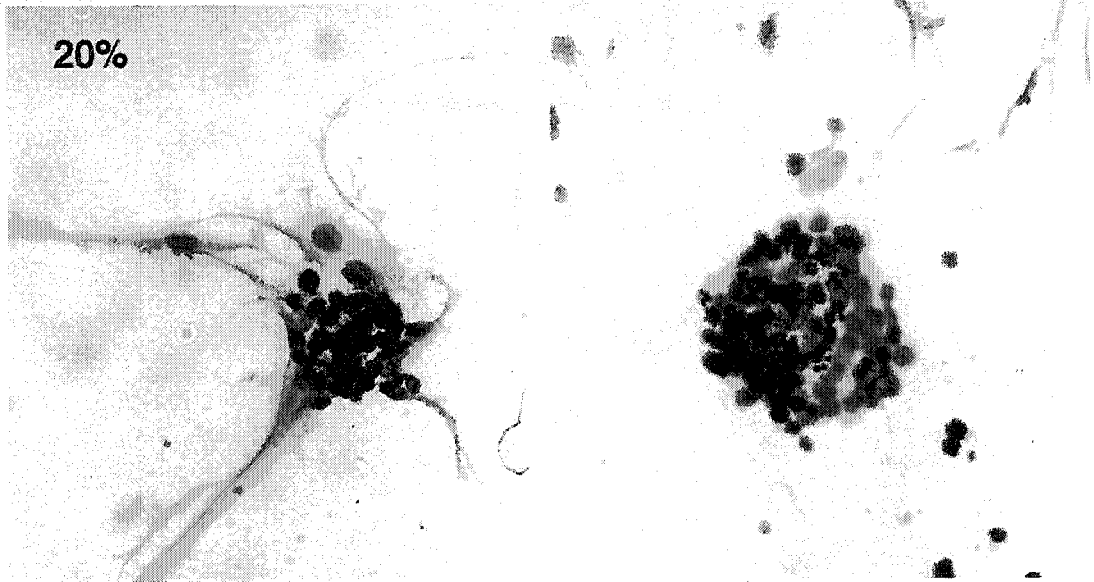


Figure 4A.

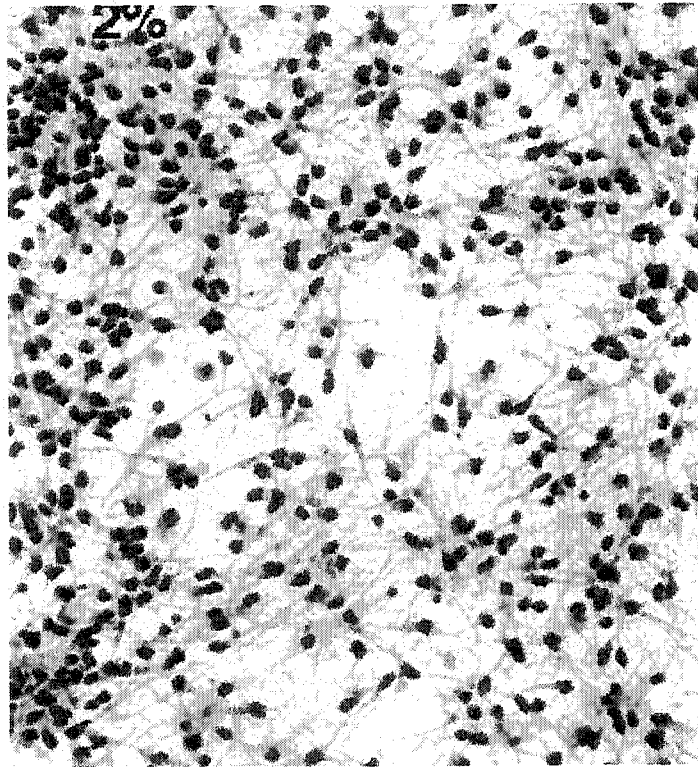


Figure 4B.

Figure 5.

Striatal precursors expanded for 5 days in bFGF-containing growth medium, then allowed to differentiate for 5 days after bFGF withdrawal in either low or 20% oxygen.

Immunocytochemistry was performed to identify nestin-positive precursors, Tuj1-positive neurons, GalC-positive oligodendrocytes, and GFAP-positive astrocytes. A greater percentage of neurons (46% vs. 34%) were generated in low oxygen vs. 20% oxygen, as well as astrocytes (6% vs. 2%), both $p < 0.05$. Nestin immunoreactivity was grossly reduced at the end of this differentiation period in low oxygen conditions.

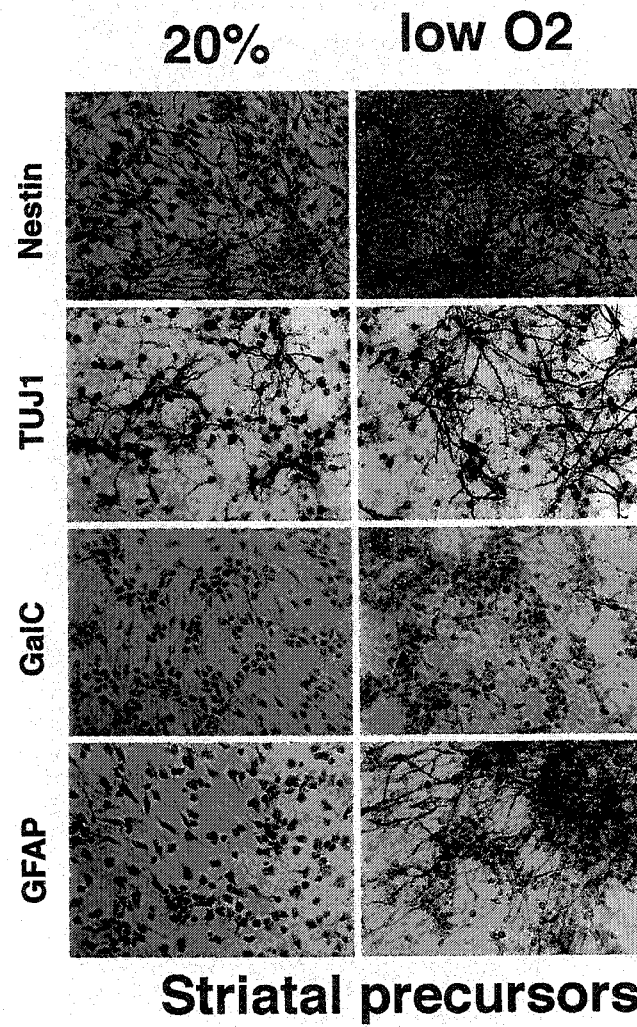


Figure 5.

Figure 6.

O4 immunoreactivity showing early oligodendrocytes appeared earlier in low oxygen vs. 20% oxygen conditions.

A. Two days after bFGF withdrawal early oligodendrocytes could not be detected by immunohistochemistry.

B. A small proportion of cells were O4-immunoreactive in low oxygen conditions, characteristically in small clusters.

C. Higher power view of O4 staining in low oxygen cultures

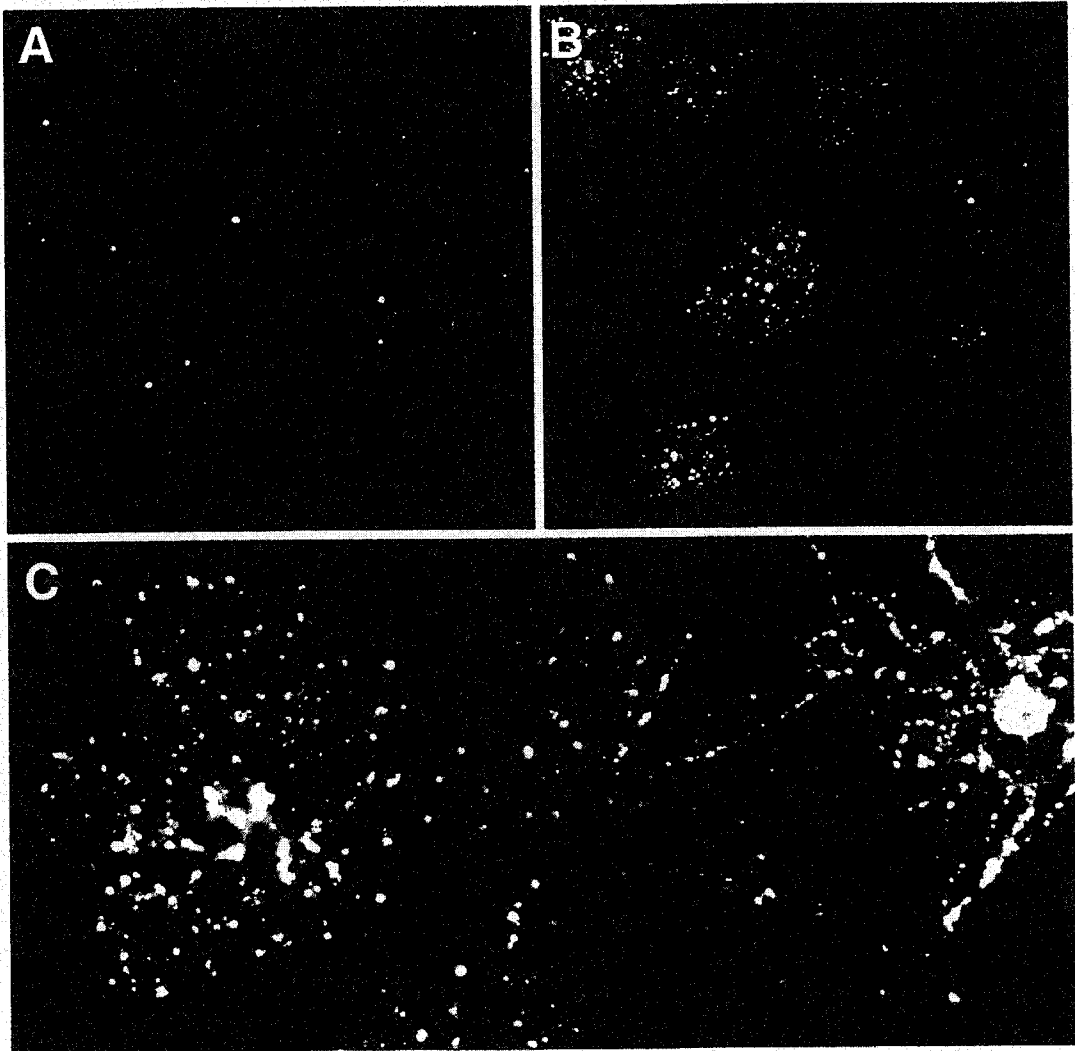


Figure 6.

Figure 7.

Immunohistochemistry performed after 5 days of differentiation of striatal precursors in either low or 20% oxygen.

In low oxygen clusters of dopaminergic neurons were common, whereas GABA-ergic neurons were more commonly identified in 20% oxygen cultures. Floor-plate cells and engrailed immunopositivity were more frequent in low vs. 20% oxygen. The neuroblast marker PSA-NCAM was less frequently identified in low oxygen than 20%, paralleling nestin-immunoreactivity patterns.

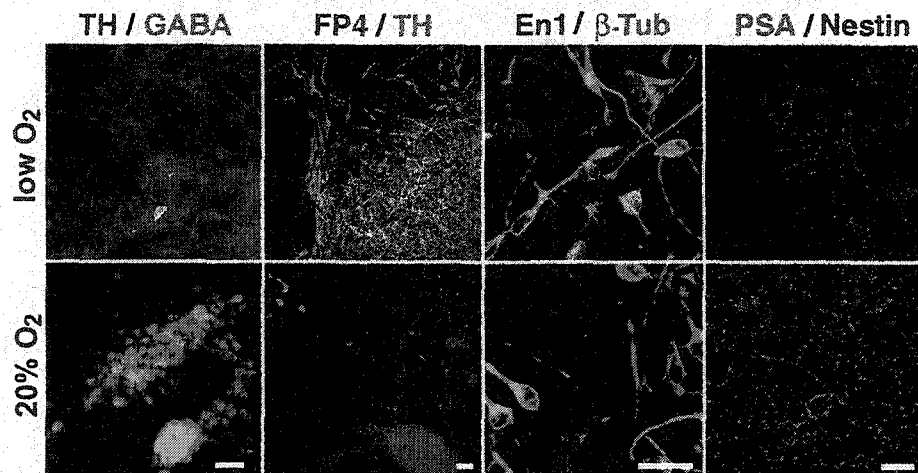


Figure 7.

Figure 8.

Clonal analysis of cultured CNS precursors.

The frequency of (multipotent) clone formation in low oxygen was three-fold greater in low vs. 20% oxygen cultures. In addition the average clone size was significantly larger in low oxygen conditions.

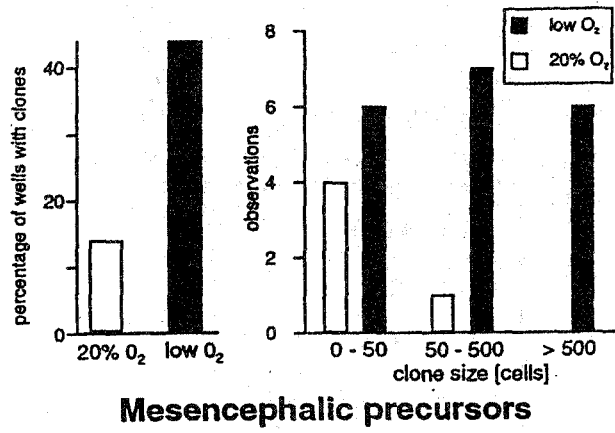


Figure 8.

Figure 9.

Neuronal subtype differentiation from mesencephalic precursors in lowered vs. 20% O₂.

Double immunocytochemical labeling revealed that lowered O₂ culturing markedly increased the representation of dopaminergic (TH) and serotonergic (Ser) neuronal (Tuj1+) subtypes, but decreased the representation of GABA+ and Glutamate+ neurons. Scale bars = 20 μm

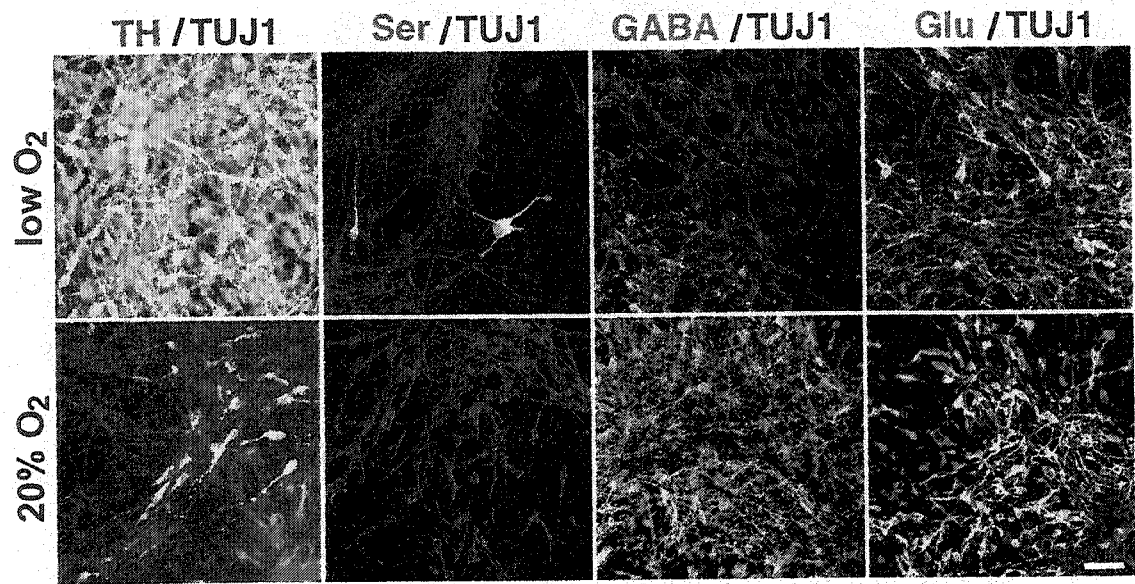


Figure 9.

Figure 10.

Western analysis of tyrosine hydroxylase protein.

Tyrosine hydroxylase protein was more abundant in extracts of differentiated CNS precursors grown in low vs. 20% oxygen conditions. (Each lane 2.5 μ g total protein.)

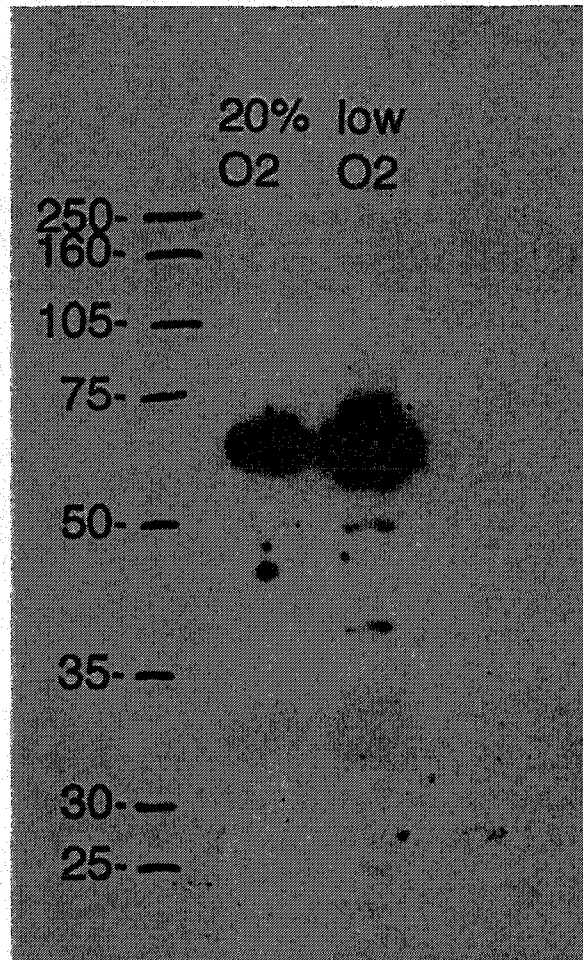


Figure 10.

Figure 11.

High pressure liquid chromatographic assessment of dopamine production from differentiated CNS precursors grown in either low or 20% oxygen.

rp-HPLC with electrochemical detection was used to quantify dopamine in culture media. Significantly more dopamine was detected in cultures maintained at lowered O₂ compared to those grown at 20% O₂. At left, dopamine content of 24-hour conditioned medium revealed significantly more dopamine in medium from low oxygen cultures, as did basal release in HBSS, and evoked release after KCl was added. A typical chromatogram for dopamine detection in lowered and 20% O₂ cultures is shown on the right.

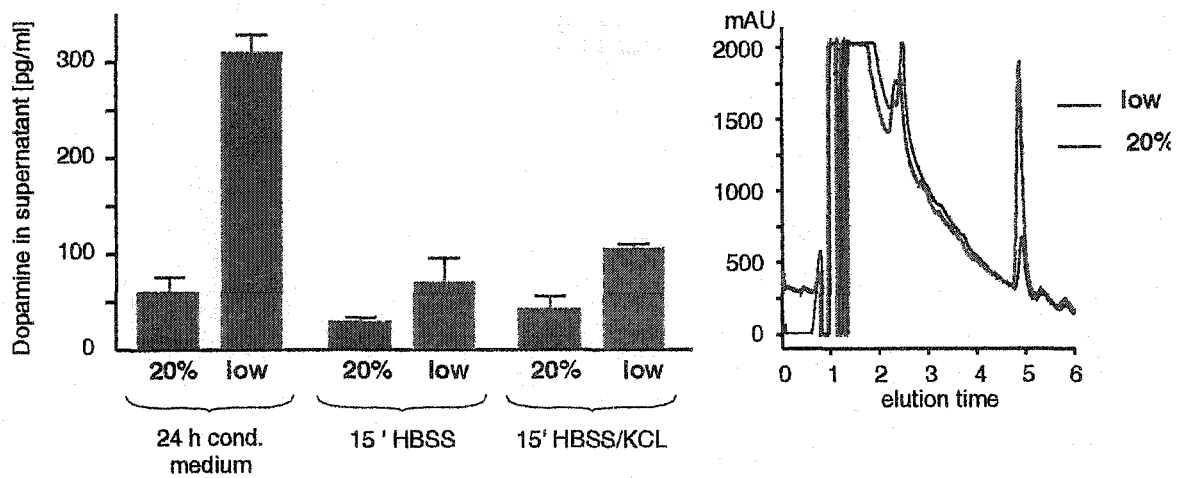


Figure 11.

Figure 12.

Low oxygen culturing during expansion of CNS precursors is critical for the augmented yield of dopaminergic neurons.

In order to test whether low oxygen exerted its effect on dopaminergic neuron yield during expansion or differentiation, cells were grown in low oxygen then either maintained in low oxygen or switched to 20% oxygen. Another group of precursors was grown in 20% oxygen then either maintained in 20% oxygen or switched to low oxygen at the time of bFGF withdrawal.

The major effect of low oxygen on augmenting dopaminergic neuron yield is during expansion of precursors. Cultures maintained in low oxygen but differentiated in 20% oxygen regenerated almost as many dopaminergic neurons as those cells grown in low oxygen throughout. Cultures switched from 20% oxygen to low oxygen at the time of differentiation had greater dopaminergic neuron yield than those grown at 20% throughout, but these yields were significantly lower than those from any cultures expanded in low oxygen.

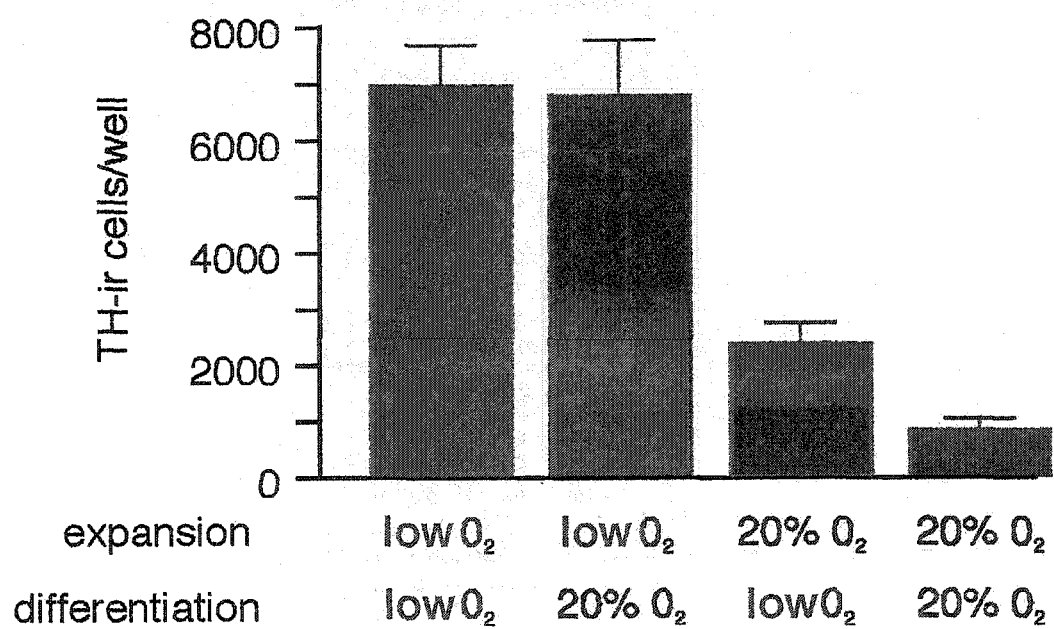


Figure 12.

Figure 13.

Differential gene expression in mesencephalic precursors at lowered and 20% O₂ assessed by semiquantitative RT-PCR.

Candidate genes involved in midbrain development were tested for O₂-dependent differential expression. Increased expression of TH and Ptx-3 during differentiation confirmed the larger number of functional dopaminergic neurons in lowered O₂ cultures. Significant lowered O₂-mediated changes in expression of En1 and especially FGF8 were also detected. TH expression was not dramatically upregulated in low oxygen conditions.

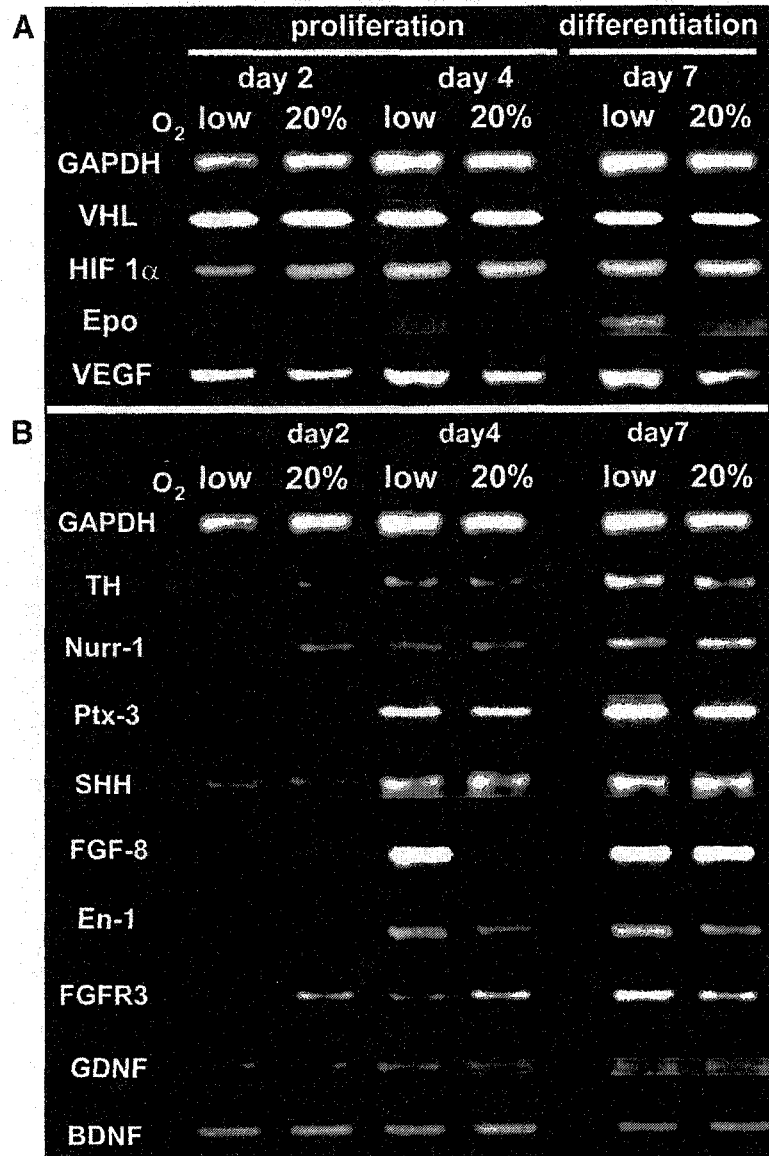


Figure 13.

Figure 14.

Expression of genes involved in the physiological response to changes in O₂ analyzed by semiquantitative RT-PCR.

Messages for EPO and von Hippel Lindau protein (involved in regulation of HIF-1 α) were assessed after 2 or 6 days of expansion and after differentiation (day 4 of differentiation = day 10 of culture) in lowered and 20% O₂. Data are normalized to GAPDH expression. EPO message, as expected, was more abundant in low oxygen cultures vs. 20% oxygen after differentiation.

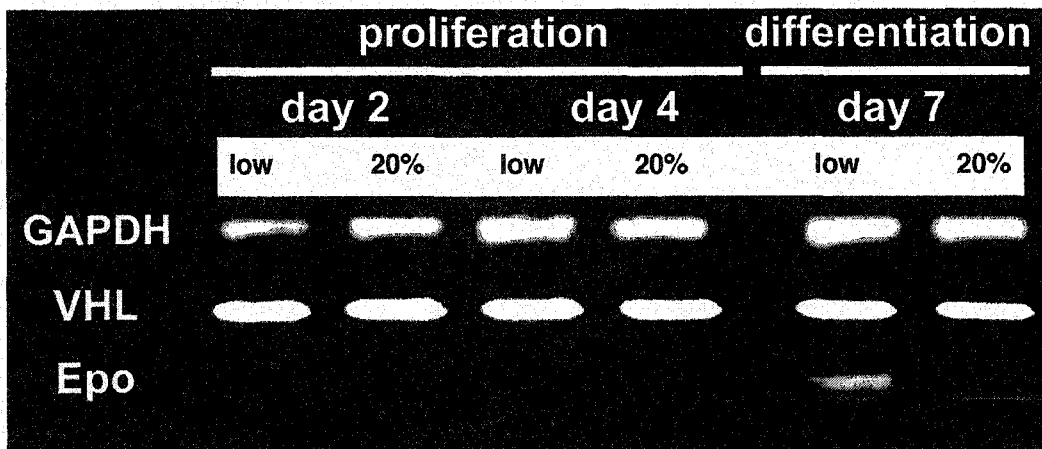


Figure 14.

Figure 15.

EPO mimics the lowered O₂ effect on dopaminergic differentiation.

Saturating concentrations of EPO or EPO neutralizing antibody were added to E12 mesencephalic precursor cultures during both proliferation and differentiation phase (10 days total) in lowered or 20% O₂. EPO supplementation significantly increased TH+ cell numbers in 20% O₂ cultures (n=6, p < 0.05). EPO neutralizing antibody decreased TH+ cell numbers in both lowered O₂ (n=6, p < 0.01) and 20% O₂ cultures (n=6, p < 0.05). Scale bar = 20µm.

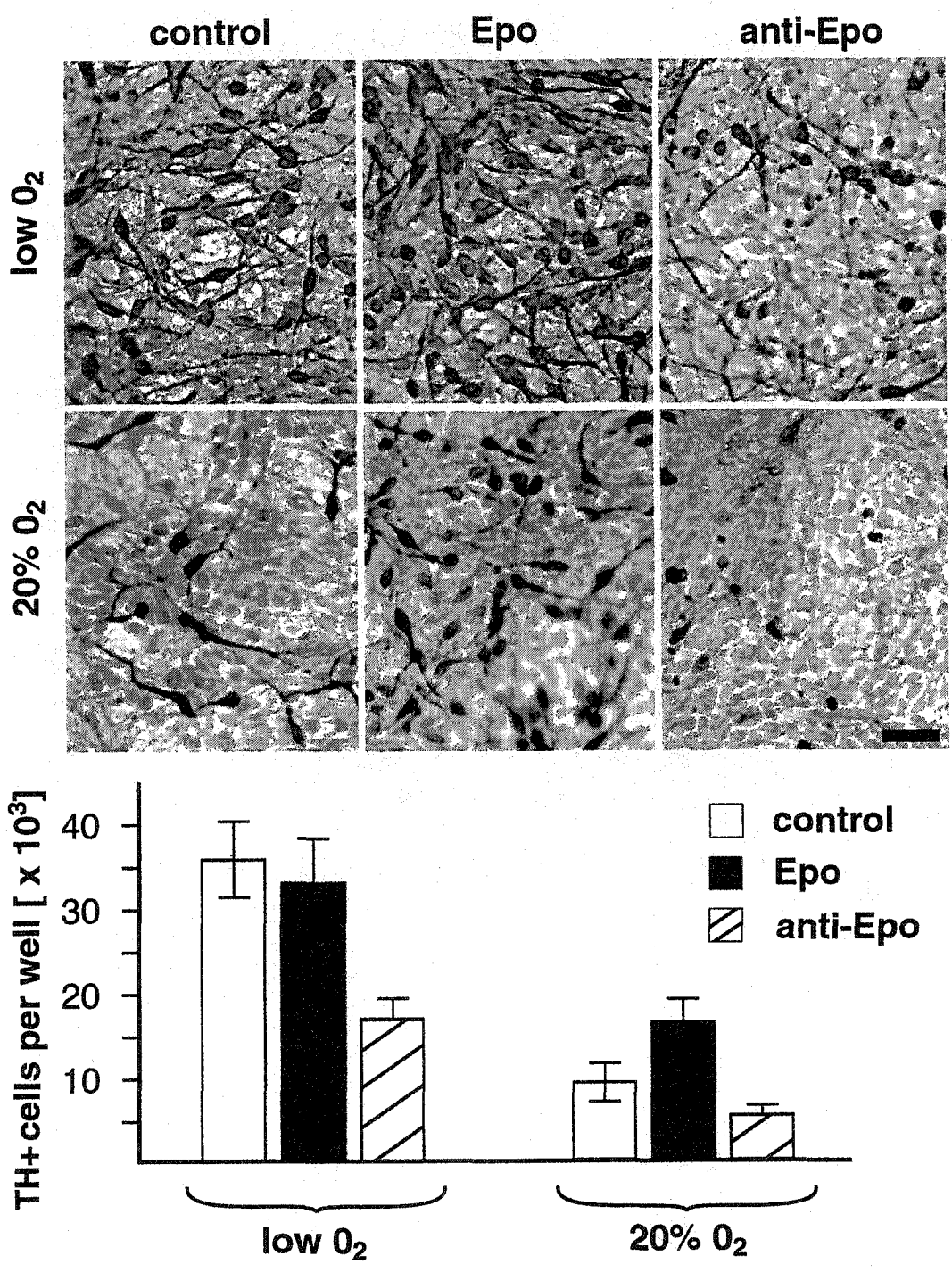


Figure 15.

Figure 16.

6% oxygen compared to 20% oxygen, indicating a lower TUNEL analysis of retinal precursors cultured in either 6% or 20% oxygen for one week.

- A. DAPI (top). Many cells with intense fluorescence (green, bottom) in 20% oxygen, indicating a high rate of apoptosis.

- B. DAPI (top). Fewer cells with intense fluorescence indicating a lower rate of apoptosis in low oxygen than in 20% cultures.

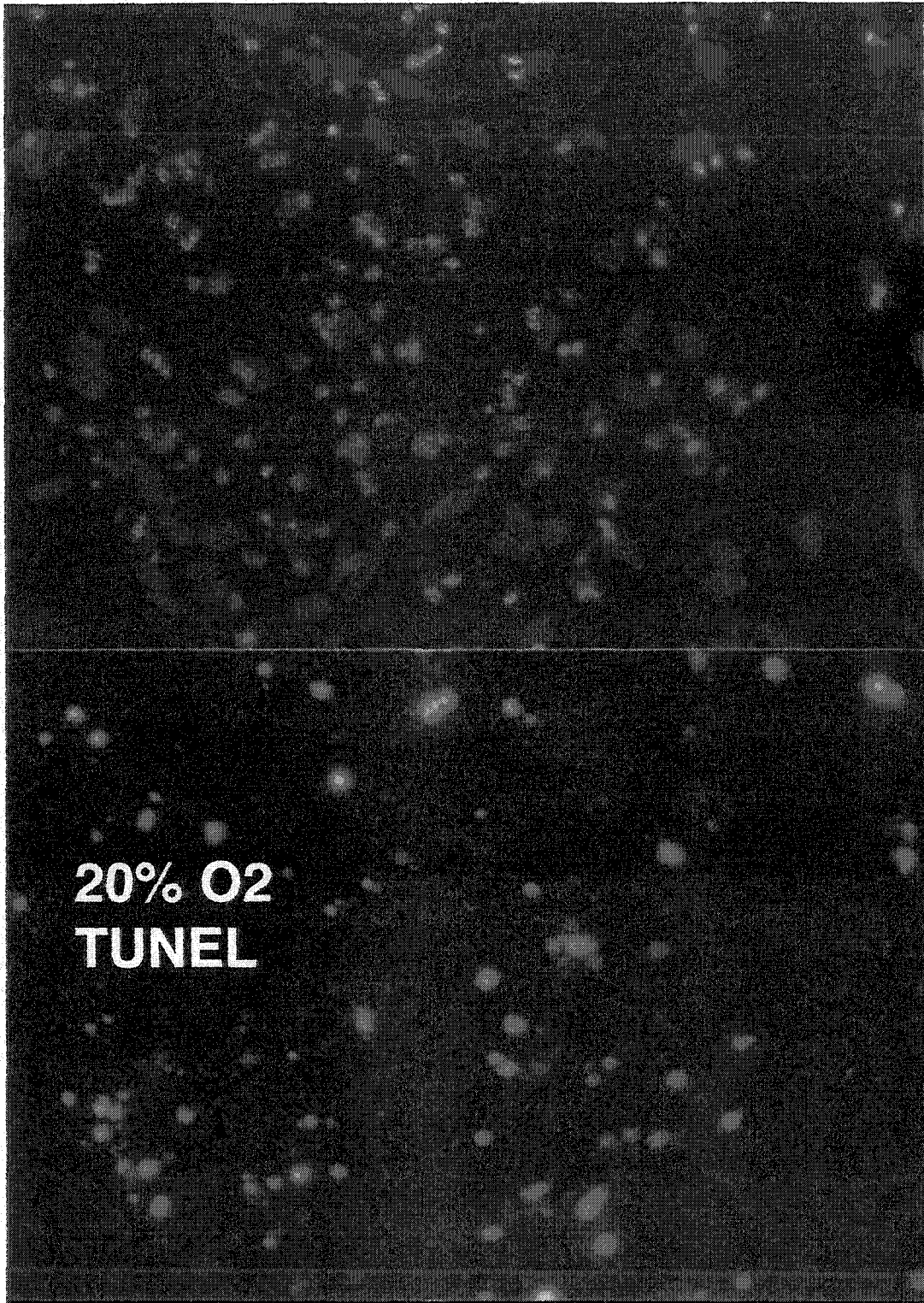


Figure 16A.

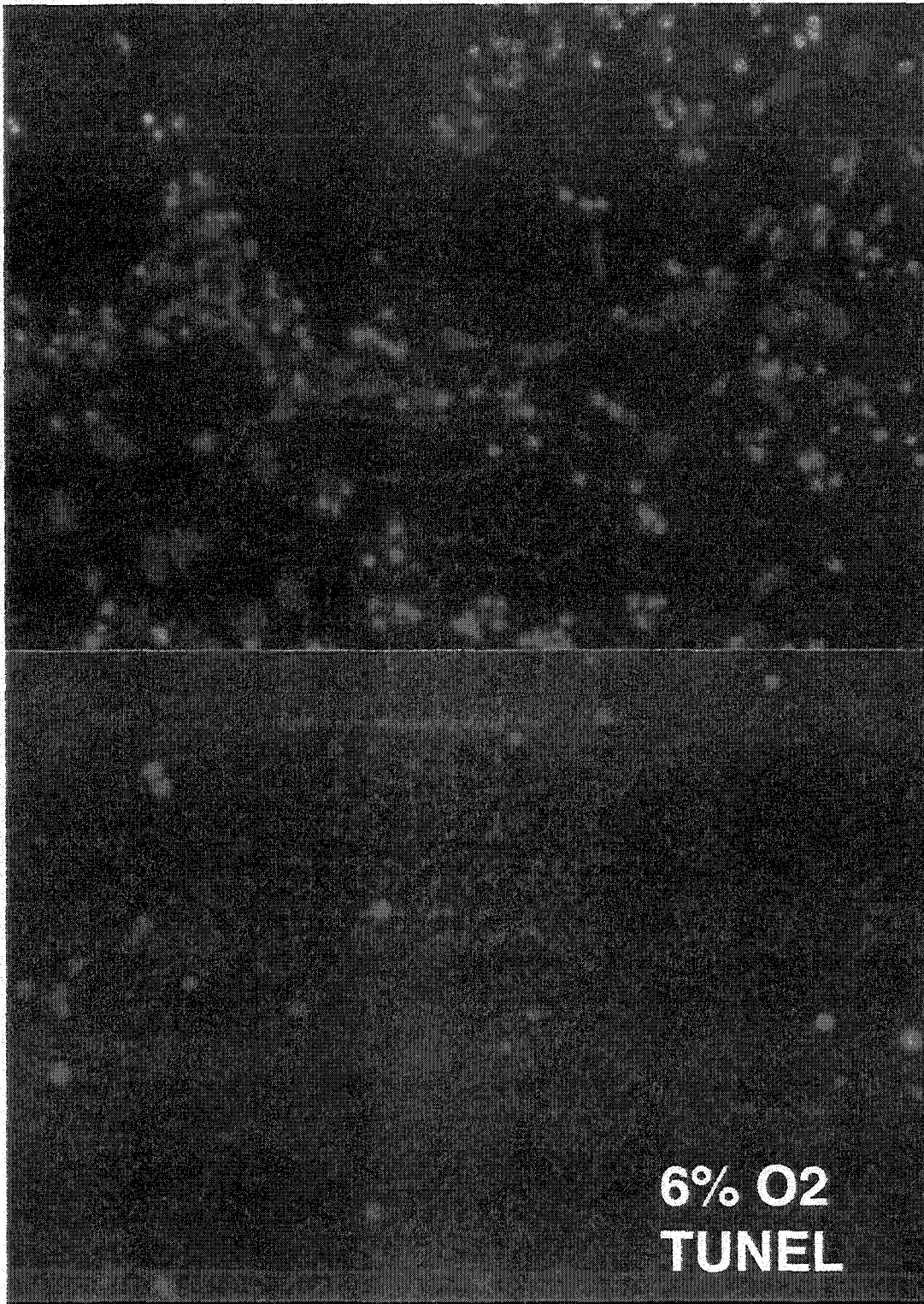


Figure 16B.

Figure 17.

TOP: Immunohistochemical stain for neurons (Tuj1 staining) in retinal cultures grown in 20% oxygen for 2 weeks. Small clusters (or single) neurons were present in about half the cultures.

BOTTOM: Neuron clusters, identified by immunoreactivity to Tuj1 antibody, were observed in all retinal cultures grown in 6% oxygen after 2 weeks.

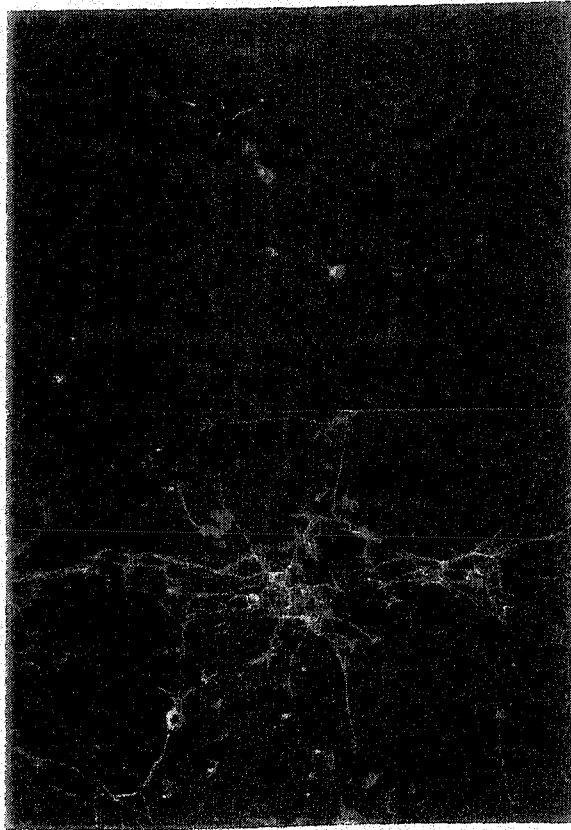


Figure 17.

References

- Bany-Mohammed, F.M., Slivka, S., Hallman, M. (1996). Recombinant human erythropoietin: possible role as an antioxidant in premature rabbits. *Pediatr. Res.* 40, 381-387.
- Belliveau, M.J., Cepko, C.L. (1999). Extrinsic and intrinsic factors control the genesis of amacrine and cone cells in the rat retina. *Development* **126**, 555-566.
- Bjornson, C.R.R., Rietze, R.L., Reynolds, B.A., Magli, M.C., Vescovi, A.L. (1999). Turning brain into blood: A hematopoietic fate adopted by adult neural stem cells in vivo. *Science* **283**, 534-537.
- Brewer, G.J., Cotman, C.W. (1989). Survival and growth of hippocampal neurons in defined medium at low density: advantages of a sandwich culture technique or low oxygen. *Brain Res.* **494**, 65-74.
- Briscoe, J., Sussel, L., Serup, P., Hartigan-O'Connor, D., Jessell, T.M., Rubenstein, J.L.R., Ericson, J. (1999). Homeobox gene *Nkx2.2* and specification of neuronal identity by graded Sonic hedgehog signalling. *Science* **398**, 622-627.

- Campana, W.M., Misasi, R., O'Brien, J.S. (1998). Identification of a neurotrophic sequence in erythropoietin. *Bioorg. Med. Chem. Lett.* **1**, 235-241.
- Choi-Lundberg, D.L., Lin, Q., Chang, Y-N., Chiang, Y.L., Hay, C.M., Mohajeri, H., Davidson, B.L., Bohn, M.C. (1997). Dopaminergic neurons protected from degeneration by GDNF gene therapy. *Science* **275**, 838-841.
- Colton, C.A., Pagan, F., Snell, J., Colton, J.S., Cummins, A., Gilbert, D.L. (1995). Protection from oxidation enhances the survival of cultured mesencephalic neurons. *Exper. Neurol.* **132**, 54-61.
- Czyzyk-Krzeska, M.F., Furnari, B.A., Lawson, E.E., Millhorn, D.E. (1994) Hypoxia increases rate of transcription and stability of tyrosine hydroxylase mRNA in pheochromocytoma (PC12) cells. *J. Biol. Chem.* **269**, 760-764.
- Danelian, P.S., McMahon, A.P. (1996). Engrailed-1 as a target of the Wnt-1 signalling pathway in vertebrate midbrain development. *Nature* **383**, 332-334.
- Echelard, Y., Epstein, D.J., St-Jacques, B., Shen, L., Mahler, J., McMahon, J.A., McMahon, A.P. (1993). Sonic hedgehog, a member of a family of putative

signaling molecules, is implicated in the regulation of CNS polarity. *Cell* **75**, 1417-1430.

Ericson, J., Muhr, J., Placzek, M., Lints, T., Jessell, T.M., Edlund, T. (1995). Sonic hedgehog induces the differentiation of ventral forebrain neurons: A common signal for ventral patterning within the neural tube. *Cell* **81**, 747-756.

Freeman, T.B., Vawter, D.E., Leaverton, P.E., Godbold, J.H., Hauser, R.A., Goetz, C.G., Olanow, C.W. (2000). Use of placebo surgery in controlled trials of a cellular-based therapy for Parkinson's disease. *N. Engl. J. Med.* **341**, 988-992.

Gage, F.H., Ray, J., Fisher, L.J. (1995). Isolation, characterization, and use of stem cells from the CNS. *Annu. Rev. Neurosci.* **18**, 159-192.

Gage, F.H. (2000). Mammalian neural stem cells. *Science* **287**, 1433-1438.

Gemel, J., Jacobsen, C., MacArthur, C.A. (1999). Fibroblast growth factor-8 expression is regulated by intronic engrailed and Pbx1-binding sites. *J. Biol. Chem.* **274**, 6020-6026.

Goda, F., O'Hara, J.A., Liu, K.J., Rhodes, E.S., Dunn, J.F., Swartz, H.J. (1997). Comparisons of measurements of

pO₂ in tissue in vivo by EPR oximetry and micro-electrodes. *Adv. Exp. Med. Biol.* **411**, 543-549.

Gritti, A., Parati, E.A., Cova, L., et al. (1996). Multipotential stem cells from the adult mouse brain proliferate and self-renew in response to basic fibroblast growth factor. *J. Neurosci.* **16**, 1091-1100.

Gross, J., Ungethum, U., Andreeva, N., Heldt, J., Gao, J., Marschhausen, G., Altmann, T., Muller, I., Husemann, B., Andersson, K. (1999). Hypoxia during early developmental period induces long-term changes in the dopamine content and release in a mesencephalic cell culture. *Neuroscience* **92**, 699-704.

Gundersen, H.J., et al. Some new, simple and efficient stereological methods and their use in pathological research and diagnosis. (1988) *APMIS* **96**, 379-394.

Guyton, A.C., Hall, J.E., "Transport of oxygen and carbon dioxide in the blood and body fluids," In: *Textbook of Medical Physiology*, WB Saunders Co., Philadelphia, 1996, pp. 513-523.

Hazel, T. and Muller, T. (1998). Culture of neuroepithelial stem cells. In *Current Protocols in Neuroscience*, John Wiley and Sons, Inc., pp. 3.1.1-3.1.6.

- Hewett, S.J., Muir, J.K., Lobner, D., Symons, A., Choi, D.W. (1996). Potentiation of oxygen-glucose deprivation-induced neuronal death after induction of iNOS. *Stroke* **27**, 1586-1591.
- Husain, J., Juurlink, B.H. (1995). Oligodendroglial precursor cell susceptibility to hypoxia is related to poor ability to cope with reactive oxygen species. *Brain Res.* **698**, 86-94.
- Hynes, M., Poulsen, K., Tessier-Lavigne, M., Rosenthal, A. (1995). Control of neuronal diversity by the floor plate: Contact-mediated induction of midbrain dopaminergic neurons. *Cell* **80**, 95-101.
- Hynes, M., Rosenthal, A. (1999). Specification of dopaminergic and serotonergic neurons in the vertebrate CNS. *Curr. Opin. Neurobiol.* **9**, 26-36.
- Ibi, M., Sawada, H., Kume, T., Katsuki, H., Kaneko, S., Shimohama, S., Akaike, A. (1999). Depletion of intracellular glutathione increases susceptibility to nitric oxide in mesencephalic dopaminergic neurons. *J. Neurochem.* **73**, 1696-1703.
- Jensen, A.M., Raff, M.C. (1997). Continuous observation of multipotential retinal progenitor cells in clonal density culture. *Dev. Biol.* **188**, 267-279

- Johe, K.K., Hazel, T.G., Muller, T., Dugich-Djordjevic, M.M., McKay, R.D. (1996). Single factors direct the differentiation of stem cells from the fetal and adult central nervous system. *Genes Dev.* **10**, 3129-3140.
- Joyner, A.L. (1996). *Engrailed*, *Wnt*, and *Pax* genes regulate midbrain-hindbrain development. *Trends Genet.* **12**, 15-20.
- Juul, S.E., Stallings, S.A., Christensen, R.D. (1999). Erythropoietin in the cerebrospinal fluid of neonates who sustained CNS injury. *Pediatr. Res.* **46**, 543-547.
- Juul, S.E., Yachnis, A.T., Rojiani, A.M., Christensen, R.D. (1999). Immunohistochemical localization of erythropoietin and its receptor in the developing human brain. *Pediatr. Dev. Pathol.* **2**, 148-158.
- Kalyani, A.J., Piper, D., Mujtaba, T., Lucero, M.T., Rao, M.S. (1998). Spinal cord neuronal precursors generate multiple neuronal phenotypes in culture. *J. Neurosci.* **18**, 1856-1868.
- Kaplan, F.S., Brightman, C.T., Boytim, M.J., Selzer, M.E., Lee, V., Spindler, K., Silberberg, D., Black, J. (1986). Enhanced survival of rat neonatal cerebral cortical neurons at subatmospheric oxygen tensions in vitro. *Brain Res.* **384**, 199-203.

- Konishi, Y., Chui, D.H., Hirose, H., Kunishita, T., Tabira, T. (1993). Trophic effect of erythropoietin and other hematopoietic factors on central cholinergic neurons in vitro and in vivo. *Brain Res.* **609**, 29-35.
- Koos, B.J., Power, G.G. (1987). Predict fetal brain PO₂ during hypoxaemia and anemia in sheep. *J. Develop. Physiol.* **9**, 517-726.
- Koury, M.J., Bondurant, M.C. (1990). Erythropoietin retards DNA breakdown and prevents programmed death in erythroid progenitor cells. *Science* **248**, 378-381.
- Kuo, M.F., Song, D., Murphy, S., Papadopoulos, M.D., Wilson, D.F., Pastuszko, A. (1998). Excitatory amino acid receptor antagonists decrease hypoxia induced increase in extracellular dopamine in striatum of newborn piglets. *Neurochem. Int.* **32**, 281-299.
- Laszkiewicz, I., Mouzannar, R., Wiggins, R.C., Konat, G.W. (1999). Delayed oligodendrocyte degeneration induced by brief exposure to hydrogen peroxide. *J. Neurosci. Res.* **55**, 303-310.
- Lauro, K.L., LaManna, J.C. (1997). Adequacy of cerebral vascular remodeling following three weeks of hypobaric hypoxia. Examined by an integrated composite analytical model. *Adv. Exp. Med. Biol.* **411**, 369-376.

- Le, W., Conneely O.M., Zou, L., He, Y., Saucedo-Cardenas, O., Jankovic, J., Mosier, D.R., Appel, S.H. (1999). Selective agenesis of mesencephalic dopaminergic neurons in *Nurr1*-deficient mice. *Exp. Neurol.* **159**, 451-458.
- Lendahl, U., Zimmerman, L.B., McKay, R.D. (1990). CNS stem cells express a new class of intermediate filament protein. *Cell* **60**, 585-595.
- Liu, K.J., Hoopes, P.J., Rolett, E.L., Beerle, B.J., Azzawi, A., Goda, F., Dunn, J.F., Swartz, H.M. (1997). Effect of anesthesia on cerebral tissue oxygen and cardiopulmonary parameters in rats. *Adv. Exp. Med. Biol.* **411**, 33-39.
- Masuda, S., Nagao, M., Takahata, K., Konishi, Y., Gallyas, F. Jr., Tabira, T., Sasaki, R. (1993) Functional erythropoietin receptors of cells with neural characteristics - Comparison with receptor properties of erythroid cells. *J. Biol. Chem.* **268**, 11208-11216.
- Max, S.R., Bossio, A., Iacovitti, L. (1996) Co-expression of tyrosine hydroxylase and glutamic acid decarboxylase in dopamine differentiation factor-treated striatal neurons in culture. *Dev. Brain Res.* **91**, 140-142.

- Maxwell, P.H., Wiesener, M.S., Chang, G.W., Clifford, C.S., Vaux, E.C., Cockman, M.E., Wykoff, C.C., Pugh, C.W., Maher, E.R., Ratcliffe, P.J. (1999). The tumour suppressor protein VHL targets hypoxia-inducible factors for oxygen-dependent proteolysis. *Nature* **399**, 271-275.
- McKay, R.D. (1997). Stem cells in the central nervous system. *Science* **276**, 66-71.
- Morishita, E., Masuda, S., Nagao, M., Yasuda, Y., Sasaki, R. (1997). Erythropoietin receptor is expressed in rat hippocampal and cerebral cortical neurons, and erythropoietin prevents in vitro glutamate-induced neuronal death. *Neurosci.* **76**, 105-116.
- Morrison, S.J., White, P.M., Zock, C., Anderson, D.J. (1999). Prospective identification, isolation by flow cytometry, and in vivo self-renewal of multipotent mammalian neural crest stem cells. *Cell* **96**, 737-749
- Nieber, K. (1999). Hypoxia and neuronal function under in vitro conditions. *Pharmacol. Ther.* **82**, 71-86.
- Nurse, C.A., Vollmer, C. (1997) Role of basic FGF and oxygen in control of proliferation, survival, and neuronal differentiation in carotid body chromaffin cells. *Dev. Biol.* **184**, 197-206.

- Olanow, C.W., Kordower, J.H., Freeman, T.B. (1996). Fetal nigral transplantation as a therapy for Parkinson's disease. *Trends Neurosci.* **19**, 102-109.
- Panchinsion, D., Hazel, T., McKay, R. (1998). Plasticity and stem cells in the vertebrate nervous system. *Curr. Opin. Cell Biol.* **10**, 727-733.
- Paulding, W.R., Czyzyk-Krzeska, M.F. (1999) Regulation of tyrosine hydroxylase mRNA stability by protein binding, pyrimidine-rich sequence in the 3'untranslated region. *J. Biol. Chem.* **274**, 2532-2538.
- Paulson, O. B., Strandgaard, S. and Edvinsson, L. (1990) Cerebral autoregulation. *Cerebrovasc. Brain Metab. Rev.* **2**, 161-192.
- Perez Velazquez, J.L., Frantseva, M.V., Carlen, P.L. (1997). In vitro ischemia promotes glutamate-mediated free radical generation and intracellular calcium accumulation in hippocampal pyramidal neurons. *J. Neurosci.* **17**, 9085-9094.
- Quelle, F.W., Wang, J., Feng, J., Wang, D., Cleveland, J.L., Ihle, J.N., Zambetti, G.P. (1998). Cytokine rescue of p53-dependent apoptosis and cell cycle

arrest is mediated by distinct Jak kinase signaling pathways. *Genes Dev.* **12**, 1099-1107.

Sacchetti, P., Brownschidle, L.A., Granneman, J.G., Bannon, M.J. (1999). Characterization of the 5'-flanking region of the human dopamine transporter gene. *Brain Res. Mol. Brain Res.* **74**, 167-174.

Sadamota, Y., Igase, K., Sakanaka, M., Sato, K., Otsuka, H., Sakaka, S., Masuda, S., Sasaki, R. (1998). Erythropoietin prevents place navigation disability and cortical infarction in rats with permanent occlusion of the middle cerebral artery. *Biochem. Biophys. Res. Comm.* **253**, 26-32.

Sakanaka, M., Wen, T.C., Matsuda, S., Masuda, S., Morishita, E., Nagao, M., Sasaki, R. (1998) In vivo evidence that erythropoietin protects neurons from ischemic damage. *Proc. Natl. Acad. Sci.* **95**, 4635-4640.

Sakurada, K., Ohshima-Sakurada, M., Palmer, T.D., Gage, F.H. (1999). Nurr1, an orphan nuclear receptor, is a transcriptional activator of endogenous tyrosine hydroxylase in neural progenitor cells derived from the adult brain. *Development* **126**, 4017-4026.

Saucedo-Cardenas, O., Quintana-Hau, J.D., Le, W.D., Smidt, M.P., Cox, J.J., De Mayo, F., Burbach, J.P., Conneely, O.M. (1998). *Nurr1* is essential for the induction of the dopaminergic phenotype and the survival of ventral mesencephalic late dopaminergic precursor neurons. *Proc. Natl. Acad. Sci.* **95**, 4013-4018.

Scandurro, A.B., Beckman, B.S. (1998). Common proteins bind mRNAs encoding erythropoietin, tyrosine hydroxylase, and vascular endothelial growth factor. *Bioch. Biophys. Res. Comm.* **246**, 436-440.

Shamim, H., Mahmood, R., Logan, C., Doherty, P., Lumsden, A., Mason, I. (1999). Sequential roles for *Fgf4*, *En1* and *Fgf8* in specification and regionalisation of the midbrain. *Development* **126**, 945-959.

Silver, I., Erecinska, M. Oxygen and ion concentrations in normoxic and hypoxic brain cells. In *Oxygen Transport to Tissue XX*, 7-15, edited by Hudetz and Bruley, Plenum Press, New York (1988).

Simone, H.H., Saueressig, H., Wurst, W., Goulding, M.G., O'Leary, D.D. (1998). *En-1* and *En-2* control the fate of the dopaminergic neurons in the substantia nigra and ventral tegmentum. *Eur. J. Neurosci.* **10**, 389-399.

Smidt, M.P., van Schaick, H.S., Lanctot, C., Tremblay, J.J., Cox, J.J., van der Kleij, A.A., Wolterink, G., Drouin, J., Burbach, J.P. (1997). A homeodomain gene Ptx 3 has highly restricted brain expression in mesencephalic dopaminergic neurons. *Proc. Natl. Acad. Sci.* **94**, 13305-13310.

Studer, L., Psylla, M., Buhler, B., Evtouchenko, L., Vouga, C.M., Leenders, K.L., Seiler, R.W., Spenger, C. (1996). Non-invasive dopamine determination by reversed phase HPLC in the medium of free-floating roller tube cultures of rat fetal ventral mesencephalon. A tool to assess dopaminergic tissue prior to grafting. *Brain Res. Bull.* **41**, 143-150.

Studer, L., Tabar, V., McKay, R. (1998). Transplantation of expanded mesencephalic precursors leads to recovery in parkinsonian rats. *Nature Neurosci.* **1**, 290-295.

Tammela, O., Song, D., Olano, M., Delivoria-Papadopoulos, M., Wilson, D.F., Pastuszko, A. (1997). Response of cortical oxygen and striatal extracellular dopamine to metabolic acidosis in newborn piglets. *Adv. Exp. Med. Biol.* **411**, 103-111.

Taylor, D.L., Edwards, A.D., Mehmet, H. (1999). Oxidative metabolism, apoptosis and perinatal brain injury. *Brain Pathol.* **9**, 93-117.

- Ursino, M., and Lodi, C.A. (1998). Interaction among autoregulation, CO₂ reactivity, and intracranial pressure: a mathematical model. *Am. J. Physiol.* **274**, H1715-H1728.
- Wallen, A., Zetterstrom, R.H., Solomin, L., Arvidsson, M., Olson, L., Perlmann, T. (1999). Fate of mesencephalic AHD2-expressing dopamine progenitor cells in NURR1 mutant mice. *Exp. Cell Res.* **253**, 737-746.
- Wang, M.Z., Jin, P., Bumcrot, D.A., Marigo, V., McMahon, A.P., Wang, E.A., Woolf, T., Pang, K. (1995) Induction of dopaminergic neuron phenotype in the midbrain by Sonic hedgehog protein. *Nature Med.* **1**, 1184-1188.
- Wurst, W., Auerbach, A.B., Joyner, A.L. (1994). Multiple developmental defects in Engrailed-1 mutant mice: An early mid-hindbrain deletion and patterning defects in forelimbs and sternum. *Development* **120**, 2065-2075.
- Xu, L., Lee, J.E., Giffard, R.G. (1999). Overexpression of bcl-2, bcl-XL or hsp70 in murine cortical astrocytes reduces injury of co-cultured neurons. *Neurosci. Lett.* **277**, 193-197.
- Yamada, T., Placzek, M., Tanaka, H., Dodd, J., Jessell, T.M. (1991). Control of cell pattern in the

developing nervous system: polarizing activity of the floor plate and notochord. *Cell* **64**, 635-647.

Ye, W., Shimamura, K., Rubenstein, J.L., Hynes, M.A., Rosenthal, A. (1998) FGF and Shh signals control dopaminergic and serotonergic cell fate in the anterior neural plate. *Cell* **93**, 755-766.

APPENDIX I

Methods

Animals were housed and treated following NIH guidelines. Cells dissected from rat embryonic lateral ganglionic eminence (E14) or mesencephalon (E12) were mechanically dissociated, plated on plastic 24-well plates or 12 mm glass cover slips precoated with polyornithine/fibronectin, and grown in defined medium with bFGF.^{2,6} In general, bFGF was withdrawn from the medium after 4 - 6 days of culture. Clonal assays were carried out in plastic 48-well plates. In some studies, recombinant human (rh)EPO, rhVEGF₁₆₅ or recombinant mouse (rm)FGF8b, or their neutralizing antibodies (all from R&D Systems) were added to cultures at the following concentrations: EPO 0.5 U/ml, EPO neutralizing antibody 10 µg/ml, FGF8 250 ng/ml, FGF8b neutralizing antibody 5 µg/ml, VEGF 50 ng/ml, VEGF neutralizing antibody 0.5 µg/ml. Dose response for EPO was carried out at 0.05, 0.5, 5, and 15 U/ml; for anti-EPO at 10 µg/ml and 100 µg/ml. Results of all experiments were confirmed by ≥ 2 independent series.

Lowered O₂ culture

Cultures were placed in humidified portable isolation chambers (Billups-Rothenberg, Del Mar, CA), flushed daily with a gas mixture 1% O₂, 5% CO₂ + 94% N₂. Precise O₂ levels in the chamber depended on the length of flush (90 sec at 15 L/min achieved 6% O₂, 6 minutes of flush achieved 1.5% O₂), which was not standardized until availability of an O₂-sensitive electrode system (OS2000, Animus Corp., Frazer, PA). Thus "lowered O₂" conditions represent a range of O₂ of 3±2%, approximating brain tissue levels (Table 1). The chamber was housed in an incubator to maintain temperature at 37°C.

BrdU uptake and TUNEL analysis

Bromodeoxyuridine (10 µM) was added to cultures for 60 minutes prior to fixation. Anti-BrdU staining was performed according to manufacturer's protocol (Amersham Life Sciences). The TUNEL reaction was also performed according to manufacturer's protocol (Boehringer-Mannheim). TUNEL+ cells were visualized by metal-enhanced DAB reaction (Pierce) after peroxidase conversion of the FITC label.

Immunohistochemistry

Cells were fixed in 4% paraformaldehyde + 0.15% picric acid/PBS. Standard immunohistochemical protocols were followed. The following antibodies were used: Stem cell/progenitor characterization: Nestin polyclonal #130 1:500 (Martha Marvin & Ron McKay), PSA-NCAM, En1 and FP4 (all monoclonal 1:2, Developmental Studies Hybridoma Bank). Stem cell differentiation: β -tubulin type III (Tuj1) monoclonal 1:500 and polyclonal 1:500 (both BabCO), O4 monoclonal 1:5 (Boehringer-Mannheim), galactocerebroside (GalC) monoclonal 1:50 (Boehringer-Mannheim), glial fibrillary acidic protein (GFAP) 1:100 (ICN Biochemicals). Neuronal subtype differentiation: Tyrosine hydroxylase (TH) polyclonal 1:200-1:500 (PelFreeze, Rogers, AK) or monoclonal 1:2000 (Sigma), GABA polyclonal 1:500 (Sigma), glutamate 1:500 (Sigma), dopamine- β -hydroxylase (DBH) 1:100 (Protos Biotech). Appropriate fluorescence-tagged (Jackson Immunoresearch) or biotinylated (Vector Laboratories) secondary antibodies followed by metal-enhanced DAB reaction were used.

Cell counts and statistical procedures

Uniform random sampling procedures were used for cell counts and quantified using the fractionator technique.³⁹

Statistical comparisons were made by ANOVA with posthoc Dunnett test when more than 2 groups were involved. If data were not normally distributed, Mann-Whitney U was used to compare results. Data are expressed as mean \pm SEM.

Reverse-phase HPLC determinations of dopamine content

Culture supernatants of medium, HBSS, and HBSS+56 mM KCl were stabilized with orthophosphoric acid and metabisulfite, and stored at -80°C until analysis. Stabilization, aluminum adsorption, equipment, and elution of dopamine were previously described (Studer et al., 1996; Studer et al., 1998). Results were normalized against dopamine standards at varying flow rates and sensitivities.

Western blots

Stored (-80°C) pellets were lysed in 20 mM Hepes, pH 7.6, 20% glycerol, 10 mM NaCl, 1.5 mM MgCl_2 , 0.2 mM EDTA, 0.1% Triton-X-100, with protease inhibitors, homogenized, and incubated on ice for 1 hr. Protein concentration was assayed by BCA (Pierce). For western, block was 5% milk in TBST, primary TH antibody (Pel-Freeze) was used at 1:500, and secondary was HRP-conjugated goat anti-rabbit (Pierce) at 1:5000. Signal was detected with SuperSignal (Pierce).

RT-PCR

Cells were washed once in PBS before solubilization in 2 ml Trizol (Life Technologies) then stored at -80°C . RNA extraction was carried out according to manufacturer's recommendations (Gibco Life Technologies). The Superscript kit (Gibco Life Technologies) was used for reverse transcription of 10 μg RNA per condition. PCR conditions were optimized by varying MgCl concentration and cycle number to determine linear amplification range. Amplification products were identified by size and confirmed by DNA sequencing. Primer sequences, cycle numbers, and annealing temperatures were:

GAPDH: f.: *CTCGTTCATAGACAAGATGGTGAAG*

r.: *AGACTCCACGACATACTCAGCACC*, 28 cyc., 59°C , 305bp

VHL: f: *CCTCTCAGGTCATCTTCTGCAACC*

r: *AGGGATGGCACAACAGTTCC*, 35 cyc., 60°C , 208bp

HIF1 α : f.: *GCAGCACGATCTCGGCGAAGCAAA*

r.: *GCACCATAACAAAGCCATCCAGGG*, 30 cyc., 59°C , 235bp

EPO: f.: *CGCTCCCCCAGCCTCATTG*

r.: *AGCGGCTTGGGTGGCGTCTGGA*, 30cyc., 60°C , 385 bp

VEGF: f.: *GTGCACTGGACCCTGGCTTTACT*

r.: *CGCCTTGCAACGCGAGTCTGTGTT*, 30 cycles, 60°C, 474bp (detects VEGF-A, B and C)

Nurr1: f.: *TGAAGAGAGCGGAGAAGGAGATC*

f.: *TCTGGAGTTAAGAAATCGGAGCTG*, 30 cyc., 55°C, 255 bp

TH: Provided by Vera Vikodem, NIDDK, 30 cyc., 56°C, 300bp

Ptx3: f.: *CGTGCGTGGTTGGTTCAAGAAC*

r.: *GCGGTGAGAATACAGGTTGTGAAG*, 35 cyc., 60°C, 257 bp

SHH: f.: *GGAAGATCACAAGAAACTCCGAAC*

r.: *GGATGCGAGCTTTGGATTCATAG*, 30 cyc., 59°C, 354bp

FGF8: f.: *CATGTGAGGGACCAGAGCC*

r.: *GTAGTTGTTCTCCAGCAGGATC*, 35 cyc., 60°C, 312bp

En1: f.: *TCAAGACTGACTACAGCAACCCC*

r.: *CTTTGTCCTGAACCGTGGTGGTAG*, 30 cyc., 60°C, 381bp

FGFR3: f.: *ATCCTCGGGAGATGACGAAGAC*

r.: *GGATGCTGCCAAACTTGTTC*, 30 cyc., 55°C, 326 bp

BDNF: f.: *GTGACAGTATTAGCGAGTGGG*

r.: *GGGTAGTTCGGCATTGC*, 35 cycles, 56°C, 213 bp

Retinal precursor preparation.

B6D2F1 pups, 1 day old, were euthanized by decapitation. The heads were dipped into 70 EtOH and the orbits removed using ophthalmic scissors, and placed into iced DMEM + Pen/Strep. The retinae were removed intact in two steps. First the orbits were placed on DMEM-soaked sterile

Kimwipes to immobilize them. A puncture is made just posterior to the lens opacity with a 26 g needle. Ophthalmic scissors are inserted into the hole and a circumferential, superficial incision was made around the lens, which is then removed. Then the remaining retina tissue was transferred to a small droplet of DMEM and pigmented epithelium was pulled away from the unpigmented retina using two fine forceps. The retinae were pooled into iced DMEM. Medium was removed with a sterile transfer pipet and the retinae digested with 0.5 mL 0.2% trypsin in a 37°C water bath for 3 min. The trypsin was removed; remaining enzyme was neutralized with 5 mL DMEM + 20% fbs with 2 ul Dnase (Boehringer-Mannheim). The cells were gently triturated with a 1000 ul pipet tip about 15 times, then centrifuged for 5 min at 2000 rpm. The supernatant was removed and replaced with 1 ml medium with serum. The trituration was repeated then the cells were gently forced through a nylon filter (8 micron). These were washed three times by gently swirling in DMEM + Pen/Strep, then the cells settled for about a min, and the medium was removed with a transfer pipet. A final spin at 2000 rpm for 5 min was followed by repeat trituration. Cells were counted in a hemacytometer and plated at 5×10^5 cells/well in 24-well places on cover slips previously coated with poly-D-lysine.

The culture medium is DMEM:F12 + 10% fbs + N2 supplement (Gibco) + antibiotics + glutamine + 20 ng/ml epidermal growth factor. Half the medium was exchanged twice weekly. After 1 week EGF was removed from the medium to encourage differentiation.

Chapter 4. A simple mathematical model

The mathematical modeling in this chapter is a first step in describing the qualitative features of stem cell regeneration and differentiation in response to oxygen changes in the simplest possible terms. By modeling the system, we hope to gain insights into the population dynamics as a whole in response to oxygen perturbations. While most of the discussion could be accomplished in words, the use of a few simple equations and standard results from linear systems theory and optimal control actually simplifies and clarifies the discussion. The long-term goal is to build on this model with more sophisticated models as data become available, to yield a quantitative analysis.

The simplest possible mathematical model for the dynamics of early stage stem cell regeneration and differentiation *in vitro* is the linear system described by two equations:

$$(1) \quad \dot{s} = ds/dt = (r-d)*s$$

s is stem cell population size, r is the rate of stem cell self-renewal, d is the rate of differentiation, and \dot{s} is the rate of change of stem cell number.

$$(2) \quad \dot{p} = dp/dt = d * s - x * p$$

Here again s is stem cell number and p is the population size of early progeny, the states of the system. d is the rate of differentiation, and x is the rate of progeny death or further differentiation. \dot{p} is the rate of change in the size of the early progeny population.

This representation assumes that the numbers of cells are sufficient to treat as continuous concentrations, and that stem cell division can also be viewed as a continuous process yielding some net rate of change in stems cells via renewal and progeny by differentiation. The total rate of stem cell division is given by $r+d$.

Thus overall, the model is as follows:

$$\begin{bmatrix} \dot{s} \\ \dot{p} \end{bmatrix} = \begin{bmatrix} (r-d) & 0 \\ d & -x \end{bmatrix} \begin{bmatrix} s \\ p \end{bmatrix}$$

There are obviously many simplifying assumptions underlying such a model, which will be discussed in more detail at the end of the chapter. For example, the model assumes that r , d , and x are constants (that they change much more slowly than s and p). Nevertheless, a surprising amount of

insight can be gained from even such a simple model. We will explore a variety of increasingly complex assumptions about the parameters, to frame a discussion of the potential effects of oxygen levels on the process. First, assume that the parameters are constant as functions of time, but vary with the oxygen tension.

Starting with the simplest scenario, steady state:

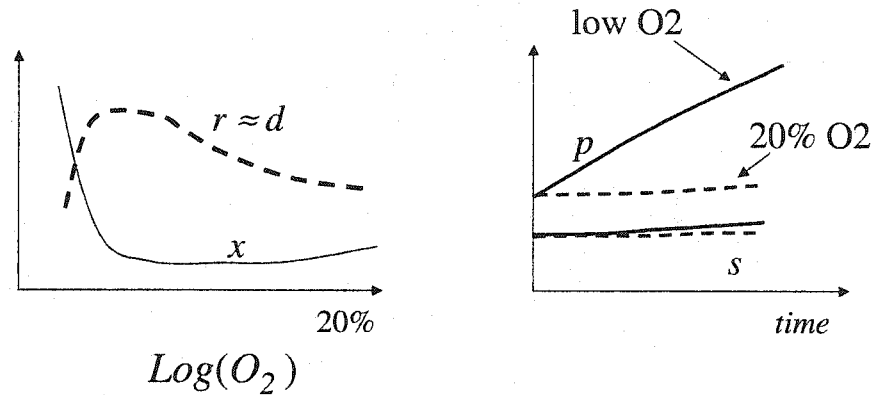
In steady state, $\dot{s} = \dot{p} = 0$, so $r = d$, and

$$p = \frac{d}{x} s$$

From any initial condition, for constant parameters with $r = d$, the progeny will change linearly in time until this steady state is reached. If $r \neq d$ then the rate of renewal and differentiation of stem cells is imbalanced and both populations will grow or decay exponentially. We hypothesize that lowered oxygen increases both r and d , and decreases x . This would lead to increased progeny, though not necessarily stems, as that would depend on $r - d$.

As another simple example, suppose that the parameters vary roughly as shown in Figure 1, under the assumption that $r = d$. In this figure, as the oxygen is lowered, the rate of stem

Figure 1



cell division increases until some critical oxygen level is achieved, and then the rate drops. Similarly, the rate of progeny death decreases until some critical oxygen level. The resulting time histories would have very little differences between the low and high oxygen case for stem cell numbers and yet large differences between progeny numbers. Thus dramatic effects of oxygen tension need not show up as changes in stem cell populations, if self-renewal and differentiation maintain a balance. The stem cell growth rate $r-d$ may be greater at low oxygen if, for example, r increased more than d .

Another way to use the model is to explore the possible patterns of stem cell population changes under conditions in which r and d are no longer assumed to be constant

parameters, but can vary with time. We will also assume that there is some limitation on total stem cell division rate. For convenience, assume without loss of generality that the units are chosen so that $r+d \leq 1$. Then a natural question to address is the *optimal* trajectories of renewal and differentiation that would either maximize the progeny in a given time, or minimize the time to reach a given concentration of progeny, subject to $r+d \leq 1$ and perhaps a lower limit on stem cell density. No mechanism is implied here for stem cell renewal and differentiation, or how mechanism might change with oxygen tension. But identification of optimal trajectories might help guide expectation for optimal trajectories in experiments.

The particular optimal control problems described in the previous paragraph are simple enough to be easily solved analytically, and produce "bang-bang" solutions where stem cells undergo only renewal ($r=1$) for some period of time, and then switch to only differentiation ($d=1$) until the problem goal is reached. The time at which switching occurs is also easily computed. Although we will omit the details, the intuition can be explained as follows: Suppose that we are interested in the minimum time T to reach a desired progeny regeneration level. There is then

a level of stem cell density s_s , that is required at the switching time T_s , so that the pool of stem cells just reaches its minimum constrained level at the final time T . Before T_s , the stem cells will self-renew with $r=1$, until they reach the required density s_s , during which time the progeny population does not increase. Thus depending on the desired final stem and progeny levels, stem cell levels may go up or down initially.

This exercise illustrates that the optimal time trajectories of cell populations can be complex, even when the model and objective are simple. Thus without much greater understanding of the constraints on the process of stem cell renewal and differentiation, we should not expect to see any particular characteristic patterns. The effect of lowered oxygen should be evident however in the changing rates of renewal and differentiation.

This extremely simplified mathematical setting would need to be expanded substantially to reflect actual biology. For future work some considerations of how one might add more detail to this highly aggregate model are important to consider. The deterministic dynamical system could be made

to reflect more realistic stochastics in a variety of ways, from modifying the existing equations to include noise terms to replacing the differential equations themselves with a hybrid Markov process that viewed each division as an event with transition probabilities (Yakovlev et al., 1998). Such stochastic models could in turn be viewed as aggregations of underlying deterministic processes of cell fate determination, which could then be modeled in more detail as mechanisms were discovered. The optimal control theory alluded to above could help shape the search for mechanisms by suggesting what a set of possible strategies would look like, which could potentially narrow the experimental process somewhat. Even an apparently deterministic renewal and differentiation process at the cellular level might be the result of elaborate feedback and signaling to either suppress or exploit stochastic effects at the molecular level. Modeling such multiscale dynamics is currently a rather ad hoc process, but there are vigorous research programs pursuing more systematic treatments.

An obvious weakness of the simple model above is the assumption of linearity. The most significant nonlinearity would probably arise from density dependent changes in

rates due to intercellular signaling and density-dependent changes in cell cycling. As more detailed mechanisms were included, of course, then additional nonlinear effects would complicate the analysis. In a population level model like this, the initial transients in cultures are likely to be reasonably well modeled by linear differential equations, and the dominant dynamic effects will be due to the dependence of the rates on various external quantities, like oxygen tension. This assumption tends to break down the longer the experiment is run.

Finally, the eigenvalues of the matrix (here the diagonal elements, $r-d$

$$\begin{bmatrix} (r-d) & 0 \\ d & -x \end{bmatrix}$$

and $-x$), determine the asymptotic dynamics. However, the transients and steady-state can be more affected by d , particularly if d is large. This is the simplest example of a general phenomenon, by which large transients are independent of the eigenvalues. Mathematically, this is a highly nongeneric property of a matrix or system, and rarely arises in physics, but is surprisingly common in engineering, and apparently also biology. For these reasons, the mathematical tools used in modeling

engineering systems are likely to help biologists model analagous complex systems.

Reference

Yakovlev, A.Y., Mayer-Proschel, M., Noble, M. (1998). A stochastic model of brain cell differentiation in tissue culture. *J. Math. Biol.* **37**, 49-60.

Chapter 5. Speculation

Introduction

In humans, major physiologic responses to hypoxia are mediated through a bHLH-PAS protein, hypoxia-inducible factor 1 α (Wang et al., 1995). bHLH-PAS proteins are defined by their structure: Basic helix-loop-helix motifs are found in large families of transcription factors in which the basic region mediates DNA binding and the helix-loop-helix region mediates dimerization to various partners (both homo- and heterodimerization). PAS refers to the first proteins identified in this family, the drosophila per (involved in circadian rhythms), mammalian ARNT (aryl hydrocarbon nuclear receptor translocator) and sim (involved in embryonic patterning). The PAS domain is involved in sensing not only oxygen, but redox status and light (Taylor and Zhulin, 1999).

HIF1 α with its partner ARNT mediate increased transcription of several genes that are critical in both acute and chronic responses to decreases in cellular oxygen availability. HIF-1 α -mediated acute physiologic responses

include increased transcription of tyrosine hydroxylase in the carotid body which increases respiratory minute ventilation (Zhu and Bunn, 1999), increased transcription of nitric oxide synthase II (Jung et al., 2000) and heme oxygenase (Lee et al., 1997) which increases vasodilation. In addition HIF-1 α is involved in increased expression of two glucose transporters (Iyer et al., 1998) and several glycolytic enzymes (Semenza, 1999). More longterm physiologic adaptations include increases in capillary density mediated partly by HIF-1 α -induced VEGF (Schweiki et al., 1992), and increased red cell mass mediated by HIF-1 α -induced erythropoietin production (Semenza and Wang, 1992). Thus, HIF-1 α is a master coordinator of oxygen supply via the vasculature and cellular energy metabolism (O'Rourke et al., 1997), interacting with hypoxic response elements on many genes to regulate myriad responses to oxygen stress.

HIF1 α protein is unstable in normoxic conditions but stable in hypoxic conditions (Gradin et al., 1996). HIF1 α protein stability is controlled at the level of the proteasome, with rapid ubiquitin-mediated degradation occurring in normoxic conditions (Salceda and Caro, 1997). The proteasome is the major nonlysozymal cellular control of

protein turnover. Function of HIF-1 α in regulation of hypoxia responses also requires its translocation into the nucleus, and nuclear translocation is also blocked by pharmacologic inhibitors of the proteasome (Kallio et al., 1999). Proteins targeted for proteasome breakdown are identified and escorted to the 26S proteasome by particular combinations of complexed ubiquitin ligase SCF (Skp-cullin-F box) molecules (Hochstrasser, 1996) now known to be complexed as well with Roc1/Rbx1 type-proteins (Kamura et al., 1999). Rbx1, a RING finger protein, is thought to serve as a tether for the complex as well as playing a role in ubiquitin conjugation (Tyers and Willems, 1999). The entire complex serves to dress the target protein with a ubiquitin chain recognizable to the proteasome in a series of enzymatic reactions that consist of ubiquitin activation (E1 enzyme), ubiquitin conjugation (E2) and ubiquitin ligation (E3) (Varshavsky, 1997).

For HIF-1 α , the intermediary complex that directs the protein to the proteasome is the VHL-elongin-Cul2 complex. VHL is the von Hippel Lindau tumor suppressor protein. Autosomal dominant mutations of this gene cause cancer syndromes with the most common tumors renal angiomas, cerebellar hemangiomas and clear cell renal carcinomas.

(See OMIM 193300.) VHL is now known to function specifically in the E3 ligase reaction (Lisztwan et al., 1999). Elongins B and C in the complex were previously known as transcription elongation mediators. Although their exact role in the complex is less clear than that of other components, VHL may serve to sequester elongins, thus inhibiting transcription of certain gene products. In a recent report, tyrosine hydroxylase transcript elongation in PC12 cells was halted by VHL (Kroll et al., 1999). Cullins are genes with tumor suppression function (Pause et al., 1997) and were first identified in *C. elegans* where they were found to be required for appropriate cell cycle exit after mitosis (Kipreos et al., 1996). Skp1 and skp2 are components of the E3 ubiquitin ligase, and also play a role in many other cellular functions including appropriate cell-cycle regulated centrosome duplication (Freed et al., 1999).

Direct interaction of HIF1 α and VHL appears to be important for the targeted breakdown of HIF1 α , and this complex formation appears to be iron-dependent, providing yet another regulatory mechanism for HIF1 α stability (Maxwell et al., 1999). ARNT message and protein levels are not

tightly regulated in response to the oxygen environment (Pollenz et al., 1999).

A mechanism for mediating specificity of the ubiquitin ligase complexes (for one protein over another) is the use of different components in different ratios as part of the complex. In yeast, proteasome localization is primarily nuclear (Russell et al., 1999) but in mammalian cells the complex and the proteasome itself change subcellular localization in response to progression through the cell cycle, another mechanism to reinforce specificity (Palmer et al., 1994). Different proteasome complexes distribute themselves to different compartments of the cell in the nucleus, surface of endoplasmic reticulum fraction and cytoplasm (Brooks et al., 2000). In tumor cell lines, both hypoxic and hypoglycemic conditions cause an increase in nuclear distribution of the proteasome (Ogiso et al., 1999). But in general, proteasome distribution in response to cellular stress has not been extensively studied. In normal rat CNS, the 20S complex was reported to be expressed throughout the brain. In hippocampus, the complex was most easily visualized immunohistochemically in pyramidal cells, predominantly in nuclei. The 20S proteasome was also detected in some dendrites in

hippocampus. In parallel hippocampal neuron cultures, an anti-20S signal was mostly nuclear but when cytoplasmic, it was described as homogenous (again without comment specifically on the synapse, and no data presented in photo form) (Mengual et al., 1996).

Precise roles for the proteasome in embryonic development have not been described. But because the proteasome is central to regulating appropriate abundance of gene products involved in cell cycling, the proteasome will certainly be shown to be ubiquitously involved in normal development. Abundance of positive regulators of cell cycling such as cyclin D1 (Diehl et al., 1997), cyclin E (Singer et al., 1999), and cyclin A (Michel and Xiong, 1998) are exquisitely regulated under proteasomal control. Regulation of cyclin-dependent kinase inhibitors p27 (Montagnoli et al., 1999), p21 (Rousseau et al., 1999) and p57 (Urano et al., 1999) are also under proteasome control. This list is by no means complete, nor is the regulation of these proteins completely accomplished by the proteasome. Nonetheless the list highlights the pivotal role that must be performed by the proteasome during development. (In addition, in the case of myogenesis, both MyoD (Ciechanover

et al., 1999) and c-met (Jeffers et al., 1997) abundance is partially controlled at the level of the proteasome.

Like cell cycle regulators which require very rapid turnover, normal synaptic function and plasticity is also likely to require rapid protein turnover. In *Aplysia* models, the proteasome has been implicated in protein turnover at the synapse (Hedge et al., 1993) and this turnover is essential for long-term facilitation (Hedge et al., 1997; Chain et al., 1999). Sustained changes in the efficiency of synaptic transmission (long-term potentiation or LTP) is hypothesized to be a good cellular model for learning and memory consolidation. Rapid protein synthesis and phosphorylation are emphasized as protein-level changes that contribute to LTP (McGaugh, 2000). Receptor density and trafficking are also emphasized (Kim and Huganir, 1999). Proteasome function in the synapse as a contributor to protein turnover has not been specifically investigated in mammalian systems. A possible clinical correlate pointing to the importance of proteasome function for normal synaptic function is mutation of the E3 ligase in Angelman syndrome which causes severe mental retardation (Kishino et al., 1997).

The results presented here are preliminary but suggest that oxygen influences subcellular localization of the cul2/VHL complex in cultured CNS stem cells as well as in cultured astrocytes. In addition in hippocampal neuronal cultures, the proteasome machinery can be identified early in structures that appear to be growth cones as well.

Results

Oxygen levels influence cul2 nuclear localization in cultured astrocytes

Human astrocytes were grown at either 2% oxygen or 20% oxygen, then analyzed for cul2 protein expression with immunohistochemistry. In both conditions a faint cytoplasmic signal was visible in all cells, but in a subset of cells a strong nuclear signal was visible. Counts of nuclear signals as a percentage of DAPI-positive nuclei were 104/167 or 65% for astrocytes grown in 2% oxygen vs. 19/103 or 18% for astrocytes grown in 20% oxygen ($p < 0.05$). (See Figure 1.) In separate experiments, the cul2 immunohistochemical signal was enhanced using tyramide signal amplification. In this procedure, SA-HRP on the secondary antibody produces a reactive fluorophor from tyramide that can significantly enhance signal compared to

secondary antibody alone. After amplification, the cytoplasmic signal appeared to be localized to cytoskeleton by gross morphologic examination (Figure 2).

Oxygen levels influence cul2 and VHL nuclear localization in cultured rat CNS stem cells

For details of culturing, see Appendix in Chapter 3. Embryonic rat CNS precursors were stained for cul2 and VHL using standard immunohistochemical techniques after various times in culture in either 3+2% or 20% oxygen conditions. After two days of expansion, cells were co-stained for cul2 and nestin, with DAPI in the mounting medium. Microscopy was performed with a filter that allowed simultaneous photography of all three wavelengths used for visualization (blue DAPI, red cul2, green nestin). After 2 days in culture, most cells in clusters expressed nestin in both conditions, and nuclear cul2 stains were seen in all cells (Figure 3). However, cells that were isolated from the clusters were less likely to express nestin. Furthermore, cul2 expression was very different in the two oxygen conditions: Nuclear cul2 signals were strong in most of these isolated, single cells in low oxygen whereas almost no cul2 signal was seen in 20% oxygen. In Figure 4, a representative field of these single cells from LGE is

shown. Similar single cells from mesencephalic cultures at this point revealed the same pattern of cul2 staining (not shown).

After six days of expansion of LGE-derived precursors, VHL immunofluorescence staining patterns were remarkably different in low vs. 20% oxygen conditions. VHL staining earlier in expansion revealed nuclear signals in most cells (Figure 5). At the end of expansion, the nuclear signal was retained in cells grown in low oxygen and no cytoplasmic signal was detected. However, in 20% oxygen, nuclear signal was retained in most cells, but the vast majority of cells also displayed an intense cytoplasmic signal (Figure 6).

Cullins localize to synapses in cultured hippocampal neurons

Because cul2, not previously studied in CNS tissues, was present in CNS precursors we examined cul2 staining in cultured hippocampal neurons. Embryonic rat hippocampal neurons in 20% oxygen conditions only were assayed at 2 weeks after culture. Surprisingly, cul2 appeared to localize to the synapses in these mature cultures (Figure

7). Co-labelling with the antibody against the synaptic marker densin confirmed this observation (Figure 8).

Immunohistochemical localization of cull was also performed on cultured hippocampal neurons, and it too was found to localize to the synapse (Figure 9). Again co-labelling with the synaptic marker PSD95 confirmed synaptic localization (Figure 10). However, cull staining was not as consistent as cul2 staining over the whole neuronal population in the culture dish, and some neurons appeared to have less signal than others. On light microscopic exam, it was also apparent that a strong nuclear signal for cull was present in some but not all cells in the culture (Figure 11).

Skp1 and 20S proteasome are also found in cultured hippocampal neuron synapses

Anti-Skp1 and anti-20S proteasome antibodies were used to label hippocampal neurons in culture after 2 weeks. Stains were done together with anti-densin. Skp1 (Figure 12) and the 20S proteasome (Figure 13) also were prominently found in synapses in the mature cultures.

c-met localizes to cultured hippocampal neuronal synapses

Because c-met is subject to proteasomal breakdown and because c-met expression has been reported in the hippocampus (Thewke and Seeds, 1999), we also examined c-met expression in hippocampal neuron cultures immunohistochemically. Surprisingly, c-met also localized to the synapses and appeared to be present in the vast majority of synapses labelled with densin (Figure 14). We also found c-met in astrocytes, in a focal, dotted pattern in the cytoplasm and at the surface of astrocytes attached to other astrocytes (Figure 15).

Skp1, 20S proteasome, and c-met may be localized to growth cones in developing hippocampal neurons in culture

Synapses can be visualized in hippocampal neuron cultures after about 2 weeks. Immunohistochemical stains after 1 week of culture revealed intense staining in discrete structures which appeared morphologically to be growth cones (Figures 16 and 17). Staining to mark location of skp1, 20S proteasome and c-met gave the same pattern at this time in culture.

Discussion

Despite the central role of the VHL/cul2/elongin complex in the regulation of hypoxia inducible factor 1 α (Maxwell et al., 1999) and VEGF (Pal et al., 1997) VHL/cul2 expression and subcellular localization as a function of oxygen environment has not been examined in normal, nontransformed cells. In renal cell carcinoma lines VHL is detected in both nucleus and cytoplasm but cytoplasmic staining appears to be cell cycle regulated: 87% of BrdU-positive RCC cells had cytoplasmic VHL vs. only 13% of BrdU-negative cells (Ye et al., 1998). VHL subcellular localization is also transcription dependent. In RCC cells a VHL-GFP fusion protein was used to follow subcellular localization of VHL. VHL-GFP was predominantly cytoplasmic, but when transcription was inhibited pharmacologically, nuclear VHL increased significantly (Lee et al., 1999). In NIH 3T3 cells subcellular localization of VHL was reported to be cell density dependent. When sparse, more than 70% of the cells had a nuclear signal and more than 90% of the protein was located in the nucleus. When the cells were confluent less than 15% had a nuclear signal and 50% of the protein was in the nucleus. Furthermore, in NHK cells which cluster, nuclear staining was prominent on the cluster surface but absent inside the cluster (Lee et al., 1996).

This group also identified a nuclear localization signal in VHL protein (Lee et al., 1996).

Our results with cul2 and VHL in astrocytes and in CNS precursors, though preliminary, suggest that low oxygen is associated with increased nuclear translocation of these proteins when compared to 20% oxygen conditions. On the surface, these results are contradictory to those reported above. High density cultures would be expected to be lower in oxygen availability (Marshall et al., 1986) and internal cells of a cluster would also be expected to be more hypoxic than cells on the surface of a cluster (Mueller-Klieser and Sutherland). The difference may be related to tissue of origin, use of transformed vs. primary cultures, or developmental state. Furthermore, the fraction of VHL bound to cul-2 (and vice versa) is not yet known. On the other hand, responses to oxygen may well be regulated independently of density.

The proteasomal machinery appears to be poised to act in hippocampal neuron synapses. Location of the proteasome components in the synapse may be a function of the early developmental stage of these cultured neurons, and further study in adult preparations will be required to focus on a

possible role for the proteasome in either synaptic development or later synaptic function. During synaptic development, synaptic arborization/complexity reaches a quite specific size and then is limited, probably via activity-dependent signals (Zou and Cline, 1999). CaMKII is important in development and critical for later function of the synapse. Control of CaMKII enzyme activity is complicated, and includes autophosphorylation and calmodulin binding, control over localization between cytoskeleton and synaptic targets (Shen and Meyer, 1999). Because turnover of CaMKII is central to normal synaptic function, ongoing work is directed at exploring proteasome-mediated turnover of CaMKII in hippocampal slice models of LTP.

Examination of hippocampal neurons for proteasome expression/localization was spurred by the observation that VHL and cul2 subcellular localization were dynamically regulated in response to the oxygen environment. How can oxygen be brought back into these observations? In an animal model of global brain ischemia (transient carotid occlusion), administration of intrastriatal HGF protected hippocampal neurons from ischemic (or ischemia-reperfusion-induced) death (Miyazawa et al., 1998). We have not

examined HGF as a mediator of proliferative or differentiation changes in CNS stem cells in response to oxygen, but it will be examined as part of ongoing studies. In particular, HGF is known to interact with multiple other growth factors as part of normal CNS development. Even at the synapse level, it is possible that the oxygen microenvironment is important to consider as a regulator of local expression patterns of message and proteins. Synapses are the sites of enormous energy utilization and significant local oxygen changes accompany neuronal activity. Recently microvascular oxygen changes after sensory neuronal stimulation were measured directly in cats using phosphorescence decay. Cortical activity elicits a decrease in microvascular oxygen concentration because oxygen is consumed by electrically active neurons via oxidative metabolism. This decrease in local oxygen is followed by a reactive hyperemia. Increased blood flow overcompensates, raising local oxygen levels above those before neurons were active (Vanzetta and Grinvald, 1999). Overall local oxygen levels may shift 4.5-fold during this process (over a few seconds). Similarly large shifts in glucose utilization locally accompany neuronal activity. Although models of quantitation of these changes are somewhat controversial (Magistrelli et al., 1999) the

shifts in local glucose concentrations are also likely to be very wide. Many of the same gene pathways responsive to oxygen levels are also responsive to changes in glucose levels (Semenza, 1999). Perhaps as a long-shot speculation, the proteasome is situated in the synapse to assure proper regulatory responses to these rapid fire changes in the synaptic microenvironment.

Hepatocyte growth factor is neurotrophic (Maina and Klein, 1999) both during CNS and peripheral nerve development, and in adult brain (Achim et al., 1997). HGF is essential for sensory nerve development (Maina et al., 1997). The proto-oncogene c-met, the receptor for HGF, has been localized to hippocampus prior to these studies (Jung et al., 1994), but not specifically to synapse. HGF has been reported to be produced by both developing hippocampal neurons (Jung et al., 1994), by adult human astrocytes (Yamada et al., 1997) and microglia (Di Renzo et al., 1993). HGF/c-met activity levels are associated with increased malignant grade of a variety of CNS tumors (Moriyama et al., 1999). The presence of c-met in developing synapses is intriguing because of its developmental role in other systems: HGF/c-met play a role in epithelial branching during lung development (Ohmichi et al., 1998; Kolatsi-Joannu et al.,

1997), ureteric bud branching during kidney development (Woolf et al., 1995), branching in mammary epithelial cell duct formation (Soriano et al., 1995), and terminal branching of sensory nerves (Maina et al., 1997). In all these systems, branching morphogenesis is mediated in part through HGF/c-met. Ongoing studies will evaluate a possible role for c-met in branching (arborization) of developing CNS synapses. In renal carcinoma cells, the branching morphogenesis induced by HGF is suppressed by the von Hippel-Lindau protein, such that the interaction between HGF and VHL in part determines tumor phenotype and invasiveness (Koochekpour et al., 1999).

HGF plays an important role in axon guidance in the sensory nervous system (Ebens et al., 1996; Yang et al., 1998) but it has not been studied in CNS growth cone motility. Localization of both c-met and proteasome structures in growth cones will require confirmation with known growth cone markers, and is the subject of ongoing work.

Figure legends**Figure 1.**

Human astrocytes grown in either 2% oxygen (1A) or 20% oxygen (1B) were stained with antibody against cul2 (in red). Lower panel shows DAPI staining of the views in the upper panels. In 2% oxygen, 65% of astrocytes had a nuclear signal for cul2 vs. only 18% of astrocytes grown in 20% oxygen.

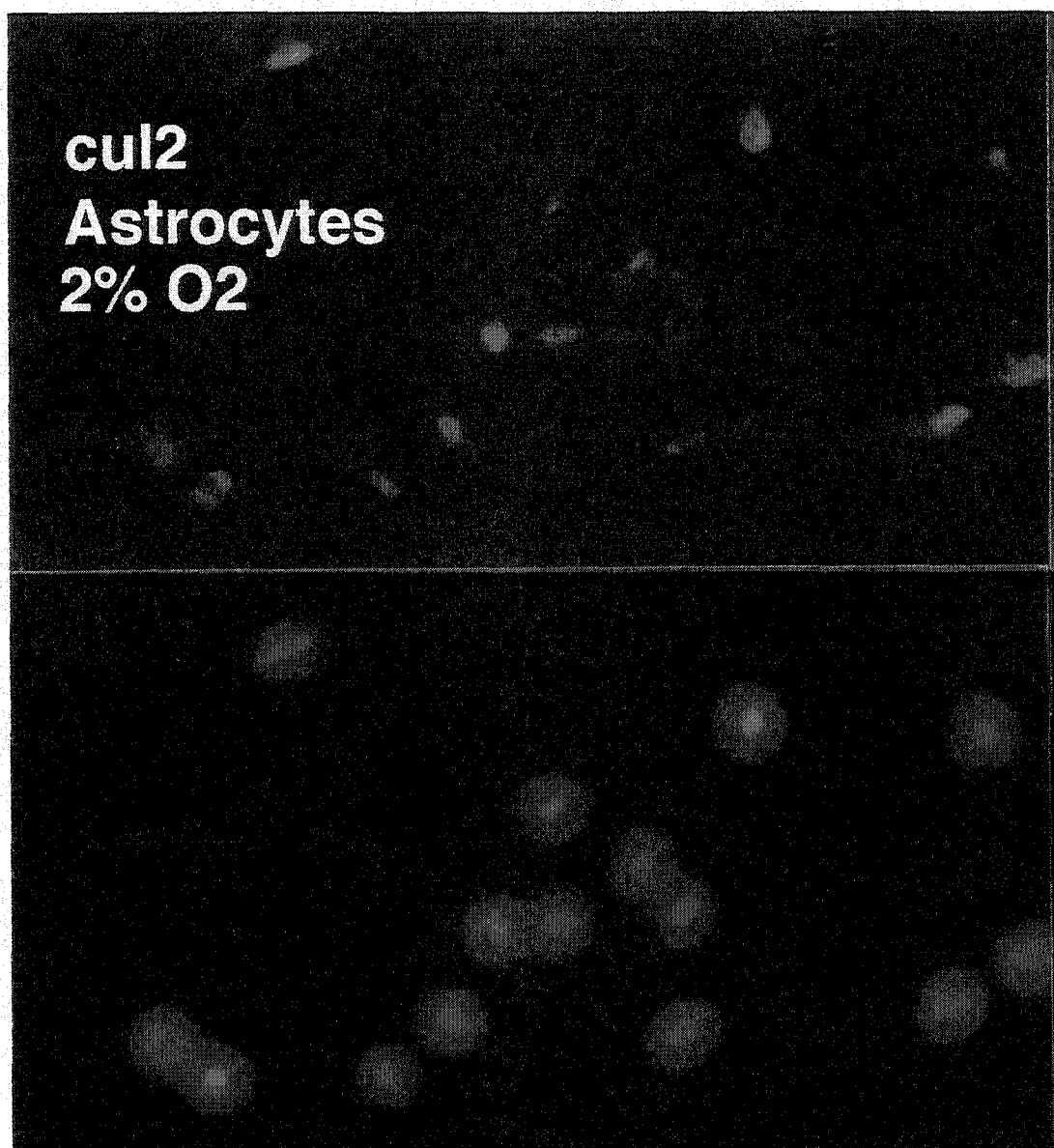


Figure 1A.

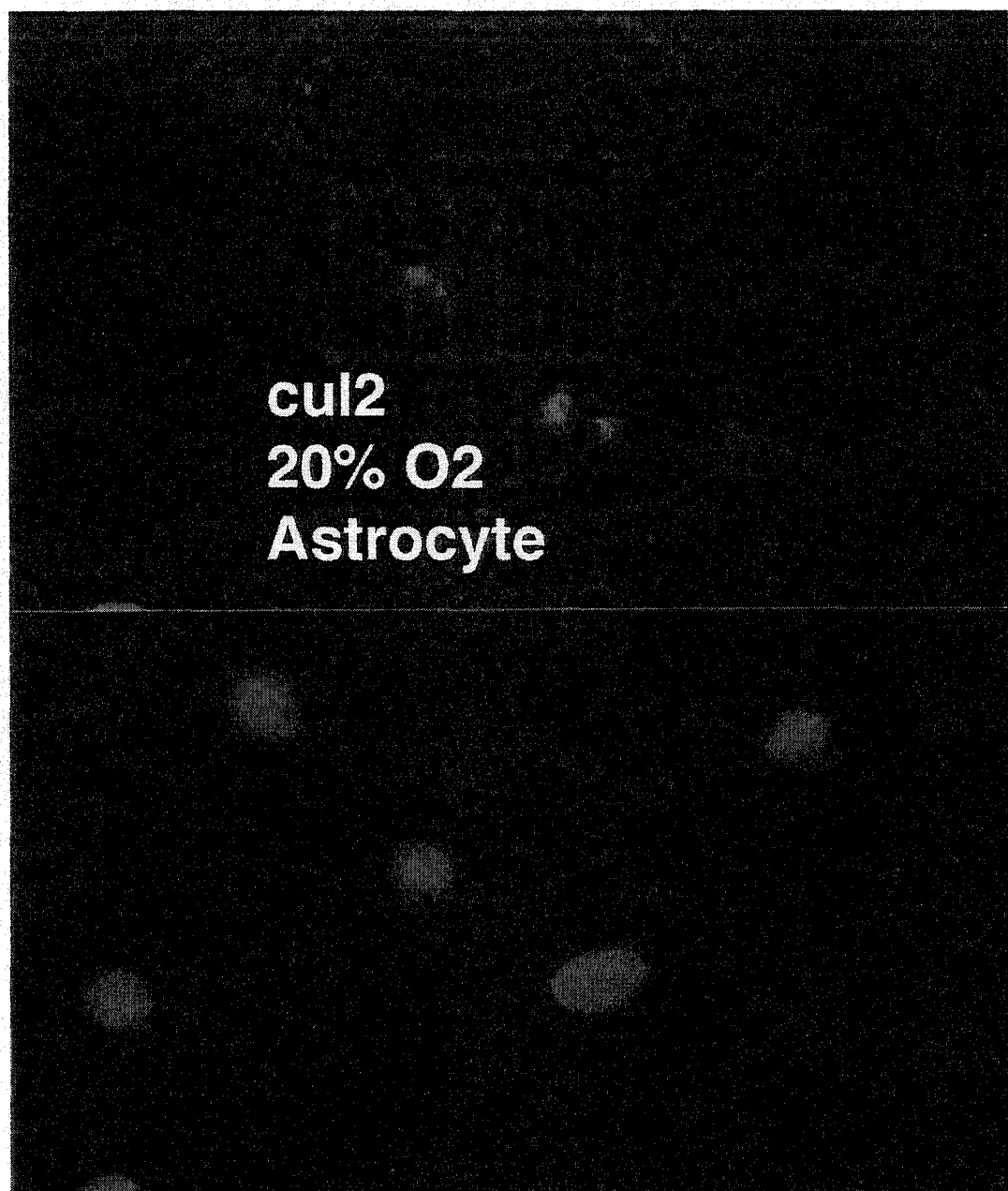


Figure 1B.

Figure 2.

Immunofluorescence amplification technique used to visualize subcellular localization of cul2 in astrocytes. In cultured human astrocytes, some of the cytoplasmic cul2 appears to localize to cytoskeletal structures.

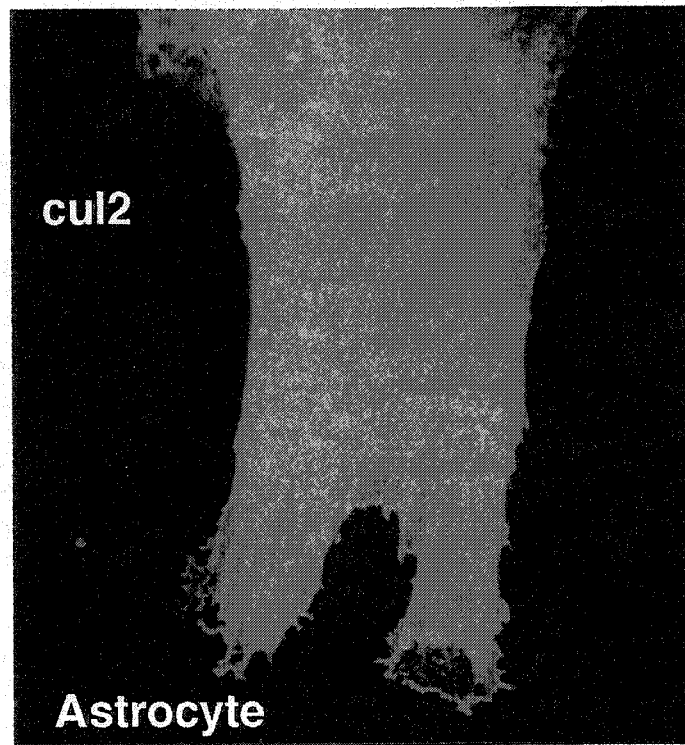


Figure 2.

Figure 3.

Embryonic rat CNS stem cells after culture for 2 days in either 3+2% or 20% oxygen. Nestin immunocytochemistry indicates that most cells were nestin-positive in either oxygen condition at this time (green). Most precursors at this time in both conditions also had strong nuclear cul2 signals (red).

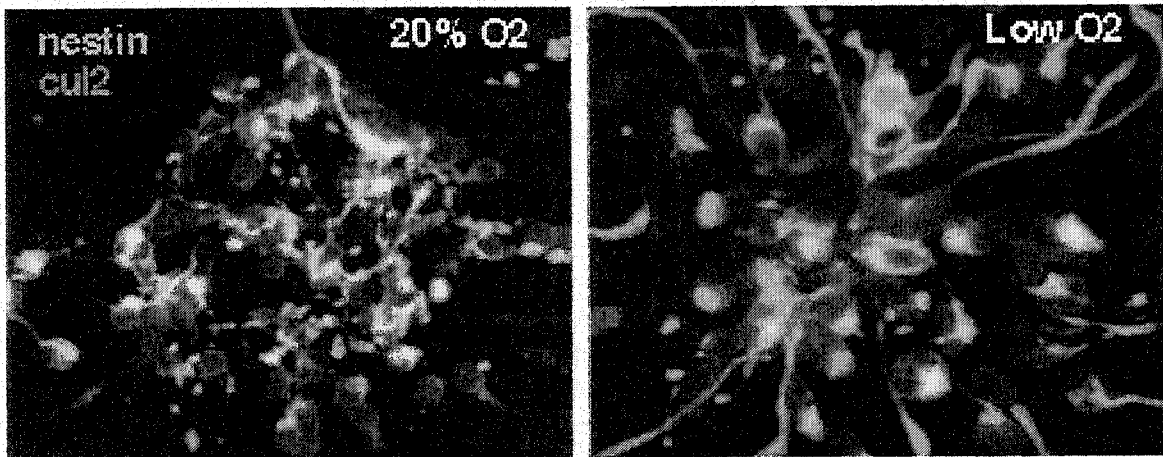


Figure 3.

Figure 4.

Embryonic rat CNS stem cells were cultured in either 3+2% or 20% oxygen for two days. At this time in culture, most cells are in small clusters and in clusters, cul2 nuclear stain was present in the vast majority of cells in both conditions. Here cells stained with antibody for cul2 showed that in low oxygen nuclear staining was common in isolated single cells, but in 20% oxygen, cul2 signal was rare.

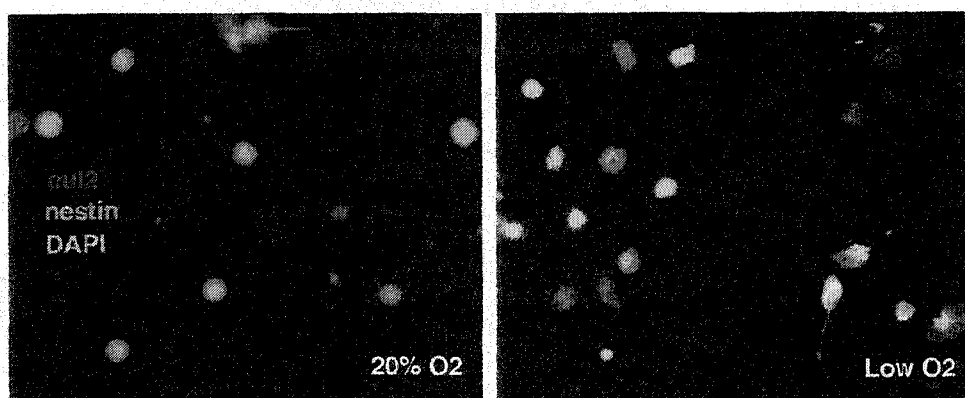


Figure 4.

Figure 5.

VHL staining of CNS precursors grown in either 3+2% or 20% oxygen. After 4 days in culture (expansion in the presence of bFGF) most cell nuclei were immunoreactive for VHL in both oxygen conditions.

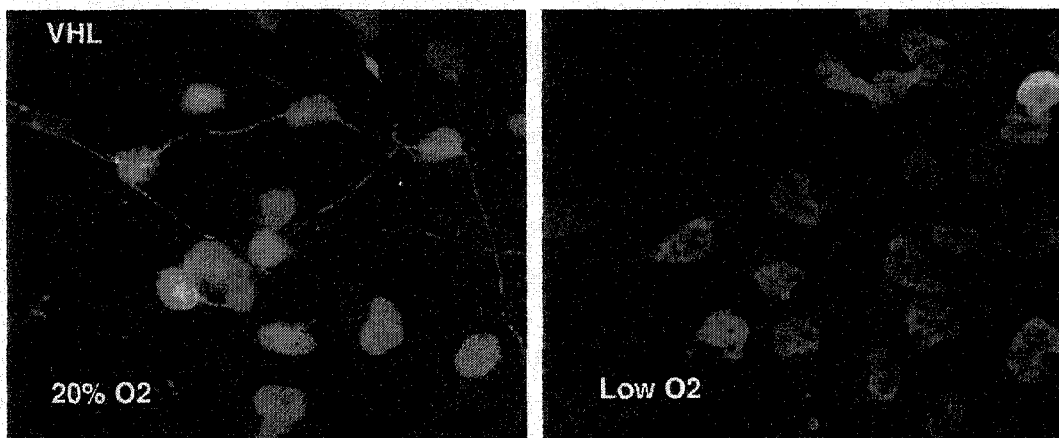


Figure 5.

Figure 6.

Rat embryonic CNS stem cells were grown in either 3+2% or 20% oxygen conditions for 6 days in the presence of bFGF. In low oxygen conditions, most precursors stained for VHL had a nuclear signal (left panel). In 20% oxygen conditions, a nuclear signal for VHL was seen in most cells but intense cytoplasmic staining was also seen in most cells (right panel). Next page: High power view of right panel.

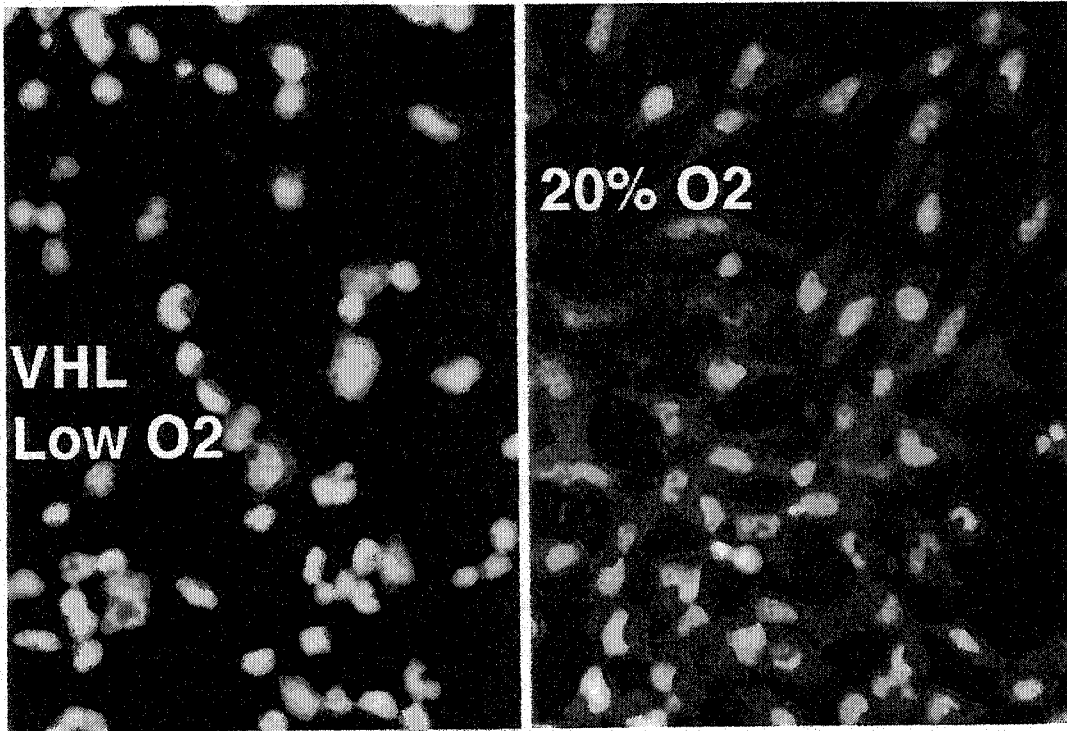


Figure 6.

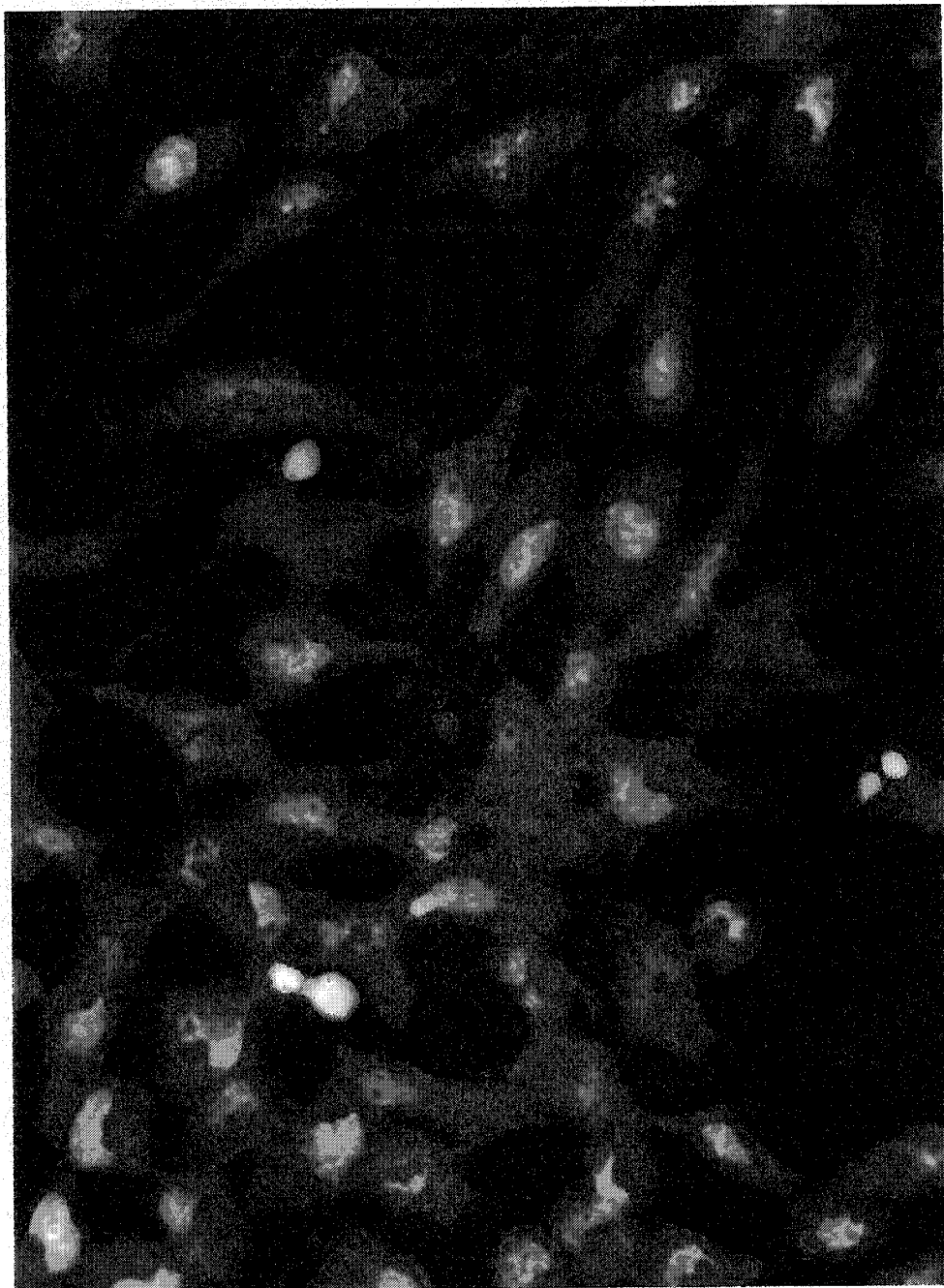


Figure 6.

Figure 7.

Embryonic mouse hippocampal neuron cultured (20% oxygen) for 2 weeks. Immunohistochemical staining with antibody against cul2 revealed a pattern of fluorescence characteristic of synaptic staining.

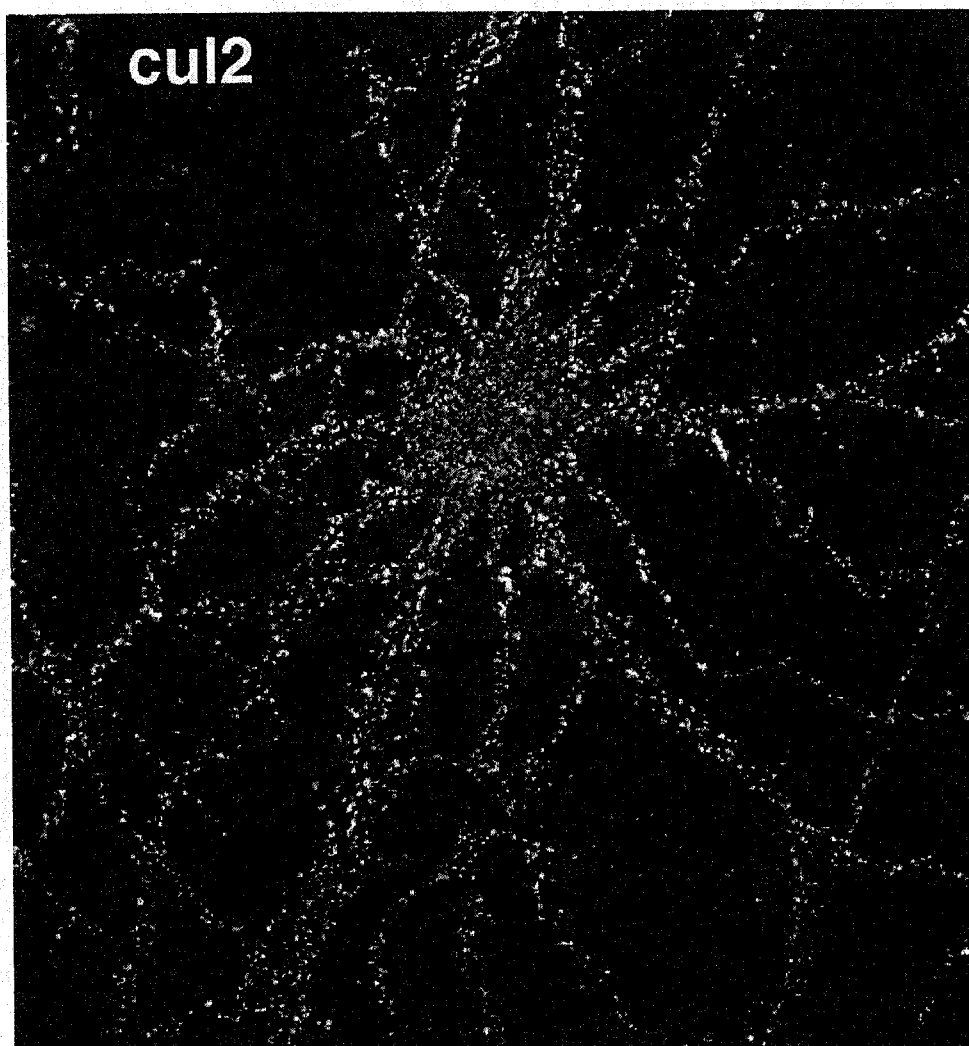


Figure 7.

Figure 8.

Embryonic mouse hippocampal neurons cultured for 2 weeks then stained for the presence of cul2 (red) and the synaptic marker, densin (green). Significant overlap of the signals (yellow) was seen in the synapses.

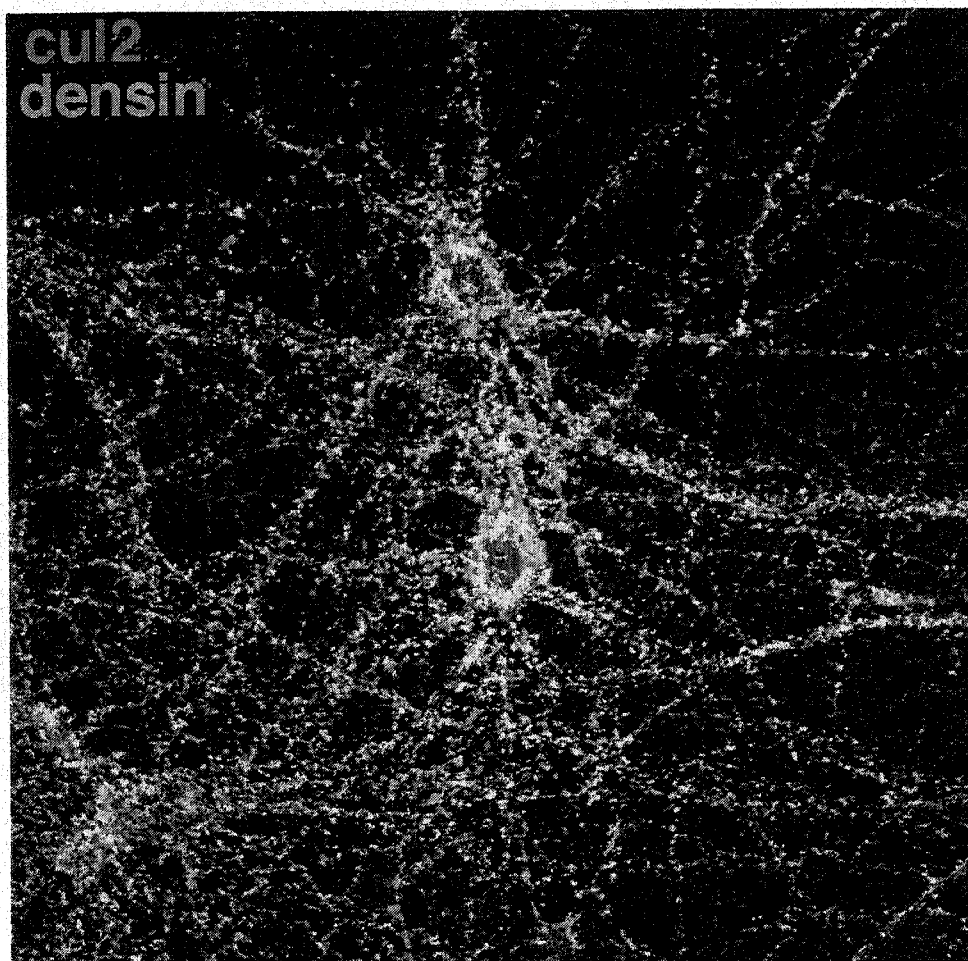


Figure 8.

Figure 9.

Embryonic hippocampal neuron stained for two weeks then stained with antibody to cull. The pattern of immunofluorescence suggested that cull is localized to the synapse.

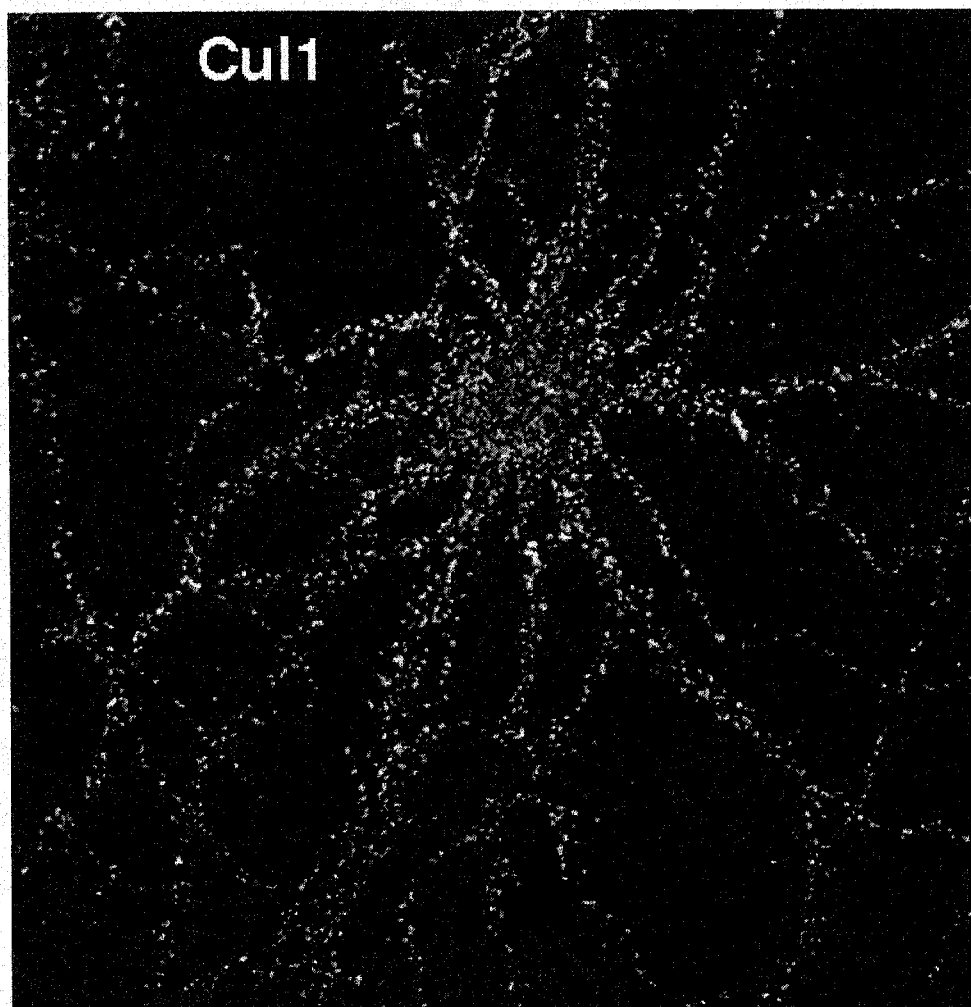


Figure 9.

Figure 10.

Embryonic mouse hippocampal neurons cultured for two weeks, then immunostained for cull1 (red) and the synaptic marker PSD95 (green). The staining pattern shows significant overlap (yellow) at synapses.

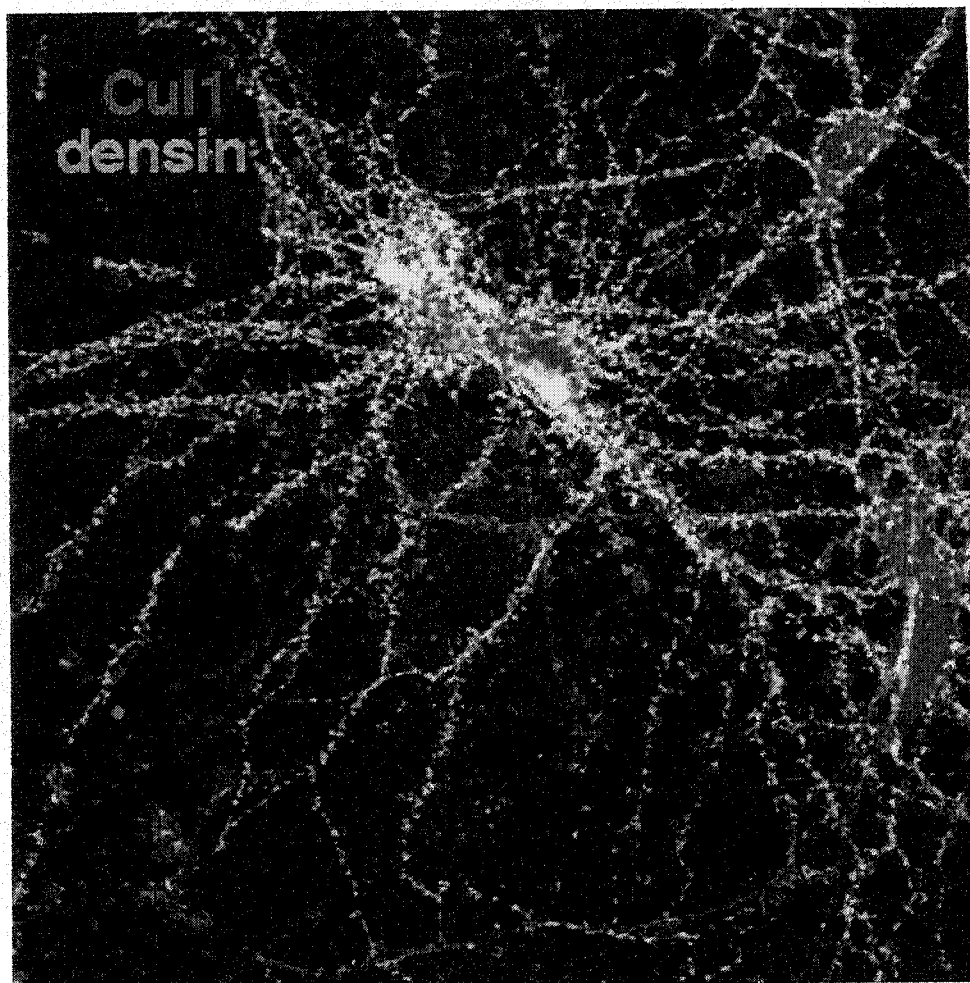


Figure 10.

Figure 11.

Hippocampal neurons from embryonic mice after two weeks in culture were stained for cull immunoreactivity. Nuclear staining was heterogeneous with some intensely bright and others at background levels.

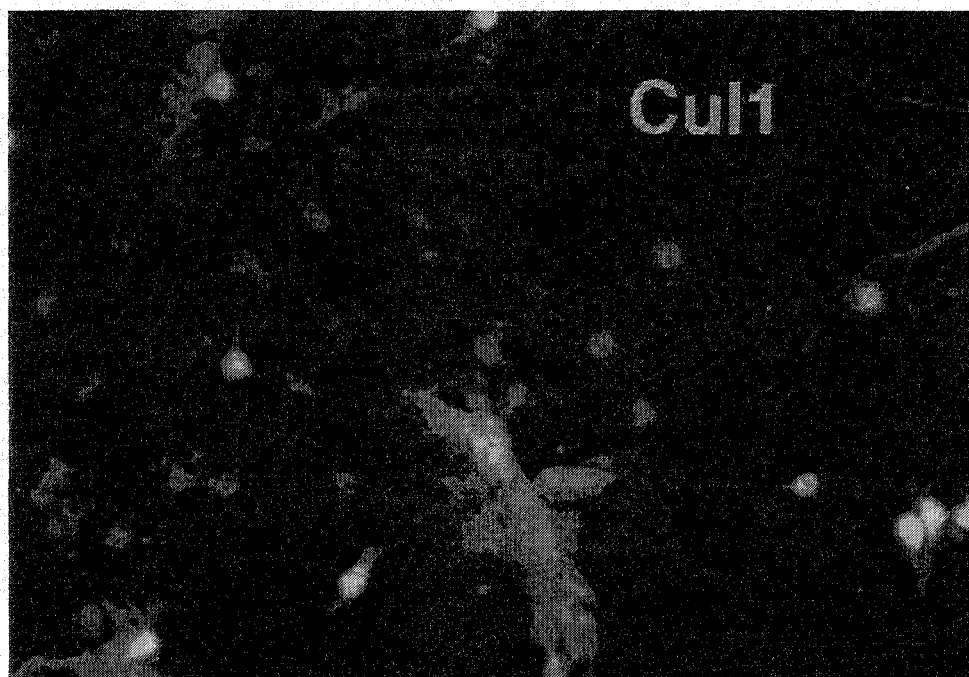


Figure 11.

Figure 12.

Embryonic mouse hippocampal neurons cultured for two weeks then stained with antibody directed against skp1 (red) and the synaptic marker densin (green). Considerable overlap of the two signals (yellow) at the synapse confirmed skp1 localization to the synapse.

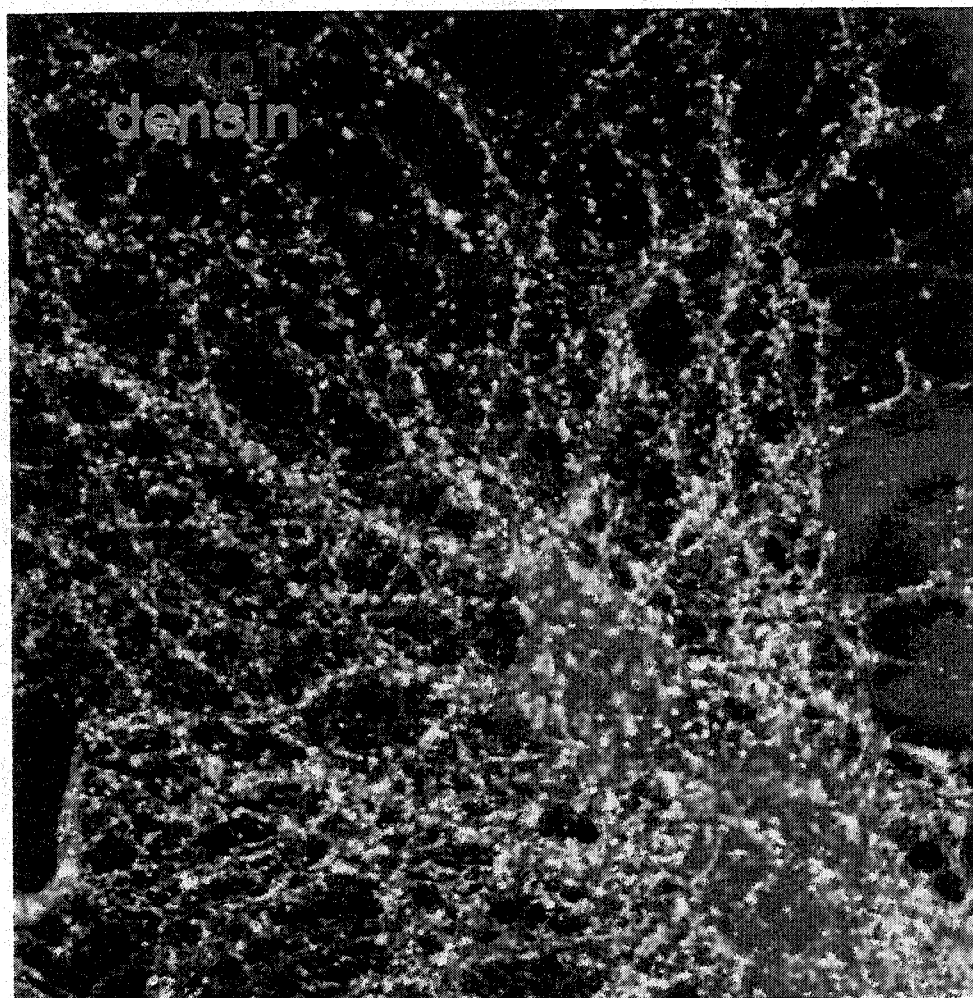


Figure 12.

Figure 13.

Embryonic mouse hippocampal neuron cultures stained with anti-20S proteasome (red) and antibody to the synaptic marker densin (green). Considerable overlap of the two signals (yellow) confirmed 20S proteasome localization to the synapse.

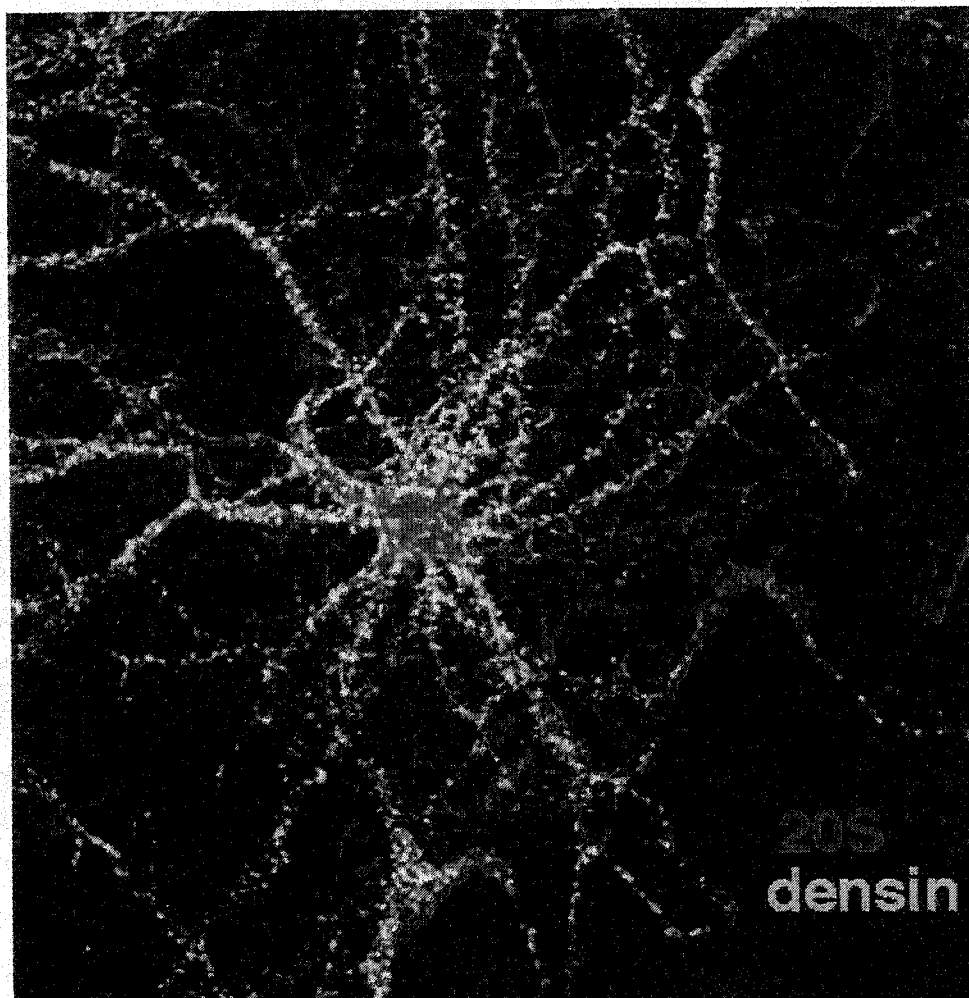


Figure 13.

Figure 14.

Embryonic mouse hippocampal cultured stained for c-met (red) and the synaptic marker densin (green), showing considerable overlap (yellow) in the two signals. C-met was localized to the synapse uniformly in these cultures.

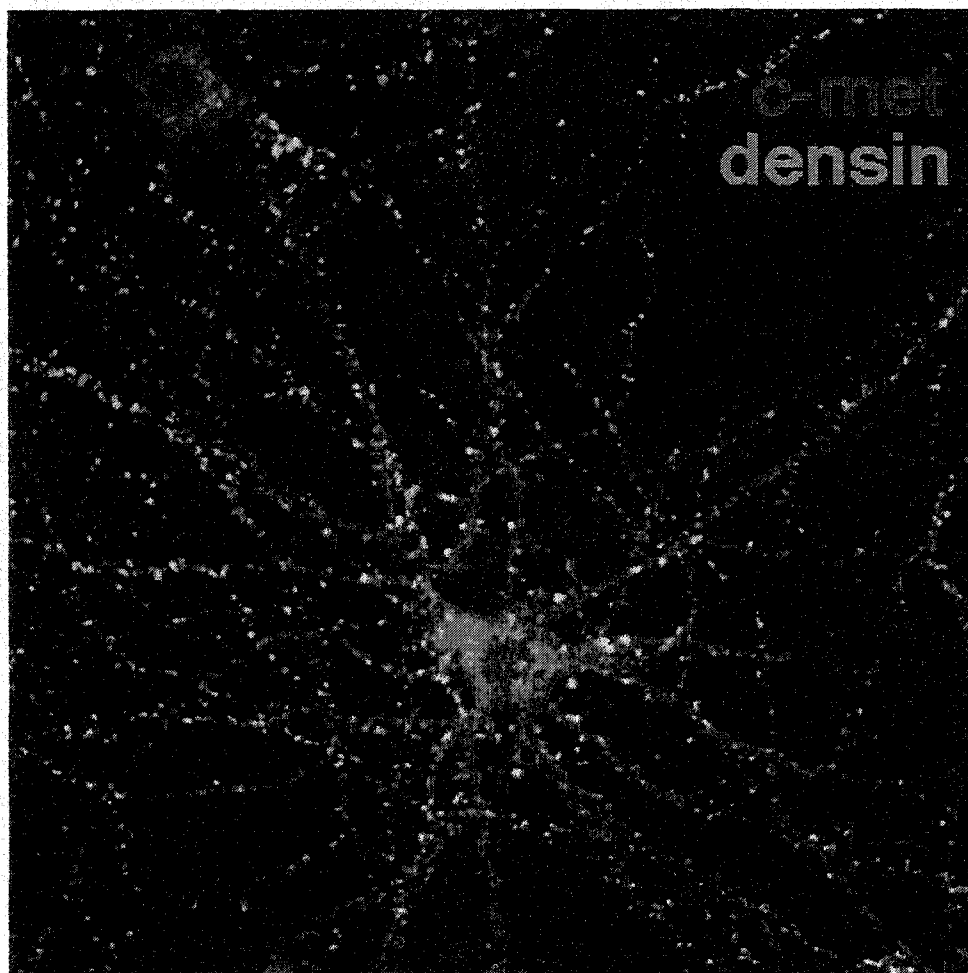


Figure 14.

Figure 15.

Astrocytes in mouse embryonic hippocampal neuron cultures after two weeks. When the cultures were stained with antibody to c-met, astrocyte clusters showed a punctate cytoplasmic (or surface) pattern and intense staining at the cell surface where cell-cell contact is made.

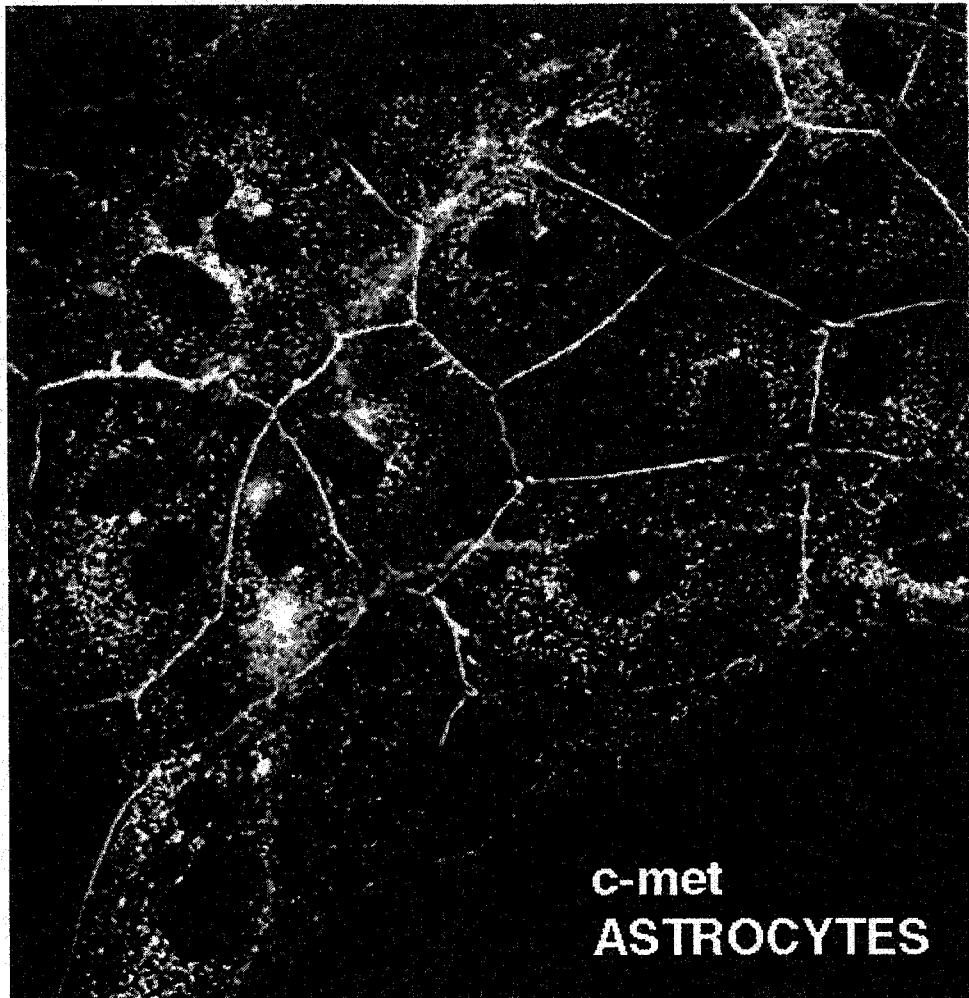


Figure 15.

Figure 16.

Embryonic mouse hippocampal neuronal cultures stained with antibody to the 20S proteasome after one week in culture. Fluorescence intensity was noted at discrete neuronal structures with the morphologic appearance of growth cones.

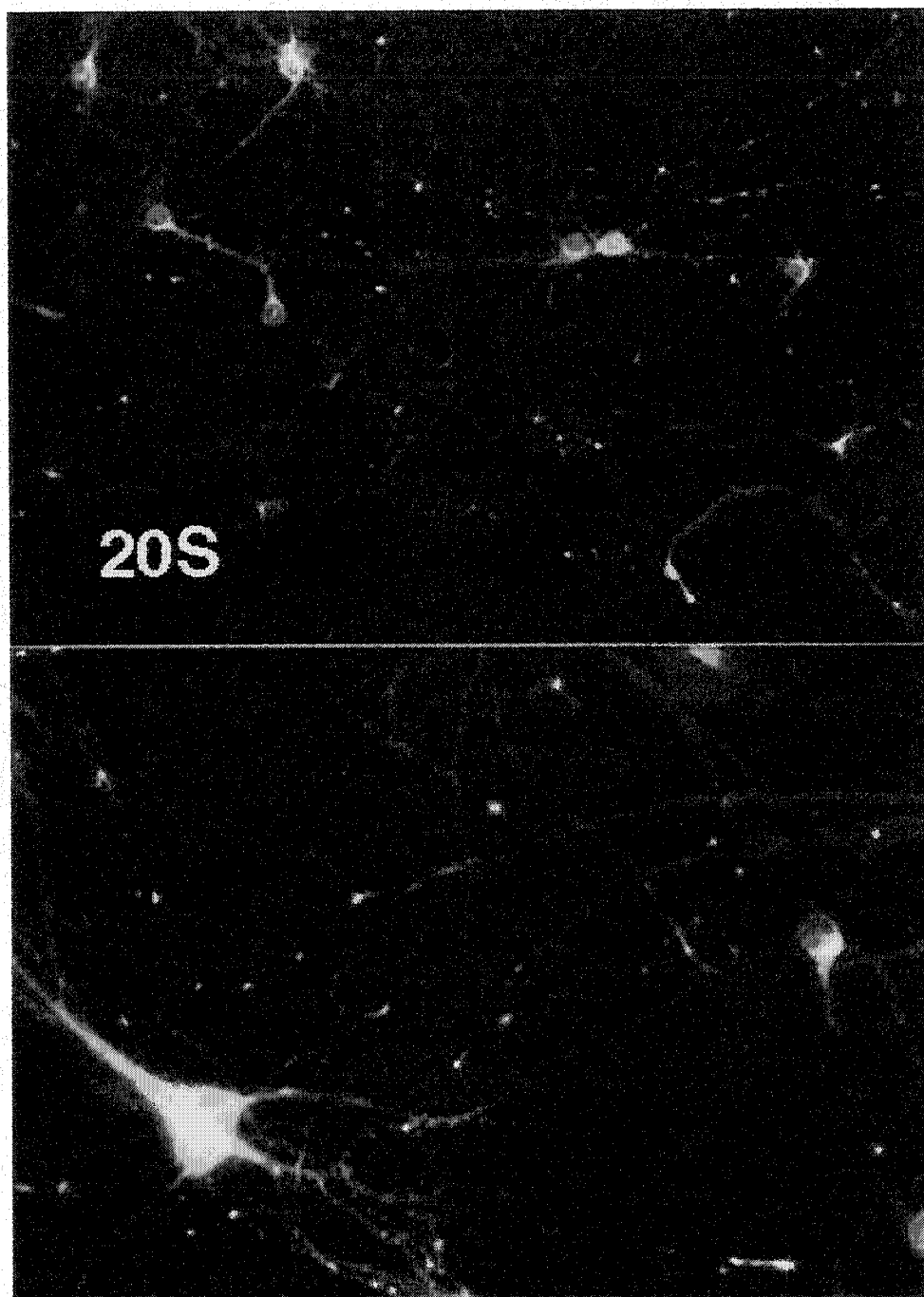


Figure 16.

Figure 17.

Embryonic mouse hippocampal neuron cultures, stained with antibody to skp1 after one week in culture. Bottom panel: Like anti-20S proteasome staining, intense immunofluorescence was noted in discrete neuronal structures that appeared morphologically to be growth cones. Top panel: Skp1 was also seen in the extensions of cells that appeared morphologically to be oligodendrocytes.

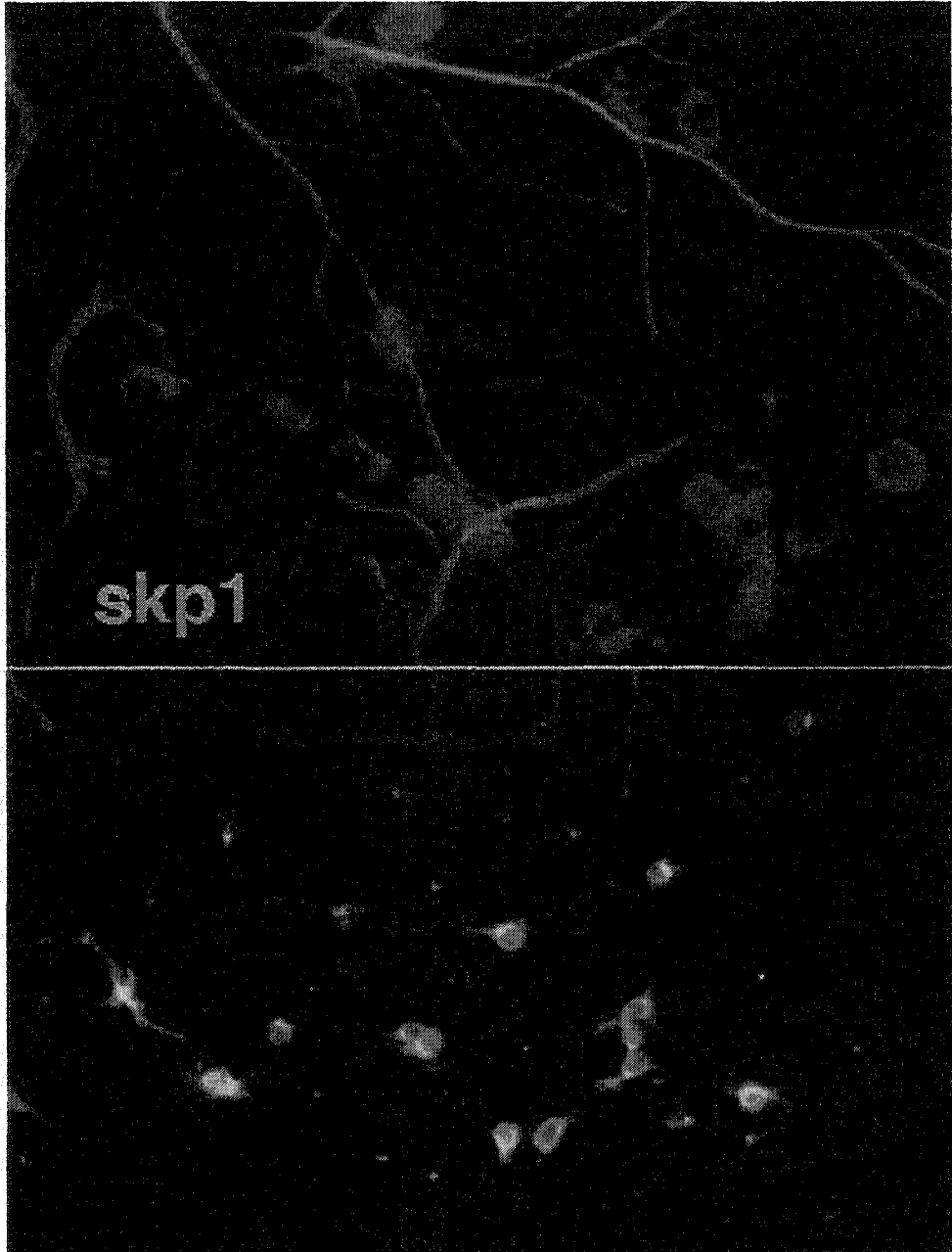


Figure 17.

References

- Achim, C.L., Katyal, S., Wiley, C.A., Shiratori, M., Wang, G., Oshika, E., Petersen, B.E., Li, J.M., Michalopoulos, G.K. (1997). Expression of HGF and cMet in the developing and adult brain. *Brain Res. Dev. Brain Res.* **102**, 299-303.
- Apperson, M.L., Moon, I-S., Kennedy, M.B. (1996). Characterization of Densin-180, a new brain-specific synaptic protein of the O-sialoglycoprotein family. *J. Neurosci.* **16**, 6839-6852.
- Brooks, P., Fuertes, G., Murray, R.Z., Bose, S., Knecht, E., Rechsteiner, M.C., Hendil, K.B., Tanaka, K., Dyson, J., Rivett, J. (2000). Subcellular localization of proteasomes and their regulatory complexes in mammalian cells. *Biochem. J.* **346**, 155-161.
- Chain, D.G., Casadio, A., Schacher, S., Hegde, A.N., Valbrun, M., Yamamoto, N., Goldberg, A.L., Bartsch, D., Kandel, E.R., Schwartz, J.H. (1999). Mechanisms for generating the autonomous cAMP-dependent protein kinase required for long-term facilitation in *Aplysia*. *Neuron* **22**, 147-156.

- Cho, K-O., Hunt, C.A., Kennedy, M.B. (1992). The rat brain post-synaptic density fraction contains a homologue of the drosophila discs-large tumor suppressor protein. *Neuron* **9**, 929-942.
- Ciechanover, A., Breitschopf, K., Hatoum, O.A., Bengal, E. (1999). Degradation of MyoD by the ubiquitin pathway: regulation by specific DNA-binding and identification of a novel site for ubiquitination. *Mol. Biol. Rep.* **26**, 59-64.
- Diehl, J.A., Zindy, F., Sherr, C.J. (1997). Inhibition of cyclin D1 phosphorylation on threonine-286 prevents its rapid degradation via the ubiquitin-proteasome pathway. *Genes Dev.* **11**, 957-972.
- Di Renzo, M.F., Bertolotto, A., Olivero, M., Putzolu, P., Crepaldi, T., Schiffer, D., Pagni, C.A., Comoglio, P.M. (1993). Selective expression of the Met/HGF receptor in human central nervous system microglia. *Oncogene* **8**, 219-222.
- Ebens, A., Brose, K., Leonardo, E.D., Hanson, M.G. Jr., Bladt, F., Birchmeier, C., Barres, B.A., Tessier-Lavigne, M. (1996). Hepatocyte growth factor/scatter factor is an axonal chemoattractant and a neurotrophic factor for spinal motor neurons. *Neuron* **17**, 1157-1172.

Freed, E., Lacey, K.R., Huie, P., Lyapina, S.A., Deshaies, R.J., Stearns, T., Jackson, P.K. (1999). Components of an SCF ubiquitin ligase localize to the centrosome and regulate the centrosome duplication cycle. *Genes Dev.* **13**, 2242-2257.

Gradin, K., McGuire, J., Wenger, R.H., Kvietikova, I., Whitelaw, M.L., Toftgard, R., Tora, L., Gassmann, M., Poellinger, L. (1996). Functional interference between hypoxia and dioxin signal transduction pathways: competition for recruitment of the Arnt transcription factor. *Mol. Cell Biol.* **16**, 5221-5231.

Hegde, A.N., Goldberg, A.L., Schwartz, J.H. (1993). Regulatory subunits of cAMP-dependent protein kinases are degraded after conjugation to ubiquitin: a molecular mechanism underlying long-term synaptic plasticity. *Proc. Natl. Acad. Sci.* **90**, 7436-7440.

Hegde, A.N., Inokuchi, K., Pei, W., Casadio, A., Ghirardi, M., Chain, D.G., Martin, K.C., Kandel, E.R., Schwartz, J.H. (1997). Ubiquitin C-terminal hydrolase is an immediate-early gene essential for long-term facilitation in *Aplysia*. *Cell* **89**, 115-126.

- Hochstrasser, M. (1996). Ubiquitin-dependent protein degradation. *Annu. Rev. Genet.* **30**, 405-439.
- Iyer, N.V., Kotch, L.E., Agani, F., Leung, S.W., Laughlin, E., Wenger, R.H., Gassmann, M., Gearhart, J.D., Lawler, A.M., Yu, A. Y., Semenza, G.L. (1998). Cellular and developmental control of O₂ homeostasis by hypoxia-inducible factor 1 alpha. *Genes Dev.* **12**,149-162.
- Jeffers, M., Taylor, G.A., Weidner, K.M., Omura, S., Vande Woude, G.F. Degradation of the Met tyrosine kinase receptor by the ubiquitin-proteasome pathway. *Mol. Cell Biol.* **17**,799-808.
- Jung, F., Palmer, L.A., Zhou, N., Johns, R.A. (2000). Hypoxic regulation of inducible nitric oxide synthase via hypoxia inducible factor-1 in cardiac myocytes. *Circ. Res.* **86**,319-325.
- Jung, W., Castren, E., Odenthal, M., Vande Woude, G.F., Ishii, T., Dienes, H.P., Lindholm, D., Schirmacher, P. (1994). Expression and functional interaction of hepatocyte growth factor-scatter factor and its receptor c-met in mammalian brain. *J. Cell Biol.* **126**,485-494.
- Kallio, P.J., Wilson, W.J., O'Brien, S., Makino, Y., Poellinger, L. (1999). Regulation of the hypoxia-

inducible transcription factor α by the ubiquitin-proteasome pathway. *J. Biol. Chem.* **274**, 6519-6525.

Kamura, T., Conrad, M.N., Yan, Q., Conaway, R.C., Conaway, J.W. (1999). The Rbx1 subunit of SCF and VHL E3 ubiquitin ligase activates Rub1 modification of cullins Cdc53 and Cul2. *Genes Dev.* **13**, 2928-2933.

Kim, J.H., Haganir, R.L. (1999). Organization and regulation of proteins at synapses. *Curr. Opin. Cell Biol.* **11**, 248-254.

Kipreos, E.T., Lander, L.E., Wing, J.P., He, W.W., Hedgecock, E.M. (1996). *Cul-1* is required for cell cycle exit in *C. elegans* and identifies a novel gene family. *Cell* **85**, 829-839.

Kishino, T., Lalonde, M., Wagstaff, J. (1997). UBE3A/E6-AP mutations cause Angelman syndrome. *Nat. Genet.* **15**, 70-73.

Kolatsi-Joannou, M., Moore, R., Winyard, P.J., Woolf, A.S. (1997). Expression of hepatocyte growth factor/scatter factor and its receptor, MET, suggests roles in human embryonic organogenesis. *Pediatr. Res.* **41**, 657-665.

Koochekpour, S., Jeffers, M., Wang, P.H., Gong, C., Taylor, G.A., Roessler, L.M., Stearman, R., Vasselli, J.R., Stetler-Stevenson, W.G., Kaelin, W.G. Jr., Linehan,

- W.M., Klausner, R.D., Gnarr, J.R., Vande Woude, G.F. (1999). The von Hippel-Lindau tumor suppressor gene inhibits hepatocyte growth factor/scatter factor-induced invasion and branching morphogenesis in renal carcinoma cells. *Mol. Cell Biol.* 19, 5902-5912.
- Kroll, S.L., Paulding, W.R., Schnell, P.O., Barton, M.C., Conaway, J.W., Conaway, R.C. (1999). Von Hippel-Lindau protein induces hypoxia-regulated arrest of tyrosine hydroxylase transcript elongation in pheochromocytoma cells. *J. Biol. Chem.* 274, 30109-30114.
- Lee, P.J., Jiang, B.H., Chin, B.Y., Iyer, N.V., Alam, J., Semenza, G.L., Choi, A.M. (1997). Hypoxia-inducible factor-1 mediates transcriptional activation of the heme oxygenase-1 gene in response to hypoxia. *J. Biol. Chem.* 272, 5375-5381.
- Lee, S., Chen, D.Y.T., Humphrey, J., Gnarr, J.R., Linehan, W.M., Klausner, R.D. (1996). Nuclear/cytoplasmic localization of the von Hippel-Lindau tumor suppressor gene product is determined by cell density. *Proc. Natl. Acad. Sci.* 93, 1770-1775.
- Lee, S., Neumann, M., Stearman, R., Stauber, R., Pause, A., Pavlakis, G.N., Klausner, R.D. (1999). Transcription-dependent nuclear-cytoplasmic trafficking is required

for the function of the von Hippel-Lindau tumor suppressor protein. *Mol. Cell Biol.* **19**, 1486-1497.

Lisztwan, J., Imbert, G., Wirbelauer, C., Gstaiger, M., Krek, W. (1999). The von Hippel-Lindau tumor suppressor protein is a component of an E3 ubiquitin-protein ligase activity. *Genes Dev.* **13**, 1822-1833.

Magistretti, P.J., Pellerin, L., Rothman, D.L., Shulman, R.G. (1999). Energy on demand. *Science* **283**, 496-497.

Maina, F., Hilton, M.C., Ponzetto, C., Davies, A.M., Klein, R. (1997). Met receptor signaling is required for sensory nerve development and HGF promotes axonal growth and survival of sensory neurons. *Genes Dev.* **11**, 3341-3350.

Maina, F., Klein, R. Hepatocyte growth factor, a versatile signal for developing neurons (1999). *Nat. Neurosci.* **2**, 213-217.

Marshall, R.S., Koch, C.J., Rauth, A.M. (1986). Measurement of low levels of oxygen and their effect on respiration in cell suspensions maintained in an open system. *Radiat. Res.* **108**, 91-101.

Maxwell, P.H., Wiesener, M.S., Chang, G-W., Clifford, S.C., Vaux, E.C., Cockman, M.E., Wykoff, C.C., Pugh, C.W., Maher, E.R., Ratcliffe, P.J. (1999). The tumour suppressor protein VHL targets hypoxia-inducible

factors for oxygen-dependent proteolysis. *Nature* **399**, 271-275.

McGaugh, J.L. (2000) Memory--a century of consolidation. *Science* **287**, 248-251.

Mengual, E., Arizti, P., Rodrigo, J., Gimenez-Amaya, J.M., Castano, J.G. (1996). Immunohistochemical distribution and electron microscopic subcellular localization of the proteasome in the rat CNS. *J. Neurosci.* **16**, 6331-6341.

Michel, J.J., Xiong, Y. (1998). Human CUL-1, but not other cullin family members, selectively interacts with SKP1 to form a complex with SKP2 and cyclin A. *Cell Growth Differ.* **9**, 435-449.

Miyazawa, T., Matsumoto, K., Ohmichi, H., Kato, H., Yamashima, T., Nakamura, T. (1998). Protection of hippocampal neurons from ischemia-induced delayed neuronal death by hepatocyte growth factor: A novel neurotrophic factor. *J. Cereb. Blood Flow Metab.* **18**, 345-348.

Montagnoli, A., Fiore, F., Eytan, E., Carrano A.C., Draetta, G.F., Hershko, A., Pagano, M. (1999). Ubiquitination of p27 is regulated by Cdk-dependent phosphorylation and trimeric complex formation. *Genes Dev.* **13**, 1181-1189.

- Moriyama, T., Kataoka, H., Koono, M., Wakisaka, S. (1999). Expression of hepatocyte growth factor/scatter factor and its receptor c-Met in brain tumors: evidence for a role in progression of astrocytic tumors. *Int. J. Mol. Med.* **3**, 531-536.
- Mueller-Klieser, W.F., Sutherland, R.M. (1982). Oxygen tensions in multicell spheroids of two lines. *Br. J. Cancer* **45**, 256-264.
- Ogiso, Y., Tomida, A., Kim, H.D., Tsuruo, T. (1999). Glucose starvation and hypoxia induce nuclear accumulation of proteasome in cancer cells. *Biochem. Biophys. Res. Commun.* **258**, 448-452.
- Ohmichi, H., Koshimizu, U., Matsumoto, K., Nakamura, T. (1998). Hepatocyte growth factor (HGF) acts as a mesenchyme-derived morphogenic factor during fetal lung development. *Development* **125**, 1315-1324.
- O'Rourke, J.F., Dachs, G.U., Gleadle, J.M., Maxwell, P.H., Pugh, C.W., Stratford, I.J., Wood, S.M., Ratcliffe, P.J. (1997). Hypoxia response elements. *Oncol. Res.* **9**, 327-332.
- Pal, S., Calffery, K.P., Dvorak, H.F., Mukhopadhyay, D. (1997). The von Hippel-Lindau gene product inhibits vascular permeability factor/vascular endothelial growth factor expression in renal cell carcinoma by

blocking protein kinase C pathways. *J. Biol. Chem.* **272**, 27509-27512.

Palmer, A., Mason G.G., Paramio, J.M., Knecht, E., Rivett, A.J. (1994). Changes in proteasome localization during the cell cycle. *Eur. J. Cell Biol.* **64**, 163-175.

Pause, A., Lee, S., Worrell, R.A., Chen, D.Y., Burgess, W.H., Linehan, W.M., Klausner, R.D. (1997). The von Hippel-Lindau tumor-suppressor gene product forms a stable complex with human CUL-2, a member of the Cdc53 family of proteins. *Proc. Natl. Acad. Sci.* **94**, 2156-2161.

Pollenz, R.S., Davarinos, N.A., Shearer, T.P. (1999). Analysis of aryl hydrocarbon receptor-mediated signaling during physiological hypoxia reveals lack of competition for the aryl hydrocarbon nuclear translocator transcription factor. *Mol. Pharmacol.* **56**, 1127-1137.

Rousseau, D., Cannella, D., Boulaire, J., Fitzgerald, P., Fotedar, A., Fotedar, R. (1999). Growth inhibition by CDK-cyclin and PCNA binding domains of p21 occurs by distinct mechanisms and is regulated by ubiquitin-proteasome pathway. *Oncogene* **18**, 4313-4325.

- Russell, S.J., Steger, K.A., Johnston, S.A. (1999). Subcellular localization, stoichiometry, and protein levels of 26S proteasome subunits in yeast. *J. Biol. Chem.* **274**, 21943-21952.
- Salceda, S., Caro, J. (1997). Hypoxia-inducible factor 1 α (HIF-1 α) protein is rapidly degraded by the ubiquitin-proteasome system under normoxic conditions: its stabilization by hypoxia depends upon redox-induced changes. *J. Biol. Chem.* **272**, 22642-22647.
- Semenza, G.L. (1999). Regulation of mammalian O₂ homeostasis by hypoxia-inducible factor 1. *Annu. Rev. Cell Dev. Biol.* **15**, 551-578.
- Semenza, G.L., Wang, G.L. (1992). A nuclear factor induced by hypoxia via de novo protein synthesis binds to the human erythropoietin gene enhancer at a site required for transcriptional activation. *Mol. Cell. Biol.* **12**, 5447-5454.
- Shen, K., Meyer, T. (1999). Dynamic control of CaMKII translocation and localization in hippocampal neurons by NMDA receptor stimulation. *Science* **284**, 162-166.
- Shweiki, D., Itin, A., Soffer, D., Keshet, E. (1992). Vascular endothelial growth factor induced by hypoxia may mediate hypoxia-initiated angiogenesis. *Nature* **359**, 843-845.

- Singer, J.D., Gurian-West, M., Clurman, B., Roberts, J.M. (1999). Cullin-3 targets cyclin E for ubiquitination and controls S phase in mammalian cells. *Genes Dev.* 13,2375-2387.
- Soriano, J.V., Pepper, M.S., Nakamura, T., Orci, L., Montesano, R. (1995). Hepatocyte growth factor stimulates extensive development of branching duct-like structures by cloned mammary gland epithelial cells. *J. Cell Sci.* **108**, 413-430.
- Taylor, B.L., Zhulin, I.B. (1999). PAS domains: Internal sensors of oxygen, redox and light. *Microbiol. Mol. Biol. Rev.* **63**, 479-506.
- Thewke, D.P., Seeds, N.W. (1999). The expression of mRNAs for hepatocyte growth factor/scatter factor, its receptor c-met, and one of its activators tissue-type plasminogen activator show a systematic relationship in the developing and adult cerebral cortex and hippocampus. *Brain Res.* 821, 356-367.
- Tyers, M., Willems, A.R. (1999). One ring to rule a superfamily of E3 ubiquitin ligases. *Science* **284**, 601-604.
- Urano, T., Yashiroda, H., Muraoka, M., Tanaka, K., Hosoi, T., Inoue, S., Ouchi, Y., Toyoshima, H. (1999). p57(Kip2) is degraded through the proteasome in

osteoblasts stimulated to proliferation by transforming growth factor beta1. *J. Biol. Chem.* **274**, 12197-12220.

Vanzetta, I., Grinvald, A. (1999). Increased cortical oxidative metabolism due to sensory stimulation: implications for functional brain imaging. *Science* **286**, 1555-1558.

Varshavsky, A. (1997). The ubiquitin system. *Trends Biochem. Sci.* **22**, 383-387.

Wang, G.L., Jiang, B.H., Rue, E.A., Semenza, G.L. (1995). Hypoxia-inducible factor 1 is a basic-helix-loop-helix-PAS heterodimer regulated by cellular O₂ tension. *Proc. Natl. Acad. Sci.* **92**, 5510-5514.

Wolf, A.S., Kolatsi-Joannou, M., Hardman, P., Andermarcher, E., Moorby, C., Fine, L.G., Jat, P.S., Noble, M.D., Gherardi, E. (1995). Roles of hepatocyte growth factor/scatter factor and the met receptor in the early development of the metanephros. *J. Cell Biol.* **128**, 171-184.

Yamada, T., Yoshiyama, Y., Tsuboi, Y., Shimomura, T. (1997). Astroglial expression of hepatocyte growth factor and hepatocyte growth factor activator in human brain tissues. *Brain Res.* **762**, 251-255.

- Yang, X-M., Toma, J.G., Bamji, S.X., Belliveau, D.J., Kohn, J., Park, M., Miller, F.D. (1998). Autocrine hepatocyte growth factor provides a local mechanism for promoting axonal growth. *J. Neurosci.* **18**, 8369-8381.
- Ye, Y., Vasavada, S., Kuzmin, I., Stackhouse, T., Zbar, B., Williams, B.R.G. (1998). Subcellular localization of the von Hippel-Lindau disease gene product is cell cycle-dependent. *Int. J. Cancer* **78**, 62-69.
- Zhu, H., Bunn, H.F. (1999). Oxygen sensing and signaling: impact on the regulation of physiologically important genes. *Resp. Physiol.* **115**, 239, 247.
- Zou, D.J., Cline, H.T. (1999). Postsynaptic calcium/calmodulin-dependent protein kinase II is required to limit elaboration of presynaptic and postsynaptic neuronal arbors. *J. Neurosci.* **19**, 8909-8918.

Appendix I

Methods

Culture of human astrocytes

Human astrocytes (Clonetics, San Diego, CA) were cultured according to supplier's protocol in F10 medium containing 5% fbs, supplemented (by the supplier) with hEGF, insulin, progesterone, transferrin and gentamicin/amphotericin. At about 80% confluence the cells were split using trypsin 0.25% to dissociate them from the plate. Stains for cul2 were done at low density 24 hr after splitting. Astrocytes were cultured at either 2% oxygen or 20% oxygen, with 5% CO₂ in both cases.

Tyramide signal amplification of fluorescent immunohistochemistry

NEN manufacturer's recommendations were followed for these assays. After PBS washes, the manufacturer's buffer was used to block the slides for 30 min at room temperature, then cul2 primary antibody was incubated overnight at 4°C. Slides were washed in manufacturer's buffer three times, then reacted with SA-HRP for 30 min at room temperature.

After washes the cells were incubated in fluorophor tyramide for 5 min, washed and mounted for microscopy.

For embryonic rat CNS stem cell culture and staining: See Appendix I in Chapter 3.

Isolation and culture of hippocampal neurons

E16 FVB/129 mouse embryos were collected after CO₂ euthanasia of the mother. The embryos were decapitated in Hanks buffer, and the brains removed and put into fresh buffer. The hippocampi were dissected out and cut into small peices, then digested in trypsin for 15 minutes at 37°C. The reaction was stopped with soyobean trypsin inhibitor (1 mg/ml) with two 5 minute treatments at room temperature. Digested cells were washed twice in Hanks buffer, then dissociated with a polished Pasteur pipet (three times) until all pieces are dispersed. The cells were counted in a hemacytometer then cultured at a density of about 200 cells/mm² on poly-D-lysine and laminin coated cover slips. Cells were initially cultured in plating medium (Neurobasal media containing B27 supplement, 0.5 mM glutamine, 25 uM glutamate, and 25 uM B-mercaptoethanol) that was pre-equilibrated in the incubator with 5% CO₂. Four days after plating, the plating media was replaced

with Neurobasal media containing B27 supplement and 0.5 mM glutamine. The cultures were maintained in this media for the duration of the experiment. After 24 hours of culture, the cover glasses were turned upside-down.

Immunohistochemical staining of hippocampal neuron cultures

Cover slips were dipped in iced D-PBS (below), then rinsed in iced methanol, which was then replaced with -20°C methanol. This fix was continued for 20 min. The slips were washed for 15 min with iced D-PBS, and then preblock (below) was applied for 1 hour at 4°C. Primary antibody incubation was in preblock at 4°C overnight. Cells were washed three times for 15 min each with preblock at room temperature. The appropriate secondary was applied in preblock at 1:100 dilution for 1 hour at room temperature. Final washes were two with preblock for 15 min and two with PBS for 15 min. Cells were postfixed with 2% paraformaldehyde in PBS, then washed twice with PBS for 5 minutes, then twice with 0.1 M carbonate buffer (below) for 5 min. Cells were mounted on a slide warmer set to 37°C with 4% n-propylgallate in 90% glycerol and 10% 0.5 M carbonate buffer, pH 9. Cover slips were sealed and analyzed with confocal microscopy.

Primary antibody concentrations used in these studies were:

Primaries:

Anti-**c-met** rabbit polyclonal 1:50 (Santa Cruz)

Anti-**20S proteasome** rabbit polyclonal 1:100 (Calbiochem)

Anti-**skp1** rabbit polyclonal 1:600 (courtesy of Dr. Peter Jackson, Stanford University)

Anti-**cul2** rabbit polyclonal 1:100 (Zymed)

Anti-**cull1** mouse monoclonal 1:500 (courtesy of Svetlana Lyapina and Dr. Ray Deshaies, Caltech)

Anti-**densin** mouse polyclonal 1:500, courtesy of Dr. Mary Kennedy (Apperson et al., 1996)

Anti-**PSD95** rabbit polyclonal 1:500, courtesy of Dr. Mary Kennedy (Cho et al., 1992)